UNIVERSITY OF ŽILINA


# TRANSCOM PROCEEDINGS 2015

## 11-th EUROPEAN CONFERENCE OF YOUNG RESEARCHERS AND SCIENTISTS

under the auspices of

Tatiana Čorejová
Rector of the University of Žilina

## SECTION 3

## INFORMATION AND COMMUNICATION TECHNOLOGIES

ŽILINA June 22 - 24, 2015
SLOVAK REPUBLIC

Edited by Peter Šarafín, Ján Račko, Michal Kvet, Michal Mokryš

ISBN: 978-80-554-1045-6
ISSN of Transcom Proceedings CD-Rom version: 1339-9799
ISSN of Transcom Proceedings online version: 1339-9829
(http://www.transcom-conference.com/transcom-archive)

**TRANSCOM 2015**
**11th European conference of young researchers and scientists**

TRANSCOM 2015, the 11th international conference of young European scientists, postgraduate students and their tutors, aims to establish and expand international contacts and co-operation. The main purpose of the conference is to provide young scientists with an encouraging and stimulating environment in which they present results of their research to the scientific community. TRANSCOM has been organised regularly every other year since 1995. Between 160 and 400 young researchers and scientists participate regularly in the event. The conference is organised for postgraduate students and young scientists up to the age of 35 and their tutors. Young workers are expected to present the results they had achieved.

The conference is organised by the University of Žilina. It is the university with about 13 000 graduate and postgraduate students. The university offers Bachelor, Master and PhD programmes in the fields of transport, telecommunications, forensic engineering, management operations, information systems, in mechanical, civil, electrical, special engineering and in social sciences incl. naturalsciences.

SECTIONS AND SCIENTIFIC COMMITTEE

**1. TRANSPORT AND COMMUNICATIONS TECHNOLOGY.**

Scientific committee: Adamko Norbert (SK), Bugaj Martin (SK), Buzna Ľuboš (SK), Drozdziel Paweł (PL), Jánošíková Ľudmila (SK), Madleňák Radovan (SK), Rievaj Vladimír (SK), Teichmann Dušan (CZ)

**2. ECONOMICS AND MANAGEMENT.**

Scientific committee: Blašková Martina (SK), Hittmár Štefan (SK), Borkowski Stanisław (PL), Gregor Milan (SK), Kucharčíková Alžbeta (SK), Matuszek Józef (PL), Mičieta Branislav (SK), Rostášová Mária (SK), Sroka Włodzimierz (PL), Tomová Anna (SK), Zhivitskaya Helena (BLR)

**3. INFORMATION AND COMMUNICATION TECHNOLOGIES.**

Scientific committee: Dado Milan (SK), Hudec Róbert (SK), Kharchenko Vyacheslav (UKR), Klimo Martin (SK), Kršák Emil (SK), Matiaško Karol (SK), Pancerz Krzysztof (PL), Spalek Juraj (SK), Švadlenka Libor (CZ), Vaculík Juraj (SK), Vašinek Vladimír (CZ), Vrček Neven (HR)

**4. ELECTRIC POWER SYSTEMS. ELECTRICAL AND ELECTRONIC ENGINEERING.**

Scientific committee: Altus Juraj (SK), Brandštetter Pavel (CZ), Bury Peter (SK), Cacciato Mario (I), Čápová Klára (SK), Dobrucký Branislav (SK), Chernoyarov Oleg Vyacheslavovich (RU), Janoušek Ladislav (SK), Luft Mirosław (PL), Szychta Elżbieta (PL), Špánik Pavol (SK), Vittek Ján (SK)

**5. MATERIAL ENGINEERING. MECHANICAL ENGINEERING TECHNOLOGIES.**
Scientific committee: Adamczak Stanisław (PL), Guagliano Mario (I), Konečná Radomila (SK), Kunz Ludvík (CZ), Kuric Ivan (SK), Meško Jozef (SK), Neslušan Miroslav (SK), Takács János (H), Ungureanu Nicolae Stelian (RO)

**6. MACHINES AND EQUIPMENT. TRANSPORT MEANS. APPLIED MECHANICS.**
Scientific committee: Gerlici Juraj (SK), Chudzikiewicz Andrzej (PL), Malcho Milan (SK), Medvecký Štefan (SK), Zapoměl Jaroslav (CZ), Žmindák Milan (SK)

**7. CIVIL ENGINEERING.**
Scientific committee: Bujňák Ján (SK), Ižvolt Libor (SK), Segalini Andrea (I)

**8. NATURAL SCIENCES (APPLIED MATHEMATICS). SOCIAL SCIENCES.**
Scientific committee: Dopita Miroslav (CZ), Dzhalladova Irrada (UKR), Grecmanová Helena (SK), Katuščák Dušan (SK), Marčoková Mariana (SK), Růžičková Miroslava (SK), Šindelářová Jaromíra (CZ)

**9. SECURITY ENGINEERING. FORENSIC ENGINEERING.**
Scientific committee: Kasanický Gustáv (SK), Kohút Pavol (SK), Navrátil Leoš (CZ), Řehák David (CZ), Sventeková Eva (SK), Šimák Ladislav (SK), Zagorecki Adam (UK), Zamiar Zenon (PL)

## ORGANIZING COMMITTEE

**CHAIRPERSONS** Čelko Ján, Bokůvka Otakar
**EXECUTIVE SECRETARY** Vráblová Helena

**MEMBERS** Bašťovanský Ronald, Belan Juraj, Bendík Ján, Brída Peter, Brůna Marek, Bulej Vladimír, Číba Jakub, Čičmancová Silvia, Dulina Ľuboslav, Ďurovec Martin, Florková Zuzana, Gašová Zuzana, Grajcaríková Petra, Grejták Marek, Herda Miloš, Hőger Marek, Hrbček Jozef, Hruboš Marián, Hudák Martin, Koman Gabriel, Kutaj Milan, Kuzmová Mária, Kvet Michal, Magdolen Marián, Malichová Eva, Maňurová Mária, Masárová Gabriela, Metruk Rastislav, Murgašová Veronika, Nosek Radovan, Odrobiňák Jaroslav, Olešnaníková Veronika, Oriešková Veronika, Palkechová Marcela, Porubiaková Andrea, Pšenáková Zuzana, Račko Ján, Rusinková Jana, Rypáková Martina, Semanová Štefánia, Stankovičová Zuzana, Šarafín Peter, Šimková Ivana, Šušlik Ľuboš, Vaško Alan, Vincúrová Gabriela.

# SECTION 3 INFORMATION AND COMMUNICATION TECHNOLOGIES

## REVIEWERS:

Blaško Rudolf
Brída Peter
Bubeníková Emília
Čorejová Tatiana
Dubovan Jozef
Fabuš Juraj
Jarina Roman
Juraj Vaculík
Káčik Daniel
Klimo Martin
Kolarovszki Peter
Koziorek Jiří
Kršák Emil
Kuba Michal
Madleňák Radovan
Machaj Juraj
Matiaško Karol
Matuška Slavomír
Miček Juraj
Pancerz Krzysztof
Švadlenka Libor
Vestenický Martin
Vestenický Peter
Vrček Neven

**Note:**

**Author/s are responsible for language contents of their papers**

# CONTENTS

**TRANSCOM 2015, 22-24 June 2015**
University of Žilina, Žilina, Slovak Republic

# Application of artificial neural networks to prediction of success of bank telemarketing campaign

[*]Michał Grosicki
[*]Kielce University of Technology, Faculty of Electrical Engineering, Automatic Control and Computer Science, al. Tysiąclecia Państwa Polskiego 7, 25-314 Kielce, Poland, mgrosicki@tu.kielce.pl

**Abstract.** The following paper presents example of application of artificial neural networks to prediction of success of bank telemarketing campaign. The prediction is being made based on phone call to a client and various informations obtained during that phone call. Training of the network is divided in two stages: unsupervised learning of denoising auto-encoder and supervised learning of dropout-regularized neural network using back-propagation algorithm. Obtained predictive model allowed for nearly 90% prediction accuracy. Obtained system can be used as tool to help bank personnel decide who to call to maximize bank's profits.

**Keywords:** neural networks, denoising auto-encoder, dropout, machine learning, telemarketing

## 1. Introduction

In modern world telemarketing campaigns are used by companies in almost every branch of industry to reach the largest number of the potential clients with their products and services. Unfortunately this method is very inefficient. Most of the phone calls does not end up with desired outcome. In this paper we present neural network based model for prediction of telemarketing campaign. We strongly believe that such model may be very helpful in targeting clients that are most likely to positively respond to our campaign. The biggest advantages of use of such model are better use of resource and bigger profits.

The rest of this paper is organized as follows: in section 2 we describe training of neural networks used in our model, in section 3 we present used data and results of our simulations and finally in section 4 we conclude the paper with several final remarks.

## 2. Training of neural networks for telemarketing outcome prediction

For many years training of neural networks with two or more hidden layers was hard or almost impossible [1]. Recent advances in the field proposed solutions to this problem based on restricted Boltzmann machines [2] or denoising auto-encoders [3]. The basic idea behind the first two is to pre-train a restricted Boltzmann machine or denoising auto-encoder in unsupervised manner and use the obtained parameters to initialize weights of multilayer perceptron (MLP) type network and continue training using supervised algorithm like back-propagation.

Denoising auto-encoder is an artificial neural network model composed of two modules: encoder and decoder. Each of them has one visible and one hidden layer. During learning algorithm tries to find a code (represented by hidden layer of the encoder) that allows for good reconstruction of the inputs using learned decoder. In most cases code layer has smaller size than the number of dimensions of the data. This is necessary so the network would not learn trivial representations of the data such as identity function. This allows for the denoising auto-encoders to be used as dimensionality reduction tool. Code layer of the network computes hidden representation of the data according to (1):

$$y = \sigma(Wx + b). \tag{1}$$

In similar manner is computed output of the reconstruction layer:

$$\dot{x} = \sigma(W'y + c). \quad (2)$$

The learning is performed using stochastic gradient descent algorithm which minimizes the appropriate for the data reconstruction cost. In case of real-valued data this cost is L2-cost given by (3):

$$E(x, \dot{x}) = \|x - \dot{x}\|_2^2. \quad (3)$$

To help the network learn useful representation of the data noise is introduced on the inputs of the network. Here we outline learning process of the denoising auto-encoder:

1. Choose data vector x.
2. Create noisy version of the data – x". In most case we want to perturb 10% to 50% of the attributes.
3. Compute code y using (1) and x".
4. Compute reconstruction of the data x' using (2) and y.
5. Compute reconstruction error using (3), reconstruction x' and original data x.
6. Update parameters using stochastic gradient descent algorithm; repeat until last iteration is reached.

After finished learning parameters of the auto-encoder are used to initialize weights of the multilayer perceptron network. This network is later trained using standard back-propagation algorithm with momentum and dropout regularization technique. It is also worth noting, that instead of using learned parameters as a initialization point for other network, we can use auto-encoder as a preprocessor of the data and use this new representation as input to other classification algorithms like support vector machines.

## 3. Simulations

### 3.1. Data set

During simulations we used data related with direct marketing campaigns of a Portugeses banking institution [4]. Our task is to predict if the client will subscribe a term deposit. Data set contains over 41000 examples with 20 inputs. During our experiments we used 19 of them discarding duration attribute which caused severe bias in our model. Data was split into training, validation and test set. Training set consists of 80% randomly selected examples, validation set of 20% and test set of the rest.

### 3.2. Models parameters

During simulations we used denoising auto-encoder with a code layer consisting of 50 neurons to with logistic activation function. Since the data set is real-valued we utilize linear layer as our reconstruction layer. Data were presented to the model in batches of ten and training lasted for 100 epochs. As our optimization target we used function given in (3). Parameters of encoder and auto-encoder were tied. Summarization of parameters of auto-encoder is given in Tab. 1.

| Parameter | Value |
|---|---|
| Learning rate | 0.01 |
| Momentum | 0.9 |
| Number of training epochs | 100 |
| Batch size | 20 |
| Noise ratio | 30% |

**Tab. 1.** Learning parameters of denoising auto-encoder.

Subsequently learned parameters of denoising auto-encoder were used to initialized MLP network with a hidden layer of the same size. On top of the hidden layer we placed output layer with one neuron. We used logistic function for the output. Network was trained using back-

propagation algorithm with momentum, dropout regularization and early stopping. As a cost function we utilized cross-entropy cost (4):

$$E(t,y) = -tlny - (1-t)ln(1-y). \quad (3)$$

Learning process process ended after roughly 200 epochs. Summarization of parameters of MLP network is given in Tab. 2.

| Parameter | Value |
|---|---|
| Learning rate | 0.03 |
| Momentum | 0.9 |
| Number of training epochs | 200 |
| Batch size | 20 |
| Dropout rate | 50% |

**Tab. 2.** Learning parameters of MLP.

### 3.3. Results

After successful learning we measured accuracy on the test set. Network achieved accuracy of 89.8%. This result is better than the one obtained with neural network trained without unsupervised pre-training and dropout by 5%. It is also slightly better than result obtained with support vector machine with RBF kernel, which was able to correctly classify 88.2% of the test cases. Classification accuracy for each set is presented is Tab. 3.

| Set | Accuracy |
|---|---|
| Training | 89.86% |
| Validation | 89.41% |
| Test | 89.77% |

**Tab. 3.** Accuracies obtained with trained model.

## 4. Conclusion

In this paper we presented application of artificial neural networks to prediction of bank telemarketing campaign outcomes. Accuracy of 89.2% achieved by trained model is satisfactory and bodes well for the practical use of such model for this task. Recent developments in the field of neural networks allowed to achieve good results. During our simulations we tested models with more than one hidden layer. In case of traditional neural network this resulted in severe overfitting, while in case of pre-trained networks accuracy dropped only slightly. This leads us to believe that it may be possible to train deeper network that would achieve better results. We plan on investigating this matter in our future research.

Proposed model worked well for the given task. Its predictive power may allow banking institutions to better target their client base with more personalized products minimizing the effort needed for the campaign and maximizing profits. We also believe that presented model could be used, given appropriate dataset, used various other types of companies which utilizes telemarketing as one of the tools for contacting the clients.

## References

[1] BENGIO, Y. *Learning of deep architectures for AI*. Foundations and Trends in a Machine Learning, 2009.

[2] HINTON, G. E., OSINDERO S., TEH, Y-W. *A fast learning algorithm for deep belief nets*. Neural Computations Vol. 18, No. 7, 2006.

[3] VINCENT, P., LAROCHELLE, H., BENGIO, Y., MANZAGOL P-A. *Extracting and composing robus features with denoising autoencoders*. ICML '08 Proceedings of the 25th International Conference on Machine learning, 2008.

[4] MORO, S., CORTEZ P., RITA P. *A data-driven approach to predict the success of bank telemarketing*. Decision Support Systems, Elsevier 2014.

**TRANSCOM 2015, 22-24 June 2015**
University of Žilina, Žilina, Slovak Republic

# Learning Fuzzy Cognitive Maps using Evolutionary Algorithms – a comparative study

[*]Łukasz Kubuś, [*]Katarzyna Poczęta
[*] Kielce University of Technology, Faculty of Electrical Engineering, Automatic Control and Computer Science, Department of Information Systems, al. Tysiąclecia Państwa Polskiego 7, 25-635 Kielce, Poland, {lkubus, k.piotrowska}@tu.kielce.pl

**Abstract.** In the article developed Individually Directional Evolutionary Algorithm (IDEA) for Fuzzy Cognitive Map (FCM) learning is presented. The proposed FCMs learning algorithm was compared with elite real-coded genetic algorithms. FCMs and the proposed method of learning are described. Simulation analysis of the use of FCMs with the developed algorithm was performed on the basis of real-life case of strategic planning process of an e-business company.

**Keywords:** fuzzy cognitive map, evolutionary algorithms, individually directional evolutionary algorithm, elite real-coded genetic algorithm.

## 1. Introduction

Fuzzy cognitive map (FCM) is a universal tool for modeling and analysis of dynamic systems [19]. FCMs have been introduced by Kosko [7] as a soft computing technique combining fuzzy logic, artificial neural networks and evolutionary computing [12]. It describes problem as a collection of concepts and connections (relations) between them. With increasing of uncertainty or complexity, some extensions of the traditional FCM can be used, e.g. fuzzy grey cognitive maps [15], augmented FCMs [14] or relational fuzzy cognitive maps [16,17].

There are several methods for building a FCM model. In the first method, FCM model is created based on knowledge of experts. In this case, FCM model accuracy depends from the experts knowledge. Moreover, the manual methods can became impractical for building large models [10,14].

Historical data enable automatic construction of FCM. This issue is called "learning" of the FCM model. The learning process allows to establish the weights of the relations between concepts. There are three main groups of FCM learning algorithms: unsupervised methods based on Hebbian rule [10,12,18], supervised algorithms based on gradient method [5,13], and biology-inspired approaches, such as evolutionary algorithms (EAs) [2,3,10,13,19], artificial immune systems [6] or particle swarm optimization [11].

In this paper, developed Individually Directional Evolutionary Algorithm (IDEA) [8] for fuzzy cognitive maps learning is described, together with its comparative analysis with elite real-coded genetic algorithms. Simulation analysis of the learning algorithms were based on real-life case of strategic planning process of an e-business company [20]. Section 2 briefly describes fuzzy cognitive maps. The developed algorithm IDEA is presented in section 3. Section 4 presents selected results of comparative analysis of the chosen methods. The summary of the article is contained in section 5.

## 2. Fuzzy cognitive maps

The structure of FCM is based on a directed graph:

$$< X , R > \tag{1}$$

where: $X=[X_1,\ldots,X_n]^T$ – set of the concepts, $X_i(t)$ – the value of the $i$-th concept in $t$-th step (discrete time), $i = 1, \ldots, n$; $j=1,\ldots, n$, $n$ – the number of concepts; $R=\{r_{j,i}\}$ – relations matrix, $r_{j,i}$ – the relation weight between the $j$-th and the $i$-th concept.

A dynamic model described by the equation (2) was used:

$$X_i(t+1) = F\left( X_i(t) + \sum_{\substack{j=1 \\ j\neq i}}^{n} r_{j,i} \cdot X_j(t) \right) \tag{2}$$

where: $t$ – discrete time, $t=0,1,....,T$, $T$ – end time of simulation; $F(x)$ – sigmoid stabilizing function, described as follows:

$$F(x) = \frac{1}{1+e^{-cx}} \tag{3}$$

where: $c$ – parameter, $c>0$.

FCM can be learned with the use of evolutionary algorithms. Individually Directional Evolutionary Algorithm for fuzzy cognitive maps learning is described below.

## 3. Individually Directional Evolutionary Algorithm

Individually Directional Evolutionary Algorithm (IDEA) is a newly developed algorithm for global optimization [8]. Main principle of IDEA is to monitor and direct the evolution of selected individuals of population to explore promising areas in the search space. The algorithm uses a proportional selection method ( Roulette-Wheel Selection [1]) with dynamic linear scaling of fitness function [4] and Non-Uniform Mutation [9] uses information about the direction of change also known as Direction Vector. Applied selection method and mutation operator in IDEA allows to choose the fittest individuals and their modification to explore promising areas in the search space. The idea of IDEA is an independent evolution of individuals in current population. An independent evolution process is focused on indicating correct direction of changes in the elements of solution vector.

IDEA uses characteristic elements of EAs such as Proportionate Selection (Roulette-Wheel Selection) with dynamic linear scaling of fitness function in pre-selection stage, Directional Non-Uniform Mutation (DNUM [8]) operator as genetic operator and elite scheme in post-selection stage. Figure 1 shows the scheme of IDEA.

```
procedure IDEA
begin
t:=0
initialization P^0
evaluation P^0
P^t:=P^0
while (not stop condition) do
begin
        T^t:=pre-selection P^t
        T'^t:= directional non-uniform mutation T^t
        evaluation T'^t
        P^(t+1):=post-selection (T'^t, T^t)
        t:=t+1
end
end
```

**Fig. 1.** IDEA scheme [8].

Evolution loop of IDEA is initialized in the same way as in other EAs and is made up of 4 steps. In the first step, temporary population **T** is created from current base population **P**. Individuals of population **T** will be subject to mutation. In the second step, another temporary population **T'** is created by mutations of individuals of temporary population **T**. Individuals of

temporary population **T'** are evaluated in third step of evolution loop. The last step of evolution loop is to select individuals from temporary population **T** and **T'**, that will create the next base population **P**.

## 4. Selected results of the analysis

The goal of the simulation analysis is to evaluate performance of IDEA and elite genetic algorithms in fuzzy cognitive maps learning problem on the basis of a real-life case of strategic planning process of an e-business company [20].

### 4.1. Problem definition

All simulations was made using developed software. The developed software is a collection of Java classes, that include useful tools for implementation (in Java language) and analysis evolutionary algorithms. New module was made for the purposes of this paper that allow to create FCM model by using evolutionary algorithms. The software is still developed.

### 4.2. Problem definition

The objective of learning is to find candidate FCM that behaves similarly to the referenced map for different initial state vectors [19].

Total error (4) is a sum of absolute value of difference between FCM response and expected value from learning or test data.

$$total\_error = \sum_{p=1}^{P}\sum_{t=1}^{T}\sum_{i=1}^{n} | Z_i^p(t) - X_i^p(t) | \tag{4}$$

where: $p=1,...,P$, $p$ – the number of the $p$-th initial state vector; $P$ – the number of different initial state vectors; $t=0,1,...,T-1$, $T$ – the number of the records, $Z(t) = [Z_1(t),\ldots,Z_n(t)]^T$ – the desired FCM response for the initial vector $Z(t-1)$; $X(t) = [X_1(t),\ldots,X_n(t)]^T$ – the FCM response for the initial vector $Z(t-1)$; $i = 1, \ldots, n$; $n$ – the number of concepts.

Mean error is described as follows (5):

$$mean\_error = \frac{1}{P(T-1)n} total\_error \tag{5}$$

Value of minimum error is the minimum absolute value of difference between FCM response and expected value for concept for all concepts and steps (6).

$$minimum\_error = \min_{\substack{t\in T,\\ i\in N,\\ p\in P}} \{ | Z_i(t) - X_i(t) | \} \tag{6}$$

Value of maximum error is the maximum absolute value of difference between FCM response and expected value for concept for all concepts and steps (7).

$$maximum\_error = \max_{\substack{t\in T,\\ i\in n,\\ p\in P}} \{ | Z_i(t) - X_i(t) | \} \tag{7}$$

The simulations were performed with the referenced FCM model reported in literature, which concerns business industry and financial activities [20]. This FCM model contains seven concepts described as the most important in the strategic planning process of an e-business company [20]: E-Business Profits ($X_1$), E-Business Sales ($X_2$), Prices Cutoffs ($X_3$), Customers Satisfaction ($X_4$), Staff Recruitments ($X_5$), Impact from International E-Business Competition ($X_6$) and Better E-Commerce Services ($X_7$).

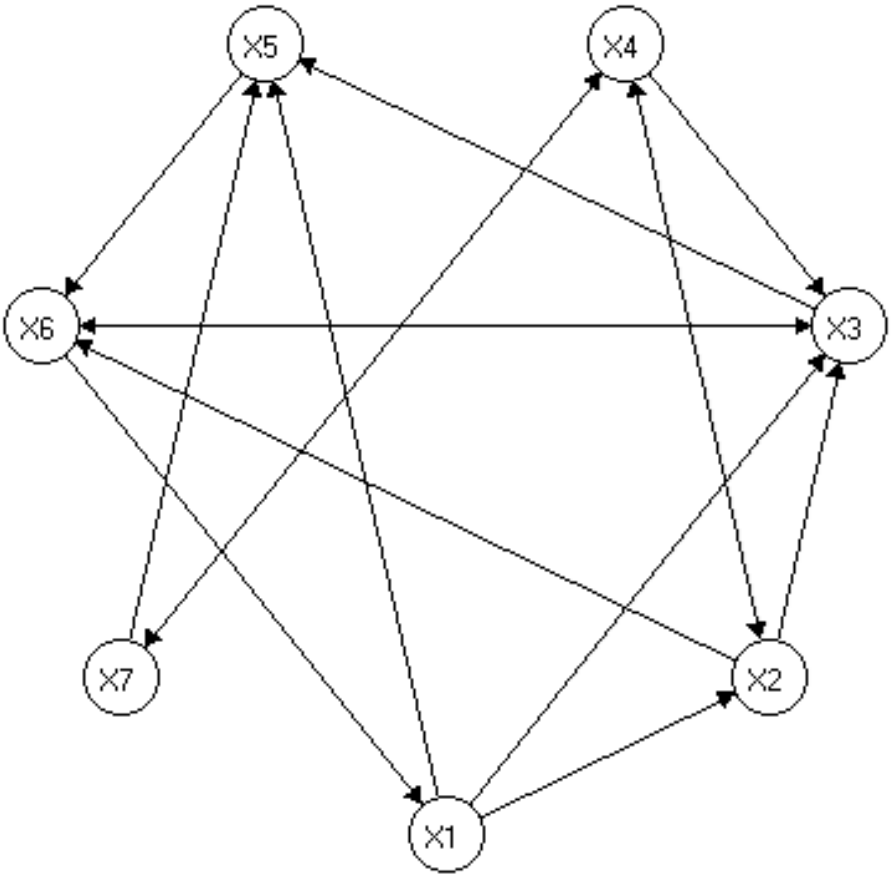


**Fig. 2.** Structure of the initialized map [20].

Graphic interpretation of the structure of the analyzed map is presented in Fig. 2. Nodes and edges of directed graph shows concepts of FCM model and relations between them. Description of nodes presents in fig. 2. refers to the description of the concepts of FCM model.

Learning data for the 10 randomly generated state vectors and testing data for the 10 different state vectors were generated on the basis of the referenced map. The following algorithms are compared: developed algorithm IDEA, elite Real-Coded Genetic Algorithm (RCGA) with the one elite individual and elite RCGA with the number of elite individuals equal to population size. All compared algorithms use the same parameters: number of individuals equal to 200 and number of generations equal to 1000 and the same selection method. Moreover, both of elite RCGAs use Single-Point Crossover and Non-Uniform Mutation operators.

### 4.3. Comparison of IDEA with elite real-coded genetic algorithms

The performance of the proposed learning method for FCMs based on IDEA was evaluated based on *mean_error*, obtained for the same data generated with the use of the reference FCM model for the strategic planning process of an e-business company. The obtained values of *mean_error* achieved by IDEA were compared with the values of mean error obtained by two other EAs: elite RCGA with the one elite individual and elite RCGA with the number of elite individuals equal to population size.

Tables 1-3 present the error value for achieved results of FCM learning by compared algorithms. These tables show errors value based on obtained the best, the worst and average result as the effect of multiple launches of compared algorithms.

Based on simulation results (Tab. 1-3) it can be observed that the IDEA gives better results in comparison with other EAs. Error values for the best, worst and average result of FCM learning is better than in case of compared algorithms. The average value of errors were calculated as average from obtained errors based on the all achieved results. The obtained criterion *mean_error* is

relatively low. It shows that the learned FCM behaves similarly to the referenced model for different input states.

| Algorithm | Elite RCGA (1) | | Elite RCGA (Population Size) | | **IDEA** | |
|---|---|---|---|---|---|---|
| Data set/ Error value | Learning data | Test data | Learning data | Test data | Learning data | Test data |
| Total error | 6.643378 | 6.495902 | 6.579157 | 6.696447 | **5.633745** | **5.996711** |
| Mean error | 0.0047453 | 0.004640 | 0.004699 | 0.004783 | **0.0040241** | **0.004283** |
| Minimum error | 0 | 0 | 0 | 0 | **0** | **0** |
| Maximum error | 0.246045 | 0.322815 | 0.216229 | 0.187713 | **0.194909** | **0.02578** |

**Tab. 1.** Errors values for the best results achieved.

| Algorithm | Elite RCGA (1) | | Elite RCGA (Population Size) | | **IDEA** | |
|---|---|---|---|---|---|---|
| Data set/ Error value | Learning data | Test data | Learning data | Test data | Learning data | Test data |
| Total error | 9.148835 | 8.013510 | 8.908233 | 9.170017 | **8.214785** | **8.187957** |
| Mean error | 0.006535 | 0.005724 | 0.006363 | 0.006550 | **0.005868** | **0.005849** |
| Minimum error | 0 | 0 | 0 | 0 | **0** | **0** |
| Maximum error | 0.430239 | 0.370065 | 0.271812 | 0.231051 | **0.2342410** | **0.333533** |

**Tab. 2.** Errors values for the worst results achieved.

| Algorithm | Elite RCGA (1) | Elite RCGA (Population Size) | **IDEA** |
|---|---|---|---|
| Data set/ Error value | Learning data | Learning data | Learning data |
| Total error | 7.937274 | 7.638351 | **6.988159** |
| Mean error | 0.039686 | 0.038192 | **0.034941** |

**Tab. 3.** Errors values for the average results achieved.

## 5. Conclusion

This article presents new and promising approach for FCMs learning based on IDEA. Fuzzy cognitive maps and developed Individually Directional Evolutionary Algorithm are described. Selected results of comparative analysis of the IDEA with elite real-coded genetic algorithms are presented. Obtained results showed that IDEA improves the obtained accuracy expressed by mean error and total error with respect to compared EAs.

## References

[1] ARABAS J.: Lectures on evolutionary algorithms, WNT, Warsaw, 2001 (in Polish).

[2] FROELICH W., JUSZCZUK P.: Predictive Capabilities of Adaptive and Evolutionary Fuzzy Cognitive Maps - A Comparative Study. In: NGUYEN N. T., SZCZERBICKI E. (eds.): Intel. Sys. for Know. Management, SCI 252, pp. 153–174, Springer-Verlag, Heidelberg, 2009.

[3] FROELICH W., PAPAGEORGIOU E.: Extended Evolutionary Learning of Fuzzy Cognitive Maps for the Prediction of Multivariate Time-Series. In. PAPAGEORGIOU E. I.: Fuzzy Cognitive maps for Applied Sciences and Engineering -- From fundamentals to extensions and learning algorithms. Intelligent Systems Reference Library, vol. 54, pp. 121–131, Springer, 2014.

[4] GOLDBERG D. E.: Genetic Algorithms in Search, Optimization, and Machine Learning, WNT, Warsaw, 1995 (in Polish).

[5] JASTRIEBOW A., POCZĘTA K.: Analysis of multi-step algorithms for cognitive maps learning. BULLETIN of the POLISH ACADEMY of SCIENCES TECHNICAL SCIENCES. Vol. 62, Issue 4, 2014, pp. 735-741.

[6] KANNAPPAN A., PAPAGEORGIOU E.: A new classification scheme using artificial immune systems learning for fuzzy cognitive mapping. Fuzzy Systems (FUZZ), 2013 IEEE International Conference on, pp. 1–8, 2013.

[7] KOSKO B.: Fuzzy cognitive maps. Int. J. Man-Machine Studies, vol. 24, pp. 65–75, 1986.

[8] KUBUŚ Ł.: Individually Directional Evolutionary Algorithm – simulation analysis. In: JASTREIBOW A., WORWA K. (eds.) Applications of Information Technologies - theory and practice. Institute for Sustainable Technologies - National Research Institute, Radom, pp. in press, 2015 (in Polish).

[9] MICHALEWICZ Z.: Genetic Algorithms + Data Structures = Evolution Programs, WNT, Warsaw, 1999 (in Polish).

[10] PAPAGEORGIOU E. I.: Learning Algorithms for Fuzzy Cognitive Maps - A Review Study. IEEE Transactions on Systems, Man, and Cybernetics – Part C: Applications and Reviews, vol. 42, no. 2, pp. 150–163, 2012.

[11] PAPAGEORGIOU E. I., PARSOPOULOS K. E., STYLIOS C. S., GROUMPOS P. P., VRAHTIS M. N.: Fuzzy Cognitive Maps Learning Using Particle Swarm Optimization. Journal of Intelligent Information Systems, 25:1, pp. 95-121, 2005.

[12] PAPAGEORGIOU E. I., STYLIOS C. D.: Fuzzy Cognitive Maps. In: PEDRYCZ W., SKOWRON A., KREINOVICH V. (eds.): Handbook of Granular Computing. John Wiley & Son Ltd., Publication Atrium, England, pp. 755–774, 2008.

[13] POCZĘTA K., KUBUŚ Ł.: Supervised and population based learning algorithms for fuzzy cognitive maps – a comparative study. In: JASTREIBOW A., WORWA K. (eds.) Modern information technologies and their application in theory and practice. Institute for Sustainable Technologies - National Research Institute, Radom, pp. 96-107, 2014.

[14] SALMERON J. L.: Augmented fuzzy cognitive maps for modelling LMS critical success factors. Knowledge-Based Systems, 22(4), pp. 275–278, 2009

[15] SALMERON J. L.: Modelling grey uncertainty with Fuzzy Cognitive Maps. Expert Systems with Applications 37, 2010, pp. 7581–7588.

[16] SŁOŃ G.: Application of Models of Relational Fuzzy Cognitive Maps for Prediction of Work of Complex Systems. In: Rutkowski L., Korytkowski M., Scherer R., Tadeusiewicz R., Zadeh L. A., Zurada J. M. (eds.), Artificial Intelligence and Soft Computing - Lecture Notes in Artificial Intelligence LNAI 8467, 13th International Conference ICAISC 2014, Zakopane 2014; 2014, pp. 307–318.

[17] SŁOŃ G., JASTRIEBOW A.: Optimization and Adaptation of Dynamic Models of Fuzzy Relational Cognitive Maps. In: KUZNETSOV S.O. Et al. (eds.) RSFDGrC 2011, Lecture Notes in Artificial Intelligence 6743, pp. 95-102, Springer-Verlag, Heidelberg, 2011.

[18] STACH W., KURGAN L., PEDRYCZ W.: Data-Driven Nonlinear Hebbian Learning Method for Fuzzy Cognitive Maps. IEEE Int. Conf. on Fuzzy Systems (FUZZ-IEEE), pp. 1975–1981, 2008.

[19] STACH W., KURGAN L., PEDRYCZ W., REFORMAT M.: Genetic learning of fuzzy cognitive maps, Fuzzy Sets and Systems 153 (3), pp. 371–401, 2005.

[20] TSADIRAS A.K.: Using fuzzy cognitive maps for e-commerce strategic planning. In: 9th Panhellenic Conference on Informatics. Thessaloniki, Greece, pp. 142–151, 2003.

**TRANSCOM 2015, 22-24 June 2015**
University of Žilina, Žilina, Slovak Republic

# The Use of Questionnaire to Evaluate the Usability of University Website

[*]Terézia Kvasnicová, [*]Iveta Kremeňová,
[*]University of Žilina, Faculty of Operation and Economics of Transport and Communications, Department of Communications, Univerzitná 1, 01026 Žilina, Slovakia, {terezia.kvasnicova, iveta.kremenova}@fpedas.uniza.sk

**Abstract.** This study evaluates the usability of University of Žilina websites. We use questionnaire to evaluate the usability of website. Respondents are students and teachers from different faculties and in different age. Results indicate that the site is not easy to use. There are many accurate opinions, what should be changed and improved to raise higher quality and usability.

**Keywords:** Usability, website, questionnaire.

## 1. Introduction

The internet is becoming a more central part of our everyday lives. We brows web pages and search information. We expect that the pages are logically arranged, and we easy find what we are looking for. Organization, which I can´t find on the Internet, as if it did not exist. This is the reason why all institutions, also schools and universities have own website. Anyone who knew them to create did it. Almost nobody knew the rules of design and usability. The strategy was to give large amounts of information and added new. Many websites are today information overload and confusing. Thanks to the theory of usability we can eliminate these mistakes.

## 2. Website Usability

Nielsen (1993) first defined usability as a quality attribute - something that is easy to use. Later Nielsen (2012) said, that usability is how easy and pleasant is something to use. We can define Website usability as an ease with which visitors are able to use a website (LLC, 2015).

On the Web, usability is a necessary condition for survival. If a website is difficult to use, people leave. If the homepage fails to clearly state what a company offers and what users can do on the site, people leave. If users get lost on a website, they leave. If a website's information is hard to read or doesn't answer users' key questions, they leave. Note a pattern here? There's no such thing as a user reading a website manual or otherwise spending much time trying to figure out an interface. There are plenty of other websites available; leaving is the first line of defence when users encounter a difficulty (Nielsen, 2012).

Similar to businesses, schools and universities have their own websites. They also need to attract “new customers” – new students and maintain “permanent customer” – students, teachers etc. Young people spent a lot of time online, so schools have to communicate online. Universities and schools have the websites, but their use is low. Here it is important to know how to communicate, what kind of information they want and need and choose the right design – company design, but also usable.

We can improve design and raise the number of visitors if we tested the old design and its usability. It means identify the good parts that we should keep and the bad parts that give users trouble (Nielsen 2012), or that they don’t use. It is also important to add new parts that they miss.

There are many methods for studying usability (user testing, eye tracking, ect.). We use questionnaire to evaluate the usability of website in this study.

## 3. Methodology

We analyzed the website www.uniza.sk, official website of University of Žilina. Web page of University of Žilina is a website that informs about events at the University; contains links to other external sites and the faculties (blue arrow). The site is organized in four navigations (Fig. 1): Menu 1 – main menu (violet arrow), Menu 2 – submenu (violet arrow left), Menu 3 – links to the websites of the faculties of the University, Menu 4 – links to Moodle, Library, Intranet, and Directory (white arrow). The middle part of the screen (red arrow) is shown the text section.

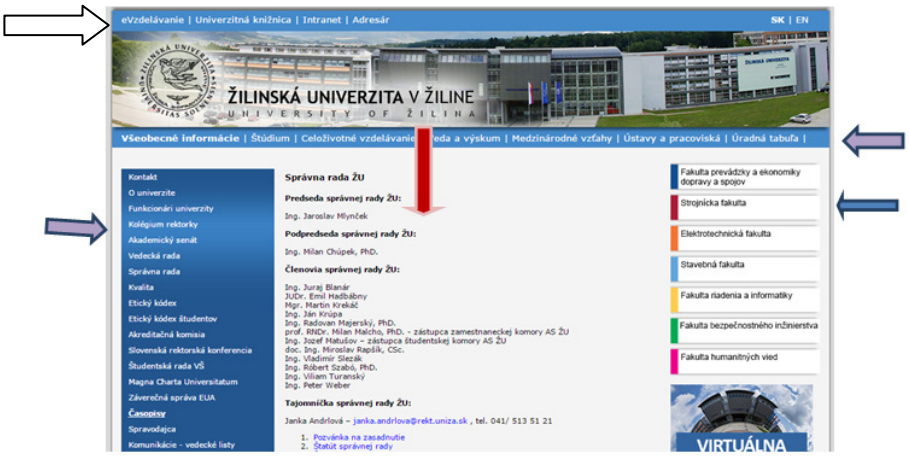


Fig. 1 Homepage www.uniza.sk

We used questionnaire to evaluate the usability of website in this study. We asked students and teachers from different faculties and in different age to answer our questions on March/April 2015 in the premises of the university canteen "Nová menza". Overall 65 respondents answered questions electronically via tablet.

The questionnaire had seven questions about preferences and the use of website, and four questions were identification, there were some closed ended question with one possible choice – some with multiple choices. There were also three open ended questions. Table 1 shows overview of questions.

| Questions | Types of Q. | Fixed set of responses | | | | |
|---|---|---|---|---|---|---|
| How often do you visit www.uniza.sk | Closed ended | Daily | Several times a week | Weekly | Monthly | I do not visit |
| Do you use "Important links " | Closed ended | YES | NO | | | |
| Do you use "Event calendar" | Closed ended | YES | NO | | | |
| I like on www.uniza.sk | Open ended | | | | | |
| I dislike on www.uniza.sk | Open ended | | | | | |
| I miss on www.uniza.sk | Open ended | | | | | |
| I search information about | Closed ended | 9 different areas of interest | | | | |
| I am | Closed ended | Man | Woman | | | |
| I am | Closed ended | Student | Teacher/PhD. student | | | |
| I have age | Closed ended | Less 25 | 25-35 | 35-55 | 55+ | |
| I am student/teacher on | Closed ended | All 7 faculties | | | | |

Tab. 1 Overview of questions

We tried to find out how often (if any) respondents use university website, what kind of information they are looking for, if they use the main areas (such as Important links, calendar etc.), what they like or dislike on the site.

## 4. Results

Overall 65 respondents answered questions electronically via tablet, 37 men, and 28 women. 43 respondents were students, 22 teachers or PhD. students. Most respondents are less than 25 years old (44 respondents), 20 respondents are 25 – 35 years old and only one more than 35.

21 respondents were from Faculty of Operation and Economics of Transport and Communications, 19 from Faculty of Electrical Engineering, 14 from Faculty of Mechanical Engineering, 7 from Faculty of Management Science and Informatics and 4 from Faculty of Civil Engineering.

In the first question we asked: How often do you visit www.uniza.sk? It was a closed ended question with five answers: Daily, Several times a week, Weekly, Monthly, I do not visit. 29 % respondents answered monthly, 28 % several times a week, 26 % weekly, 14 % daily, and 3 % they don´t visit it (Fig. 2). Respondents visit website very often, but it is very important to say, that almost all of them use it only to redirection to another pages.

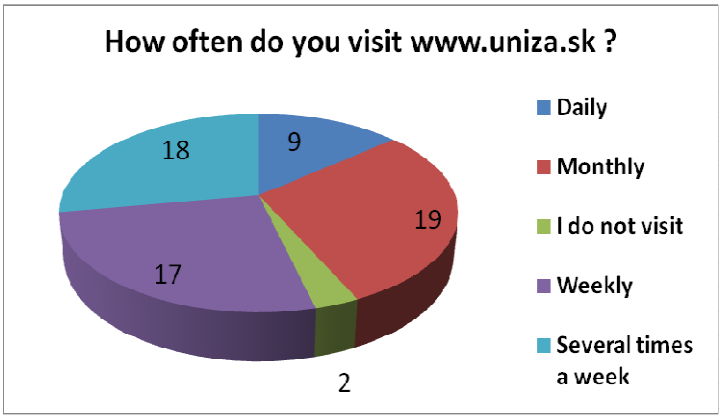


Fig. 2 Graf showing the answers to question How often do you visit www.uniza.sk.

Then we asked: Do you use “Important links”? The Figure 3 shows the answers. 61 % respondents said Yes, I use important links, 39 % don’t use it.

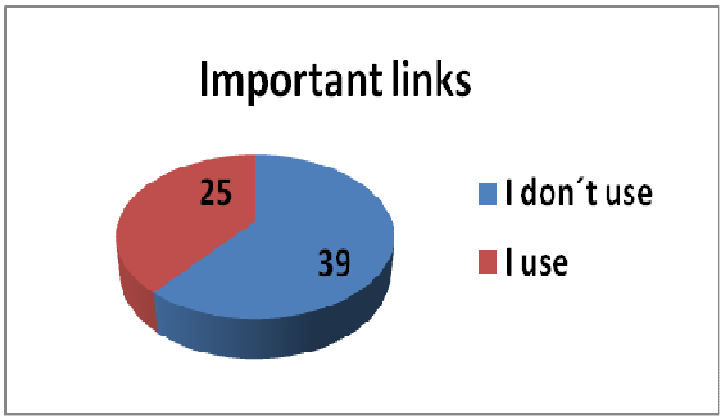


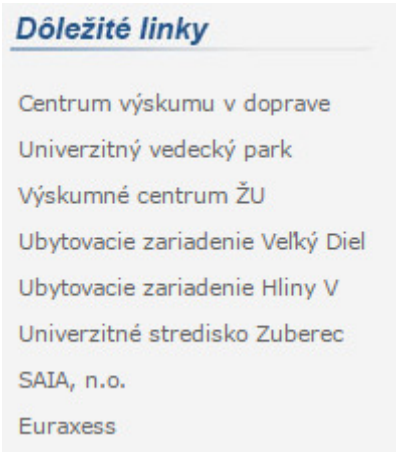


Fig. 3 Graf showing the answers to question Do you use Important links?

This area of interest – Important links is located on the right side of the page break, when viewed on a standard 15,6“ laptop. This fact is confirmed by several respondents who indicated that this part is outside the „sight view“. It should be noted that many of these links are high specific and content-oriented differently.

Next question was: Do you use “Event calendar”? The Figure 4 shows the answers. Event calendar use only 16 % of respondents. We can find a conference by date – only by months. We can´t search by topic or department and there are only conferences, not all events on University. Usability of this part is limited.

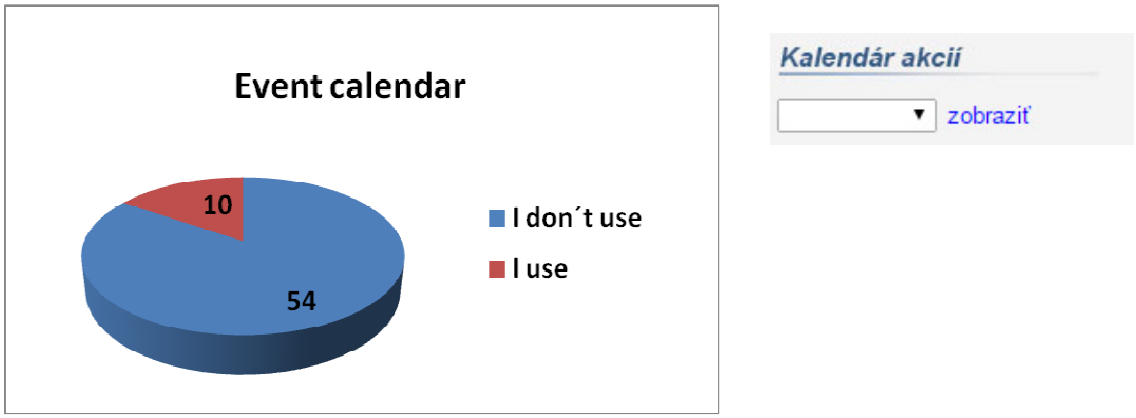


Fig. 4 Graf showing the answers to question Do you use Event calendar?

Last closed ended question was with multiple choices: Do you search information about...? More than 51 % of respondents use Links to the faculties, 50 % read News, and 50 % use website to redirection to the e-learning. Nearly 19 % use them to redirection to the Library and less than 17 % use the Directory. None of the respondents use the website to read the journals. About 5 % of respondents visit www.uniza.sk to find information about student organizations and entry to the Intranet.

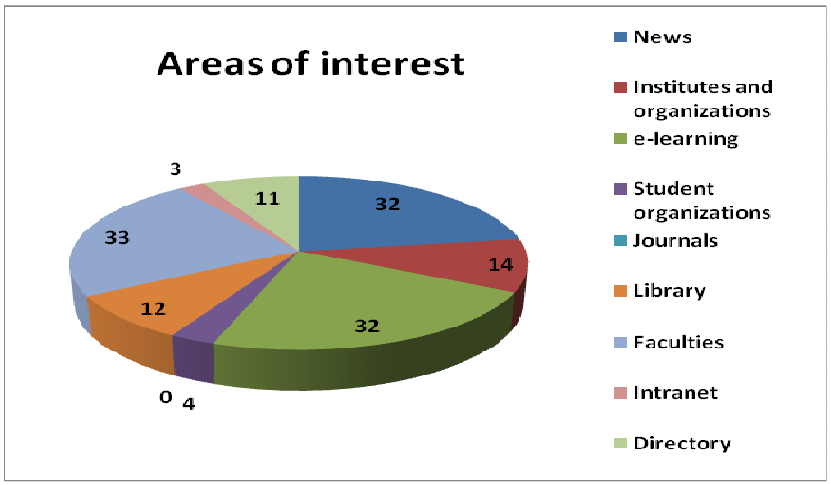


Fig. 5 Areas of interest

We also gave the opportunity to tell what our respondents like, dislike and what they miss on the website. The middle part of homepage is shown the News. Some respondents said, that they like news, some dislike, because the information is unnecessary, timeliness and they are lost in the amount of information. We miss there categorization according to the focus of news – topics of news. There is no graphical element, no picture that could be thematically attractive. The articles

are not updated in this part. There are no headlines, so the reader does not know what the article is about, until he read it.

| Open ended questions – What … ? | Answers |
|---|---|
| I like on www.uniza.sk | - Directory – contact to the teachers<br>- News<br>- Design<br>- Colours<br>- Clarity<br>- Link to the faculties<br>- Virtual tour |
| I dislike on www.uniza.sk | - Directory<br>- Design<br>- Important links - the view is out of sight<br>- The amount of information<br>- Timeliness of data<br>- Obscurity<br>- Slow updating<br>- Different design of faculties´ websites<br>- Unnecessary information |
| I miss on www.uniza.sk | - Students blog<br>- Eye catching effect<br>- Photos<br>- Jobs offer<br>- Calendar<br>- Link to the e-learning<br>- Chat<br>- Feedback questionnaire<br>- Visual simplicity<br>- Search window<br>- Links to facebook / students websites…<br>- Directory – with search function (database) |

Tab. 2 Open ended questions and answers

Respondents positively assessed the possibility of using a virtual tour. Also a very common activity is the source links for each department. Among the negative respondents indicated that each department has its own “independent design”.

Respondents missed there a chat or blog, where they can communicate and ask if they have questions. Links to social network (facebook, etc.) and students´ organization websites are also missing.

## 5. Conclusion

University of Žilina has about 10 200 students and about 1 500 employees (teachers, PhD. Students etc.). University websites are intended for students and employees, students interested in studying, partner schools, public authorities and the general public. Website could be the most important communication and information channel, and marketing tool in the near future. But it is necessary to ensure, that the website is usable and has all expected information.

We identify many usability problems, which can help the realization team to propose the new university website.

## Grant support

The paper is published as a part of the project VEGA 1/0748/14 Research methods of financing the project intents organization in a competitive environment and as a part of the research project

VEGA 1/0895/13 Research on strategic business management as promoting competitiveness in a dynamic business environment.

## References

[1] LLC. *The Digital Marketing Reference*. http://www.marketingterms.com/dictionary/web_site_usability/ 2015

[2] NIELSEN, J., LANDAUER, T. K. *A Mathematical Model of the Finding of Usability Problems.* Proceedings ACM/IFIP INTERCHI'93 Conference (Amsterdam, The Netherlands, April 24-29), 206-213. 1993

[3] NIELSEN, J. *Usability 101: Introduction to Usability*. http://www.nngroup.com/articles/usability-101-introduction-to-usability/ 2012.

**TRANSCOM 2015, 22-24 June 2015**
University of Žilina, Žilina, Slovak Republic

# Performance Evaluation of Algorithm for Identification of Minimal Cut Vectors in Multi-State Systems

Miroslav Kvassay, Jozef Kostolny
University of Zilina, Faculty of Management Science and Informatics, Department of Informatics,
Univerzitna 8215/1, 010 26 Zilina, Slovakia, {Miroslav.Kvassay, Jozef.Kostolny}@fri.uniza.sk

**Abstract.** Reliability is an important characteristic of many systems. Some tools of reliability analysis are based on the method of Minimal Cut Vectors (MCVs). A MCV represents a situation in which a repair (improvement) of any non-perfectly working component results in a repair (improvement) of the whole system. MCVs (or their equivalent in the form of minimal cut sets) have been widely used in reliability analysis of binary-state systems. However, they are not so common in the case of multi-state systems. One of the reasons is that there exist only few algorithms that can be used for their identification. One of these algorithms is based on tools of logical differential calculus. However, no performance evaluation of this algorithm has been done. For solving this issue, we have performed some experiments which results are presented in this paper.

**Keywords:** Reliability, multi-state system, minimal cut set, minimal cut vector, logical differential calculus.

## 1. Introduction

Two basic types of models are used in reliability analysis: Binary-State Systems (BSSs) and Multi-State Systems (MSSs). BSSs define only two states in system behavior that are recognized as functioning (represented by number 1) and failed (represented by number 0). These models are suitable for analyzing consequences of system failure. MSSs allow defining more than two states in system performance, i.e. from perfectly functioning (state $m$ -1) to completely failed (state 0) and, therefore, they are appropriate for analysis of processes that results in system failure.

Every system consists of one or more components that can be either binary-state (in the case of BSSs) or multi-state (for MSSs). When all components of a MSS have the same number of states as the system, then the MSS is identified as a homogeneous system [1]. Please note that BSSs can also be seen as homogeneous systems. In what follows, only homogeneous systems will be considered.

The dependency between states of individual system components and system state is defined by the structure function that has the following form for a homogeneous system [1]-[3]:

$$\phi(\boldsymbol{x}) = \phi(x_1, x_2, \ldots, x_n) : \{0,1,\ldots,m-1\}^n \rightarrow \{0,1,\ldots,m-1\}, \qquad (1)$$

where $n$ is a number of system components, $m$ is a number of possible states of the system and its components, $x_i$ is a variable representing state of the $i$-th system component for $i = 1,2,\ldots,n$, and $\boldsymbol{x} = (x_1, x_2,\ldots, x_n)$ is a vector of components states (state vector). Clearly, if $m = 2$, then (1) agrees with the structure function of a BSS.

The structure function is very useful in qualitative analysis of systems because its investigation can reveal situations in which a failure of a binary-state component or degradation of a multi-state component results in a failure of the BSS or in a degradation of the MSS. However, it cannot be used to quantify system reliability. For this purpose, the following probabilities of individual states of system components should be known:

$$p_{i,s} = \Pr\{x_i = s\}, \ \sum_{s=0}^{m-1} p_i = 1, \ \ i = 1,2,\ldots,n, \ \ s = 0,1,\ldots,m-1. \qquad (2)$$

Knowledge of these probabilities and the system structure function allows us to compute some of the basic characteristics of the system that are known as system availability and unavailability and that are defined with regard to system state *j* as follows [1], [2]:

$$A^{\geq j} = \sum_{h=j}^{m-1} \Pr\{\phi(\boldsymbol{x}) = h\},\ U^{\geq j} = \sum_{h=0}^{j-1} \Pr\{\phi(\boldsymbol{x}) = h\},\ A^{\geq j} + U^{\geq j} = 1, \quad j = 1,2,\ldots,m-1. \tag{3}$$

System availability (unavailability) computed for state *j* of the system defines a proportion of time during which the component is at least in state *j* (below state *j*). Furthermore, it can also be used in other reliability calculations that focus on identification of the most important system components, i.e. the components that have the most influence on the system proper work. One of the measures that are used for this purpose is the Fussell-Vesely's importance (FVI) that is defined as the probability that the component contributes to system unavailability [4], [5]. The computation of this measure is based not only on system unavailability but also on minimal cut sets of the considered system.

### 1.1. Minimal Cut Sets and Minimal Cut Vectors

Minimal Cut Sets (MCSs) are one of the key concepts used in reliability analysis of BSSs. They represent a minimal set of components whose simultaneous failure results in system failure [5], [6]. In terms of the structure function, they correspond to Minimal Cut Vectors (MCVs) [5].

A MCV of a BSS is defined as a state vector $\boldsymbol{x}$ such that $\phi(\boldsymbol{x}) = 0$ and $\phi(\boldsymbol{y}) = 1$ for any $\boldsymbol{y} > \boldsymbol{x}$ [1], [5]. Please note that the notation $\boldsymbol{y} > \boldsymbol{x}$ where $\boldsymbol{x} = (x_1, x_2,\ldots, x_n)$ and $\boldsymbol{y} = (y_1, y_2,\ldots, y_n)$ are two state vectors means that $y_i \geq x_i$ for $i = 1,2,\ldots, n$ and there exists at least one $i$ such that $y_i > x_i$. It can be simply shown that a MCV represents such situation in which a repair of any failed component causes that the failed system will be repaired [7].

MCSs (MCVs) have an essential role in calculation of the FVI for BSSs because they agree with situations in which system components contribute to system failure [4], [5]. This implies that the MCSs or MCVs of the system have to be known before the FVI of individual system components can be computed.

The concept of MCSs can also be applied to MSSs [2]. However, MCSs are not so often used in the analysis of MSSs since their meaning is not as intuitive as in the case of BSSs. On the other hand, MCVs can also be extended on MSSs, and this extension is more straightforward than in the case of MCSs. So, a MCV for state *j* (for $j = 1,2,\ldots,m-1$) of a MSS is defined as a state vector $\boldsymbol{x}$ such that $\phi(\boldsymbol{x}) < j$ and $\phi(\boldsymbol{y}) \geq j$ for any $\boldsymbol{y} > \boldsymbol{x}$ [1], [2]. It is easy to show that a MCV for system state *j* represents a situation in which a minor improvement (i.e. improvement by one state) of any non-perfectly working component (i.e. components that are not in state $m-1$) causes that the system achieves at least state *j* [7]. Using this definition and the relationship between MCSs and MCVs, the following definition of the FVI for MSSs has been proposed in work [8]:

$$\mathrm{FVI}_{i,s}^{\geq j} = \frac{\Pr\{\boldsymbol{x} \leq \mathrm{MCV}_{i,s-1}^{\geq j}\}}{\Pr\{\phi(\boldsymbol{x}) < j\}} = \frac{\Pr\{\boldsymbol{x} \leq \mathrm{MCV}_{i,s-1}^{\geq j}\}}{U^{\geq j}}, \tag{4}$$

where $\mathrm{FVI}_{i,s}^{\geq j}$ denotes the FVI of state *s* of component *i* with respect to system state *j*, and event $\{\boldsymbol{x} \leq \mathrm{MCV}_{i,s-1}^{\geq j}\}$ means that there is at least one MCV for system state *j* that contains component *i* in state $s-1$ and that is greater than an arbitrary state vector $\boldsymbol{x}$. Please note that this measure quantifies the contribution of degradation of state *s* of component *i* to unavailability computed for state *j* of the considered MSS.

Definition (4) implies that if we want to compute the FVI for all system components, then the MCVs for system state *j* have to be known. For this purpose, the algorithm considered in papers [7], [8] can be used.

## 2. Algorithm for Identification of Minimal Cut Vectors based on Logical Differential Calculus

Computation of MCVs for a state of a MSS has been considered in several papers [9]-[11]. These papers are primarily focused on identification of MCVs in network systems modeled as MSSs, and they are based on the assumption that all source-sink cuts (in the sense of graph theory) of the network are known. This implies that they cannot be applied to other types of systems. Because of that, authors of paper [7] have proposed another algorithm that can be used for a MSS of any type. This algorithm is based on computation of special type of Direct Partial Logic Derivatives (DPLDs) that will be referred to as Integrated Direct Partial Derivatives (IDPLDs) in the rest of this paper.

The structure function of a homogeneous MSS corresponds to formal definition of a Multiple-Valued Logic (MVL) function. This allows using some tools of MVL in reliability analysis of MSSs. One of these tools is logical differential calculus, which has been developed for analysis of dynamic properties of MVL functions [12]. DPLDs are part of logical differential calculus. They allow finding situations in which a change of MVL variable results in a change of the considered MVL function. In terms of reliability analysis, they can be used to find situations in which component degradation (improvement) results in degradation (improvement) of a given system state [3]. This derivation is defined as follows:

$$\frac{\partial \phi(j \to h)}{\partial x_i(s \to r)} = \begin{cases} 1 & \text{if } \phi(s_i, \boldsymbol{x}) = j \text{ and } \phi(r_i, \boldsymbol{x}) = h \\ 0 & \text{other} \end{cases}, \quad j,h,s,r \in \{1,2,\ldots,m-1\},\ j \neq h,\ s \neq r\,. \tag{5}$$

DPLDs carry quite little information for identification of all MCVs for system state *j* and, therefore, the next generalization of these derivatives has been proposed in paper [7]:

$$\frac{\partial \phi(h_{<j} \to h_{\geq j})}{\partial x_i(s \to r)} = \bigcup_{w=0}^{j-1} \bigcup_{v=j}^{m-1} \frac{\partial \phi(w \to v)}{\partial x_i(s \to r)} = \begin{cases} 1 & \text{if } \phi(s_i, \boldsymbol{x}) < j \text{ and } \phi(r_i, \boldsymbol{x}) \geq j \\ 0 & \text{other} \end{cases}, \quad j,s,r \in \{1,2,\ldots,m-1\},\ s \neq r\,. \tag{6}$$

This generalization is referred to as IDPLD, and it is clear that it can be used to recognize situations in which change of the *i*-th system component from state *s* to *r* causes that the system achieves at least state *j*. Please note that this partially coincides with the meaning of a MCV for system state *j*. This fact has been used in paper [7] to propose the next algorithm for computation of all MCVs for system state *j*:

1. Repeat the next two steps for all system components:
   1.1. Compute expanded IDPLDs $\partial_e \phi(h_{<j} \to h_{\geq j}) / \partial_e x_i(s \to s+1)$ for $s = 0,1,\ldots,m-2$.
   1.2. Calculate Π-conjunction $\Pi_{s=0}^{m-2} \partial_e \phi(h_{<j} \to h_{\geq j}) / \partial_e x_i(s \to s+1)$ of expanded IDPLDs computed in the previous step.
2. Calculate Π-conjunction of the Π-conjunctions computed in step 1 and identify state vectors for which it has value 1. These state vectors correspond to MCVs for level *j* of system availability.

If we repeat this algorithm for all possible system states, then all MCVs of the MSS can be found.

Please note that the aforementioned algorithm uses some special type of IDPLDs that are named as the expanded IDPLDs. This version of IDPLDs is defined as follows [7]:

$$\frac{\partial_e \phi(h_{<j} \to h_{\geq j})}{\partial_e x_i(s \to r)} = \begin{cases} 1 & \text{if } x_i = s \text{ and } \phi(s_i, \boldsymbol{x}) < j \text{ and } \phi(r_i, \boldsymbol{x}) \geq j \\ 0 & \text{if } x_i = s \text{ and } \big(\phi(s_i, \boldsymbol{x}) \geq j \text{ or } \phi(r_i, \boldsymbol{x}) < j\big), \\ * & \text{if } x_i \neq s \end{cases} \quad (7)$$
$$j, s, r \in \{1,2,\ldots,m-1\},\ s \neq r.$$

The main motivation behind the introduction of the expanded IDPLDs is the fact that some operations that are needed for identification of MCVs have to be done simultaneously for IDPLDs (6) in which variable $x_i$ changes in different ways. However, this can be quite complicated since the IDPLD is defined only for situations in which the variable $x_i$ has value $s$. Therefore, the expanded IDPLDs, which are defined for all possible values of variable $x_i$, have been proposed in paper [7].

Another term that is used in the algorithm is a Π-conjunction. This operator has been defined in paper [7] based on the rules presented in Tab. 1. It can be shown that the Π-conjunction of two expanded IDPLDs identifies situations in which improvement of every non-perfectly working component results in system improvement. Therefore, if we compute this conjunction for all possible expanded IDPLDs, then we can find all MCVs for a given system state.

| | | $\frac{\partial_e \phi(h_{<j} \to h_{\geq j})}{\partial_e x_k(s_k \to r_k)}$ | | |
|---|---|---|---|---|
| | | * | 0 | 1 |
| $\frac{\partial_e \phi(h_{<j} \to h_{\geq j})}{\partial_e x_i(s_i \to r_i)}$ | * | * | 0 | 1 |
| | 0 | 0 | 0 | 0 |
| | 1 | 1 | 0 | 1 |

**Tab. 1.** Π-conjunction of two expanded IDPLDs

## 3. Experimental Investigation of Algorithm Performance

As we mentioned firstly, the performance evaluation of the aforementioned algorithm has not been done in papers [7], [8]. Therefore, we implemented it in C++ programing language and analyzed its complexity by performing some experiments. The experiments were done on a computer with CPU Intel Core i5 (2.5 GHz), 4 GB RAM and Windows 7 OS. We analyzed time complexity of this algorithm based on the number of system components and based on the number of all system MCVs. Firstly, we focused on the dependency between the computation time and the number of all system MCVs. For this purpose, we had to generate systems that differed in the number of MCVs but not in the components count. The typical example of such system is *k*-out-of-*n* MSS that is defined as follows [13]:

> if at least *k* components are in state *m* -1, then the system is in state *m* -1;
> else if at least *k* components are in state *m* -2 or better, then the system is in state *m* -2;
> …
> else if at least *k* components are in state 1 or better, then the system is in state 1;
> else the system is in state 0.

A *k*-out-of-*n* *m*-state system generated according to these rules contains totally $(m-1)\binom{n}{k-1}$ since $\binom{n}{k-1}$ MCVs exist for every relevant system state, i.e. for system states 1,2,…, *m* -1 [13]. This implies that systems with the constant number of components and different numbers of MCVs can be obtained by generating *k*-out-of-*n* systems for some concrete *n* and variable *k*. For example, we generated 3-state systems for *n* = 13 and *k* = 1,2,…,7. It follows that we got systems with 2, 26,…,

and 3,432 MCVs. Results of these experiments for 3- and 4-state systems are presented in Fig. 1 and Fig. 2. These graphs show that the algorithm complexity does not depend on the number of MCVs that exist in the system but depends exponentially on the number of system components. This result is more obvious in Fig. 3 that illustrates the dependency between the number of system components and the running time of the algorithm for systems with the similar numbers of MCVs. Furthermore, this figure also shows that the algorithm depends exponentially on the number of components states. This implies that the considered algorithm is not very suitable for systems consisting of lots of components or whose components have many states.

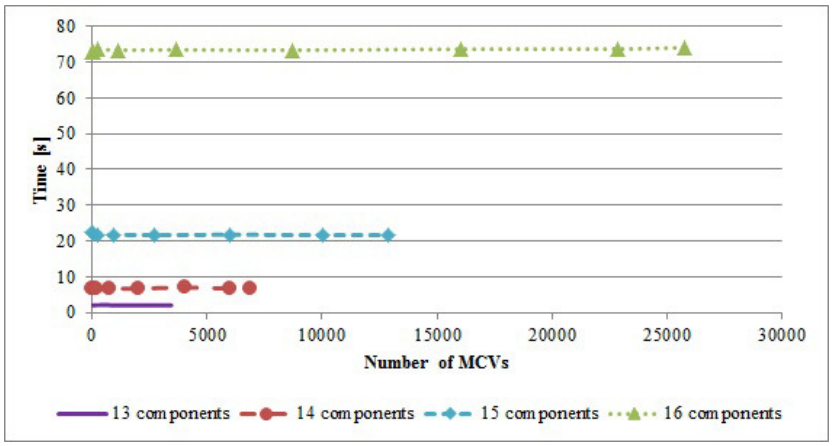


**Fig. 1.** Dependency between computation time and the number of MCVs for 3-state systems

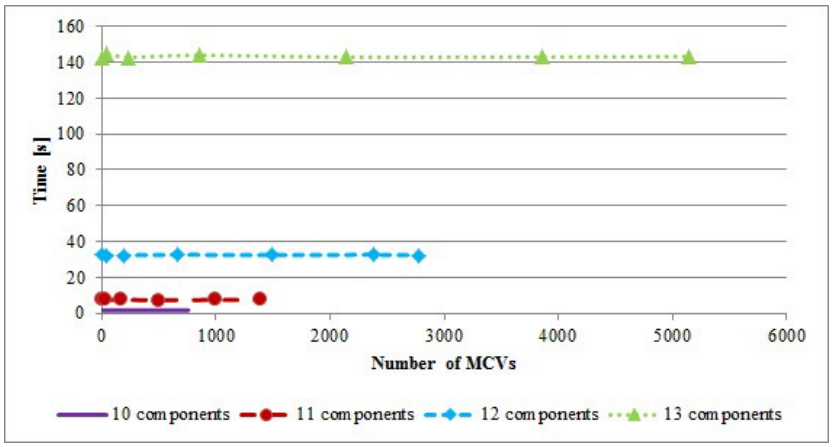


**Fig. 2.** Dependency between computation time and the number of MCVs for 4-state systems

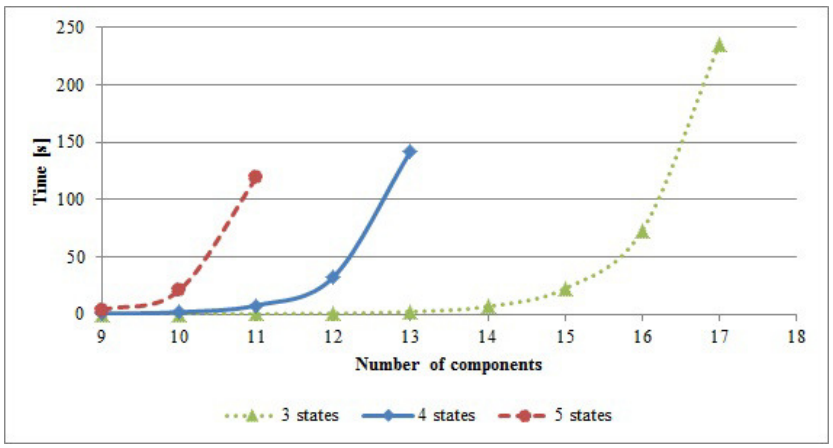


**Fig. 3.** Dependency of computation time on the number of system states for multi-state systems with the similar numbers of MCVs

## 4. Conclusion

MCSs are very useful in reliability analysis of BSSs because they can be used in both – qualitative and quantitative analysis of BSSs. From point of view of qualitative analysis, they identify minimal scenarios that cause system failure. In quantitative analysis, they are used to identify components that have the most contribution to system unavailability.

MCSs can also be expressed in the form of state vectors. These state vectors are known as MCVs. The main advantage of MCVs is that they can be very simply generalized for MSSs. This fact allows extending some measures used in reliability analysis of BSSs on MSSs. However, the main problem of using MCVs in reliability analysis of MSSs is the fact that there exist only several algorithms that can be used to find all MCVs of the system. Furthermore, most of them are based on some special assumptions and, therefore, they cannot be applied to all types of MSSs. For this purpose, the new algorithm based on logical differential calculus has been proposed in papers [7], [8]. However, the computational complexity of this algorithm has not been considered in the papers and, therefore, no information about running time of this algorithm has been known. Therefore, we performed some algorithms that focused on computation time depending on the number of system components and the number of all system MCVs. The results of the experiments showed that the running time did not depend on the number of system MCVs but depended exponentially on the number of system components and the number of components states. Because of that, the algorithm cannot be used for systems that contain a lot of components or whose components have a lot of possible states. So, the further research should be focused on finding some ways that will make this algorithm more efficient.

## References

[1] LISNIANSKI, A., FRENKEL, I., DING, Y. *Multi-state System Reliability Analysis and Optimization for Engineers and Industrial Managers*. London, UK: Springer-Verlag London Ltd., 2010.

[2] NATVIG, B. *Multistate Systems Reliability Theory with Applications*. Chichester, UK: John Wiley and Sons, Ltd, 2011.

[3] ZAITSEVA, E., LEVASHENKO, V. *Multiple-valued logic mathematical approaches for multi-state system reliability analysis. Journal of Applied Logic*, vol. 11, no. 3, pp. 350-362, 2013.

[4] FUSSELL, J. B. *How to hand-calculate system reliability and safety characteristics*. *IEEE Transactions on Reliability*, vol. R-24, no. 3, pp. 169-174, 1975.

[5] KUO W., ZHU X. *Importance Measures in Reliability, Risk, and Optimization*. Chichester, UK: John Wiley and Sons, Ltd, 2012.

[6] RAUSAND, M., HØYLAND, A. *System Reliability Theory*, Haboken, NJ: John Wiley and Sons, 2004.

[7] KVASSAY, M., ZAITSEVA, E., LEVASHENKO, V., KOSTOLNY, J. *Minimal cut vectors and logical differential calculus. IEEE 44th International Symposium on Multiple-Valued Logic (ISMVL) 2014*, pp. 167-172.

[8] KVASSAY, M., ZAITSEVA, E., LEVASHENKO, V. *Minimal cut sets and direct partial logic derivatives in reliability analysis. Safety and Reliability: Methodology and Applications - Proceedings of the European Safety and Reliability Conference, ESREL 2014*, pp. 241-248.

[9] YEH, W. *A simple approach to search for all d-MCs of a limited-flow network. Reliability Engineering and System Safety*, vol. 71, no. 1, pp. 15-19, 2001.

[10] YEH, W. *A new approach to the d-MC problem. Reliability Engineering and System Safety*, vol. 77, no. 2, pp. 201-206, 2002.

[11] YEH, W. *A fast algorithm for searching all multi-state minimal cuts. IEEE Transactions on Reliability*, vol. 57, no. 4, pp. 581-588, 2008.

[12] YANUSHKEVICH, S. N., MILLER, D. M., SHMERKO, V. P., STANKOVIC, R. S. *Decision Diagram Techniques for Micro- and Nanoelectronic Design Handbook*, vol. 2. Boca Raton, FL: CRC Press, 2005.

[13] BOEDIGHEIMER, R. A., KAPUR, K. C. *Customer-driven reliability models for multistate coherent systems. IEEE Transactions on Reliability*, vol. 43, no. 1, pp. 46-50, 1994.

**TRANSCOM 2015, 22-24 June 2015**
University of Žilina, Žilina, Slovak Republic

# Temporal Index Tablespacing

[*]Michal Kvet
[*]University of Transport, Faculty of Management Science and Informatics, Department of Informatics, Univerzitna 8215/1, 01026 Žilina, Slovakia, {Michal.Kvet}@fri.uniza.sk

**Abstract.** Temporal data processing is the fundamental requirement of intelligent signal and sensor data processing. Validity of the object is bordered and should be stored in the database with emphasis on changes. Intelligent temporal data processing requires sophisticated methods based on processing effectiveness and size of the whole structure. This paper deals with the attribute oriented temporal approach and definition of the various index structures located in the local or remote tablespaces.

**Keywords:** Temporal database, column level model, validity, index, tablespace.

## 1. Introduction

Database systems are one of the most important parts of the information technology. It is generally known that database system is usually the basic part - the root of any information system. The development of data processing has brought the need for modelling and accessing large structures based on the simplicity, reliability and speed of the system [1] [3] [4]. However, even today, when database technology is widespread, most databases process and represent the states of the data valid in this moment. Properties and states of the objects evolve over the time, become invalid and are replaced by new ones. Once the state is changed, the corresponding data are updated in the database and it still contains only the current valid data. However, temporal data processing is very important in dynamically evolving systems, industry, communication systems and also in systems processing sensitive data, which incorrect change would cause a great harm. It can also help us to optimize processes and make future decisions [2] [3] [4].

Current temporal systems are based on object level structure extending the paradigm of the conventional systems by the validity definition. Various number of data rows can define the same object. However, it requires definition new integrity constraints. The main disadvantage of the object level approach is the effectiveness based on duplicities and size of the whole structure. The main criterion is the attribute granularity and frequency of the changes.

This paper deals with the proposed and developed attribute oriented approach, which enables various sensor temporal data processing. The comparison characteristics are based on processing time. Size is also significant factor. Although large disc capacity is currently available, there is still need to effectively store and process data, because temporal data are really extensive and contain changes of the object states over the years [5] [6]. Developed types of index structures are compared based on their characteristics - local or remote tablespaces.

## 2. Extended attribute level temporal system

The solution described in the previous section manages the attributes of the objects, whereas the standard uni-temporal model works with the whole objects. Extended attribute (column) level temporal system can be considered as the improvement of the column level temporal system [6] [7] [8] in the term of the performance and the simplicity of the model management for the users. It is extended by the definition of the type of the operation. If the operation is *Update*, there is also the reference to the data type tables with historical values.

Existing applications are connected to the conventional layer with actual values, thus program can continue to operate without any changes. The main part is to manage the table containing information about the changes of temporal columns. Column, which changes need to be monitored, is temporal. If the value is changed, information about the executed *Update* is stored in the developed *temporal_table* and historical value is inserted into to the table containing historical values. Fig. 1 shows the complete structural model. Historical values are stored in the special section, each temporal data type has one table defined by the identifier (primary key) got using the sequence and trigger and the values themselves. Thus, the principle and system is similar to the column level temporal system, but historical values management and temporal table is different.

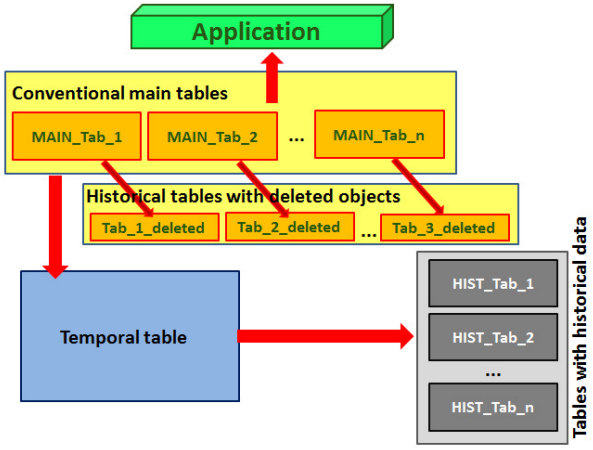


**Fig. 1.** Extended column level temporal system structure.

Management of the temporal table is completely different. It consists of these attributes (fig. 2) [7] [8]:

- *ID_change* – got using sequence and trigger – primary key of the table.
- *ID_previous_change* – references the last change of an object identified by *ID*. This attribute can also have *NULL* value that means, the data have not been updated yet, so the data were inserted for the first time in past and are still actual.
- *ID_tab* – references the table, record of which has been processed by DML statement *(Insert, Delete, Update, Restore* – renew validity of the object).
- *ID_orig* - carries the information about the identifier of the row that has been changed.
- *ID_column* – holds the information about the changed attribute (each temporal attribute has defined value for the referencing).
- *Data_type* – defines the data type of the changed attribute:
  - *C = char / varchar, N = numeric values (real, integer, …), D = date, T = timestamp*

  This model can be also extended by the definition of the other data types like binary objects.
- *ID_row* – references to the old value of attribute (if the DML statement was *Update*). Only update statement of temporal column sets not *NULL* value.
- *Operation* – determines the provided operation:
  - *I = Insert, D = Delete, U = Update, R = Restore*

  The principles and usage of proposed operations are defined the in the part of this paper.
- *BD* – the begin date of the new state validity of an object.

Complete management and principles of the DML statements are described in [9].

| Temporal_table | | | |
|---|---|---|---|
| id_change | Integer | NN | (PK) |
| id_previous_change | Integer | | |
| operation | operation_domain | NN | |
| id_tab | Integer | NN | |
| id_orig | Integer | NN | |
| id_column | Integer | | |
| id_row | Integer | | |
| bd | Date | NN | |
| data_type | data_type_domain | | |

**Fig. 2.** Temporal_table

## 3. Index structures

One of the main features of optimization is based on using index structures. Temporal databases are oriented for state management and monitoring over the time. Getting states and individual changes in the *Select* statement form the core of a major milestone of efficiency and speed of the system.

Oracle defines an index as an optional structure associated with a table or table cluster that can sometimes speed data access. By creating an index on one or more columns of a table, you gain the ability in some cases to retrieve a small set of randomly distributed rows from the table. Indexes are one of many means of reducing disk I/O. If a heap-organized table has no indexes, then the database must perform a full table scan to find a value.

The absence or presence of an index does not require a change in the wording of any SQL statement. An index is a fast access path to a data rows. However, it does not affect only the speed of execution. Given a data value that has been indexed, the index pointer reflects directly to the location of the rows containing that value. Database management system automatically maintains the created indexes – changes (*Insert*, *Delete*, *Update*) are automatically reflected into index structures. However, the presence of many indexes on a table degrades the performance because the database must also update the indexes. Moreover, the optimizer does not have to use them, if the full scan would be faster or if the index is not suitable for the query based on the conditions.

### 3.1. B-tree, B+tree

The index structure of the B+tree is mostly used because it maintains the efficiency despite frequent changes of records (*Insert, Delete, Update*). B+tree index consists of a balanced tree in which each path from the root to the leaf has the same length.

In this structure, we distinguish three types of nodes - root, internal node and leaf node. Root and internal node contains pointers $S_i$ and values $K_i$, the pointer $S_i$ refers to nodes with lower values the corresponding value ($K_i$), pointer $S_{i+1}$ references higher (or equal) values. Leaf nodes are directly connected to the file data (using pointers). B+tree extends the concept of B-tree by chaining nodes at leaf level, which allows faster data sorting. DBS Oracle uses the model of two-way linked list, which makes it possible to sort ascending and descending, too.

Limitation of this approach is a small number of records (low cardinality). In that case, using index does not produce the desired effect in terms of performance (acceleration). However, this disadvantage does not cover the temporal data characteristics. Another disadvantage is the lack of support SQL queries with functions implicitly.

### 3.2. Inverted key B+tree

Index B-tree structure with inverted key is used in case of often requirement for tree balancing (column value is obtained using the sequence and the trigger - autoincrement) caused by frequent execution of the *Insert* statement. Indexing will not use original key value, but the inverted variant. For example, for the key 123 is inverted key value 321.

Other type of index structures are described in [6].

## 4. Tablespace localization

The performance characteristics are influenced by the index location and by the type of index structure. In the first phase, data and indexes are located in the same tablespace (MODEL 1). The second type is based on indexes and data division into separate tablespaces, which are located in the separate discs (MODEL 2). This allows more flexible response to the extension of the number of data blocks and index construction changes. The last type is based on index localization in the remote storage (server) and access using the network (MODEL 3). The aim is to monitor the network traffic and response of the system.

Each user has defined tablespace in which he operates. That tablespace is called default user tablespace. However, before index definition, the location of the tablespace can be defined [9]. Next statement (fig. 3) shows the way to create tablespace. The fig. 4 shows the index definition located in explicit tablespace.

```
create tablespace
   kvet_tablespace
datafile
  '/home/kvet1/tablespace/kvet_tablespace.dat'
size 50m
autoextend on next 10m;
```

**Fig. 3.** Tablespace definition

```
create index ind12
   on temporal_table(id_orig, id_previous_change, bd) reverse
     tablespace kvet_tablespace;
```

**Fig. 4.** Index construction

## 5. Experiments

The aim of the developed structure is to address the lack of data management with different granularity and frequency of changes. The model performance is compared based on various developed index structures. *Insert*, *Update*, *Delete* (logical) and *Restore* (renew validity) operations have been monitored to highlight time consumption performance. The main criterion of quality is the speed of the processed *Select* statement, which reflects the proposed index structures. Global object changes over the time have been monitored (*Select_obj*). Another fundament is characterized by the duration to obtain actual snapshot of the temporal database (*Select_db*). This section deals with 9 different indexes, which are compared to declare the quality and usability of the system:

- no index (*ind1*).
- create index ind2 on temporal_table(id_orig);
- create index ind3 on temporal_table(id_orig, id_previous_change);
- create index ind4 on temporal_table(id_orig, bd);
- create index ind5 on temporal_table(id_orig, id_previous_change, bd);
- create index ind6 on temporal_table(id_orig) reverse;
- create index ind7 on temporal_table(id_orig, id_previous_change) reverse;
- create index ind8 on temporal_table(id_orig, bd) reverse;
- create index ind9 on temporal_table(id_orig, id_previous_change, bd) reverse;

Experiment results were provided using Oracle Database 11g Enterprise Edition Release 11.2.0.1.0 - 64bit Production; PL/SQL Release 11.2.0.1.0 – Production. Parameters of used computer are: processor: Intel Xeon E5620; 2,4GHz (8 cores), operation memory: 16GB, HDD: 500GB.

Complete number of each operation was 10 000 (*Insert*, *Update*, *Delete*, *Restore*). Number of updated temporal attributes has been generated, total number was 24 965. Minimal number of operations on the object was 3, maximal number was 26, the average value was 5,4965. *Select* statement monitors the changes over the whole time interval of object existence. Processed data were generated based on real data pattern from the intelligent transport systems – traffic monitoring. Processed table consists of five temporal columns (date, integer, number, varchar, date data type).

Next table consists of the experiment results (in seconds) based on defined models.

| Operation | Ind1 | Ind2 | Ind3 | Ind4 | Ind5 | Ind6 | Ind7 | Ind8 | Ind9 |
|---|---|---|---|---|---|---|---|---|---|
| *Insert* | 13,02 | 14,71 | 15,60 | 14,49 | 15,44 | 15,09 | 14,78 | 13,92 | 14,26 |
| *Update* | 52,18 | 21,46 | 20,62 | 24,25 | 22,70 | 21,70 | 21,72 | 21,80 | 20,85 |
| *Delete* | 40,35 | 16,01 | 17,18 | 18,34 | 18,37 | 15,56 | 16,84 | 18,07 | 17,53 |
| *Restore* | 42,97 | 17,85 | 17,65 | 17,68 | 18,32 | 17,23 | 18,76 | 16,95 | 17,78 |
| *Select* | 77,02 | 25,21 | 25,25 | 25,57 | 26,04 | 25,11 | 25,18 | 25,15 | 25,17 |

**Tab. 1.** Experiment results – MODEL 1

| Operation | Ind1 | Ind2 | Ind3 | Ind4 | Ind5 | Ind6 | Ind7 | Ind8 | Ind9 |
|---|---|---|---|---|---|---|---|---|---|
| *Insert* | 13,69 | 13,76 | 13,85 | 15,03 | 13,76 | 13,56 | 14,81 | 13,88 | 13,69 |
| *Update* | 50,65 | 21,59 | 22,32 | 22,27 | 21,10 | 21,10 | 21,01 | 21,80 | 20,59 |
| *Delete* | 39,63 | 18,85 | 14,16 | 15,95 | 16,91 | 16,29 | 16,77 | 16,23 | 15,46 |
| *Restore* | 42,79 | 19,68 | 17,96 | 18,60 | 17,68 | 20,42 | 18,46 | 17,20 | 18,02 |
| *Select* | 81,91 | 28,51 | 28,73 | 28,30 | 29,12 | 28,71 | 28,78 | 29,20 | 28,43 |

**Tab. 2.** Experiment results – MODEL 2

| Operation | Ind1 | Ind2 | Ind3 | Ind4 | Ind5 | Ind6 | Ind7 | Ind8 | Ind9 |
|---|---|---|---|---|---|---|---|---|---|
| *Insert* | 13,23 | 15,50 | 15,09 | 13,87 | 13,07 | 13,84 | 14,73 | 15,02 | 14,58 |
| *Update* | 48,89 | 20,51 | 22,33 | 20,33 | 19,75 | 20,81 | 21,29 | 21,36 | 22,82 |
| *Delete* | 38,96 | 14,98 | 17,25 | 18,13 | 18,08 | 17,86 | 17,72 | 18,34 | 15,92 |
| *Restore* | 44,96 | 19,04 | 17,36 | 17,57 | 16,60 | 16,73 | 18,25 | 18,67 | 19,55 |
| *Select* | 81,01 | 28,49 | 28,89 | 28,58 | 28,54 | 28,59 | 31,88 | 29,22 | 28,69 |

**Tab. 3.** Experiment results – MODEL 3

Evaluation is performed using three main criteria with emphasis on weight. The criterion 1 uses the same weight for all operations (statements). The criterion 2 represents the standard temporal access. The most important (most frequently used) performance statement is *Select* and *Update*. The last (third) criterion is used for uncertain wireless communication protocols. The basic element of the processing is based on number of operations, respectively importance of the operation (statement) with regards of the whole performance results. The principle of weight management is described in [6].

$$T_{\text{crit}} = \sum_{i \in I} w_i * T_i \quad I = \{\text{Insert}, \text{Update}, \text{Delete}, \text{Restore}, \text{Select}\} \tag{1}$$

| Statement | Criterion 1 | Criterion 2 | Criterion 3 |
|---|---|---|---|
| | weight | | |
| *Insert* | 1 | 0,1 | 0,02 |
| *Update* | 1 | 0,3 | 0,23 |
| *Delete* | 1 | 0,1 | 0,17 |
| *Restore* | 1 | 0,1 | 0,18 |
| *Select* | 1 | 0,4 | 0,4 |

**Tab. 4.** Criteria weights

For the first model (data and indexes are located in the same tablespace, in the same disc), the best solution provides index *ind6* based on object identifier, which value is processed reversed – crit. 1. Index *ind6* is also preferred by the criterion 3. However, the best performance based on criterion 2 is index *ind9.* Thus, it is very important to set right weights based on the application domain.

If the index is located on another disc and tablespace (model 2), the best criterion provides in all cases index *ind9*, which consists of three attributes – identifier of the processed object (*id_orig*), identifier of the last change on that object (*id_previous_change*) and begin date of the validity (*BD*). Accordingly, index *ind9* is a B+tree with inverted key (*reverse*).

Processed index can be stored also in the tablespace located in the remote server (model 3). In that case, all criteria prefer index *ind5*, which is not reverse. The global slowdown compared with the model 1 is about 2,8s (criterion 1), which corresponds 2,51% slowdown caused by the network data transfer. All data experiments were provided using university infrastructure (1Gb throughput).

## 6. Conclusion

Conventional database principles are based on management actual valid states of the objects. Temporal solution extends the definition by the validity. Standard temporal systems deal with the whole objects as granularity. Effective managing temporal approach is the main criterion. The aim of the proposed attribute level temporal model is to cover the granularity problem and variance of update frequency. A significant aspect is just performance reflected to processing time and size of the structure. Temporal index structures and their location can significantly improve performance of the system. The developed system is compared based on the index performance and tablespacing. In the future research, the system will be extended by the distribution and parallelism management.

## Acknowledgement

This publication is the result of the project implementation:

Centre of excellence for systems and services of intelligent transport, ITMS 26220120028 supported by the Research & Development Operational Programme funded by the ERDF and Centre of excellence for systems and services of intelligent transport II., ITMS 26220120050 supported by the Research & Development Operational Programme funded by the ERDF.


*"PODPORUJEME VÝSKUMNÉ AKTIVITY NA SLOVENSKU*
***Projekt je spolufinancovaný zo zdrojov EÚ"***

## References

[1] Codd, F. E.: A Relational Model of Data for Large Shared Data Banks – Communications of the ACM, Vol. 9, 1970, No. 6, pp 377-387.

[2] Date, J. C.: Date on Database. Apress, 2006.

[3] Date, J. C.- Darwen, H.- Lorentzos, A.N.: Temporal data and the relational model. Morgan Kaufmann, 2003.

[4] Jensen, S. Ch.- Snodgrass, T. R.: Temporally Enhanced Database Design. MIT Press, 2000.

[5] Johnston, T.-Weis, R.: Managing Time in Relational Databases. Morgan Kaufmann, 2010.

[6] Kvet M.: Temporal Data Approach Performance, In: Proceedings of International Conference CSSCC 2015, Wien, March 2015, pp.75-83.

[7] Kvet, M.-Matiaško, K.: Epsilon Temporal Data in MRI Results Processing, In: Proceedings of the 10th International Conference on Digital Technologies, July 2014, pp. 207-219.

[8] Kvet, M.-Matiaško, K.-Kvet, M.: Transaction Management in Fully Temporal System. In: Proceedings of UKSim-AMSS 16th international conference on computer modelling and simulation, Cambridge, March 2014, pp. 147-152.

[9] Ozsu, M.-Valduriez, P.: Principles of Distributed Database Systems, Springer, 2011

**TRANSCOM 2015, 22-24 June 2015**
University of Žilina, Žilina, Slovak Republic

# Musical Instrument Recognition Using Selected Audio Features

[*]Miroslav Malík, [*]Michal Chmulík, [*]Daša Tichá
[*]University of Žilina, Faculty of Electrical Engineering, Department of Telecommunications and Multimedia, Univerzitna 2, 01026 Žilina, Slovakia, {Miroslav.Malik, Michal.Chmulik, Dasa.Ticha}@fel.uniza.sk

**Abstract.** This article deals with a recognition of 13 types of European orchestral musical instruments by classification methods kNN and GMM with an application of 7 substantive and 2 combinations of audio features, namely MFCC, formants, LPC, LSP and derived features. The main goal was to investigate suitability of tested features for selected classification methods.

**Keywords:** recognition, musical instruments, audio features, GMM, kNN, MFCC, LPC, LSP.

## 1. Introduction

The musical instrument recognition (MIR) is one of current tasks of semantic analysis of audio content and it finds an application in the automatic audio content indexing or data retrieval systems. There is a huge amount of digital musical records available nowadays, often not very exact describable by a text, and the automatic musical instruments recognition can make this task easier. Another possible versatility of MIR is in an automatic musical record annotation, structural coding, also for several software used by musicians.

Scientists worked on the detailed analysis of musical instrument's audio features since 1950. First researches in MIR task comes in the nineties, in most cases with a small number of musical instruments and a limited scale of musical instrument. Later on, K. Martin and Y. Kim creates a system which worked with isolated tones of full pitch ranges of 14 musical instruments. In this case, the k-Nearest Neighbour algorithm (kNN) acquitted as the best method of classification. Musical instruments was classificated by a hierarchical architecture which recognize an instrument family at the first place and then it recognize a particular instrument from the given instrument family. Audio samples were divided into 70% for training and 30% for testing data and it gave the results of 72% precision for an individual instrument and 93% precision for classification into 5 musical instrument families [1]. Another extensive research in the automatic musical instrument recognition and audio features deserved A. Eronen in his works [2][3], where he experimented with 30 orchestral musical instruments and he reached the successfulness of the classification of an instrument family up to 94%.

In commercial area, the musical instrument recognition still lags behind the speaker and speech recognition. Essentially, it is caused by the fact that speech bears a far more valuable information, often easier describable than music.

## 2. Audio Features

It is necessary to describe an audio signal by the certain group of parameters which sufficiently precise represents properties of an audio signal for a possible analysis of an audio record from the view of its content. This parameters are called the audio features. In general, we could divide the audio features into 3 basic groups: temporal, spectral and statistical.

Temporal features are obtained directly from samples of an input audio signal (for example coefficients of FIR, IIR, LPC or the number of zero crossing, etc.). Spectral features are obtained by

transforming of the original signal into frequency domain, where coefficients of FFT, cepstral coefficients, or the spectral centroid may be mentioned as typical representatives and statistical parameters describes the signal properties in the term of statistics (the mean value of the signal energy, skewness coefficient, spectral slope, etc.).

Currently, there is a huge amount of audio features, the percentage of classification depends on the discrimination capability of selected audio features. For our tests have been selected groups of features listed below. The parameterization of audio recordings has been performed using the freely available tool openSmile [4] and it has been applied on frames of the length of 30 ms with the half overlapping using the Hamming window function.

### 2.1. MFCC

The Mel-Frequency Cepstral Coefficients are one of most common features in areas related to the speech processing (speech recognition, speaker recognition, speaker verification, etc.), but it finds an application in the task of semantic analysis of audio content such as the general sound recognition, the musical genres recognition and others.

The MFCC are obtained as follows. The input signal is at first transformed into the spectral domain (typically using the FFT) and then the signal enters the filter bank with the Mel frequency division, then follows a block of the cepstral transformation which is the non-linear transformation (typically the logarithm operation), and finally, the MFCC are obtained by the inverse transformation (typically the DCT). To the MFCC are also added the dynamical features of signal describing temporal changes of the spectrum, which are very important in the human perception of sound – the Δ coefficients and the ΔΔ coefficients.

### 2.2. LPC

The Linear Prediction Coefficients are obtained by the linear prediction (LP). This method which is derived from the speech production model, is based on the simple precondition that the *n*-th sample of the speech signal can be replaced by the linear combination of previous *Q* samples:

$$s(n) = -\sum_{i=1}^{Q} a_i . s(n-i). \qquad (1)$$

For a calculation of prediction coefficients is most frequently used the autocorrelation method and Levinson-Durbin's algorithm. Although the linear prediction method was originally designed for applications related to speech, it has a significant application in other areas too, because with a sufficiency high order of the predictor can very accurately describe the spectral envelope of the signal.

### 2.3 Derivates of LPC

The origins of the LP analysis dates back to the sixties of the last century and over years there have been successively proposed modifications in the form of taking into account the human perception of sound by applying the bank of filters with the Mel's scale or an application of cepstral transformation. Thus, there are new features such as the perceptual linear prediction coefficients PLP, the linear prediction cepstral coefficients LPCC or the perceptual linear prediction cepstral coefficients PLPCC.

The LPCC are obtained from the LPC by the cepstral transformation as in the case of the MFCC.

The PLP are obtained from LPC coefficients by an application of the Mel scaled filter bank, similar to the MFCC.

Applying the Mel scaled filter bank on the LPC together with the cepstral analysis gains the PLPCC.

Another derived group of features are the LSP coefficients (Line Spectral Pairs), which are gained by decomposing of the predictor to a symmetric and an asymmetric part representing zeros and poles of the LP filter. These features are typically used in the speech coding.

### 2.4 Spectral coefficients

As mentioned above, by a suitable transformation (FFT, DCT, wavelet, etc.) the original temporal signal can be converted to the spectral domain.

In our tests, the FFT coefficients has been used, filtered in octave bands supplemented by following coefficients derived from the FFT:

- spectral roll-off – determines a threshold bellow which the biggest part of signal energy resides
- spectral flux – describes a time change in a spectrum of the signal
- spectral centroid – represents the balancing point of the spectral power distribution
- spectral spread – determines variance of the spectrum
- spectral skewness
- spectral kurtosis
- spectral slope

### 2.5 Formants

The formant as a term is perhaps the most frequently used in the connection with the speech as an indication of the resonant frequency of the vocal tract model, but in general it is defined as the peak in the spectrum of signal. With formants, the spectral envelope can by described like using the LPC.

## 3. Classification methods

There are several classification techniques used for classification of audio content. They are based on comparing the similarities between unknown input audio files and known sounds. In the past, the sound processing used the intuitive comparison of functional vector patterns. Current studies of acoustical properties favour statistical models because they provides more flexible probabilistic results. The most common methods of classification are based on the Gaussian Mixture Model (GMM), Hidden Markov Model (HMM), k-Nearest Neighbours (kNN), Artificial Neural Networks (ANNs), Vector Quantisation (VQ) and Support Vector Machines (SVM).

### 3.1 Gaussian Mixture Model

The density in component models is expressed as a linear combination of density functions. A model with *M* components can be written in the form:

$$p(x) = \sum_{j=1}^{M} P(j)\, p(x \mid j), \tag{2}$$

where parameters *P(j)* are called mixture coefficients which represent probabilities of *j*-th component. Part *p(x|j)* represents parameters of density functions which typically fluctuate around *j*. The condition is that the function must not be negative and should integrate to 1 over its entire definition field. A limitation of component's coefficients

$$\sum_{j=1}^{M} P(j) = 1, \tag{3}$$

$$0 \le P(j) \le 1, \tag{4}$$

ensures that the model will represent the probability function.

The component model is generative and is useful as a process of generating samples from represented density. The first of *j*-components is randomly selected with probability *P(j).* It just depends on choosing the form of density components. Four forms of the Gaussian mixture model are known, each of these Gaussian distributions has different form of the covariant matrix:

- spherical
- diagonal
- complete
- PPCA (Probability Principal Component Analysis)

To maximise the similarity of the GMM data is used the Expectation Maximization algorithm (EM). EM is appropriate for reprocessing of problem with the equivalence of minimizing of negative record of similarity in data set using the relation:

$$E = -\Theta = \sum_{n=1}^{N} \log p\left(x^n\right), \tag{5}$$

which is regarded as an error function [5][11]. $\Theta$ represents the set of parameters of GMM which is needed to find.

After the a proper training of the model, the GMM method becomes very efficient and fast tool for classification, which is computationally inexpensive.

A disadvantage may be the absence of a higher order signal information.

### 3.2 k-Nearest Neighbours

The main principle of the kNN algorithm is very simple and it is based on a comparison of data distances in selected feature‘s space. A more similar data are closer together than a less similar data. An input data of algorithm are divided into a training and a test data. The training data are data sets which are divided into groups, each group characterize one class. The KNN seeks certain distance surroundings for each element of the test data – the neighbourhood, containing *k* training elements, respectively the reference data, and on the basis of certain criteria – most often the majority rule – algorithm assigns the tested element to one of classes. The final determination of class by the majority voting can be described as follows:

$$y^* = \arg\max_v \sum_{(x,y)\in D_z} I(v = y_i), \tag{6}$$

where the function *I(...)* is equal to *I(true) = 1; I(false) = 0;* coefficient $v$ labels the class and $y_i$ labels the class of the *i*-nearest element.

Despite the simplicity of the algorithm, this method gives good results and is used as well as a verification method. Additional advantages of the kNN include ease of implementation and flexibility. As the main disadvantage is considered the fact that the training data must be stored in memory and that the kNN do not create a complex model from the training data, thus saves some time, but very comparison is time dependant on the size of the database of training elements [6].

## 4. Database of selected musical instruments

The database of sound recordings of musical instruments is based primarily on the database of Electronic music studios at the University of Iowa. This database contains audio recordings, particular string and woodwind musical instruments that play individual notes of the chromatic scale across the full spectrum of musical instrument including various playing techniques typical for some instruments, for example *arco*, *pizzicato*, or *vibrato*. Sound recordings also involves various dynamics of played tone, *pp*, *mf* and *ff*, and thus sound samples represent the entire dynamic structure of selected musical instrument. Recordings were performed in the anechoic chamber in

Wendell Johnson Speech and Hearing Centre, mostly recorded by the condenser microphone Neumann KM 84 with cardioid characteristics, the sample frequency is 44,1 kHz and bit depth is 16 bit. [7]

Overall, 10 classes of instruments has been used for training and testing, with its durations, the number of clips and the numbers of the classes listed in Tab. 1.

| No. of class | Class | Duration [hh:mm:ss] | No. of clips |
|---|---|---|---|
| 1 | bassoon | 00:04:33 | 15 |
| 2 | flute | 00:25:56 | 43 |
| 3 | oboe | 00:05:58 | 12 |
| 4 | violin | 01:09:58 | 71 |
| 5 | clarinet | 00:28:54 | 36 |
| 6 | bass | 00:44:31 | 75 |
| 7 | French horn | 00:04:19 | 12 |
| 8 | saxophone | 00:30:29 | 42 |
| 9 | trombone | 00:17:24 | 24 |
| 10 | trumpet | 00:32:39 | 24 |
| 11 | tube | 00:04:06 | 8 |
| 12 | viola | 00:15:43 | 29 |
| 13 | cello | 01:12:15 | 76 |

**Tab. 1.** Composition of the musical instruments database.

## 5. Results

Determining of success was realized by a *F*-measure. The *F*-measure (also *F*-score or $F_1$-score) is frequently used statistical precision, for example, in a data retrieval or machine learning. It is defined by the equation:

$$F = \frac{2.P.R}{P+R}, \tag{14}$$

where *P* (Precision) is s the number of correct positive results divided by the number of all positive results, *R* (Recall) represents the number of correct positive results divided by the number of positive results that should have been returned and *F* is then a weighted average of *P* and *R*.

| Features | No. of features | F – measure accuracy (%) | |
|---|---|---|---|
| | | kNN | GMM |
| MFCC | 12+12+12 | 74,62 | 81,04 |
| LPC | 20 | 82,31 | 82,74 |
| LSP | 20 | 86,08 | 76,36 |
| PLP | 20 | 41,51 | 50,84 |
| PLPCC | 20 | 46,68 | 54,79 |
| Spectral | 24 | 55,01 | 48,72 |
| Formants | 10 | 35,96 | 37,15 |
| MFCC + LPC | 56 | 75,70 | 73,75 |
| LPC + LSP | 40 | 87,23 | 85,36 |

**Tab. 2.** Classification results.

The entire database was divided into 2 parts, 70 to 30 %, where the bigger part was used as the training data and the smaller part for testing.

According to the results of kNN method using MFCC were the results achieved 74.62% and 81.04% for GMM, and therefore it is possible to see the similarity with the results in [1] where the same division ratio was used for distribution of processed data into training and test.

## 6. Conclusion and future work

The aim of the experiment was to assess the ability of recognition of musical instruments using kNN and GMM methods. These methods achieve the best final percentage 87.23% for the combination of the LPC and the LSP coefficients for the kNN and 85.36% for the GMM. These audio features show the best results even in separate tests and they overcome in practice the most commonly used MFCC coefficients, and therefore they appear to be suitable for use in the processing of not only speech but also musical instruments. By this experiment, the long computing duration of the kNN was confirmed, so the practical application for general use can be still limited. For this application, the GMM seems more suitable because it was time-consuming just during a model creation, the classification was carried out relatively quick.

In the future, the model of experiment could be extended by other audio features such as the rise time, fall time and others, and the hierarchical distribution of musical instruments could be included. Also, the classification could be performed with use of the SVM or some other methods.

## References

[1] MARTIN, K. D., KIM, Y. E. *Musical instrument identification: A pattern-recognition approach*, Proc. of the 136th meeting of the Acoustical Society of America, USA, 1998.

[2] ERONEN, A., KLAPURI, A. *Musical Instrument Recognition Using Cepstral Coefficients and Temporal Features*, IEEE International Conference on Acoustics, Speech, and Signal Processing, Turkey, 2000.

[3] ERONEN, A. *Comparison of Features for Musical Instrument Recognition*, IEEE Workshop on Applications of Signal Processing to Audio and Acoustics, USA, 2001.

[4] *The Munich Versatile and Fast Open-Source Audio Feature Extractor*
Online:
http://www.audeering.com/research/opensmile

[5] THEODORIDIS, S., KOUTROUMBAS, K. *Pattern Recognition*. Sec. edition, Elsevier Academic Press, 2003.

[6] Chmulík, M. *Selection of audio features using stochastic evolutionary optimisation methods for content analysis of audio and speech data*, Doctoral thesis, UNIZA, Žilina, 2011.

[7] *Database of musical instruments recordings*. Electronic Music Studios, University of Iowa,
Online:
http://theremin.music.uiowa.edu/MIS.html

[8] BENADE, A. H. *Fundamentals of Musical Acoustics*. Sec. edition, Dover, 1990.

[9] MARTIN, K. D. *Toward Automatic Sound Source Recognition: Identifying Musical Instruments*, Proc. of NATO Computational Hearing Advanced Study Institute, Italy, 1998.

[10] BROWN, J. C. *Computer Identification of Musical Instruments Using Pattern Recognition With Cepstral Coefficients As Features*, Journal of Acoustic Society of America, 1999.

[11] NABNEY, I. T. *Netlab, Algorithms for Pattern Recognition, Springer*, 2004.

**TRANSCOM 2015, 22-24 June 2015**
University of Žilina, Žilina, Slovak Republic

# Antenna Circuits Analysis for GDO-based Localization of RFID Transponder

[*]Tomáš Mravec, [*]Peter Vestenický
[*]University of Žilina, Faculty of Electrical Engineering, Department of Control and Information Systems, Univerzitná 8215/1, 010 26 Žilina, Slovakia, {tomas.mravec, peter.vestenicky}@fel.uniza.sk

**Abstract.** This paper deals with localization method of single-bit inductively coupled RFID transponders (called markers) which are used to mark of underground facilities such as cables, pipes etc. The localization method based on grid dip oscillator (GDO) principle and using serial or parallel LC resonant circuit as antenna is analyzed. The proximity to the marker is detected by decreasing of current in the serial resonant antenna circuit of locator or by decreasing of voltage in the parallel resonant antenna circuit of locator. This localization method continuously radiates electromagnetic waves into the space. For mathematical modeling the differential equations are used for both cases of antenna resonant circuits. The sensitivity of localization depends mainly on the distance between coils of marker and locator antenna.

**Keywords:** Serial resonant circuit, parallel resonant circuit, single-bit RFID transponder, localization, marker.

## 1. Introduction

Inductively coupled RFID (Radio Frequency Identification) systems [1] are being used for marking of goods, animals, for electronic access control systems to building, train and bus tickets etc. In addition to these applications the RFID transponders are being used for marking of underground facilities location. Such RFID transponders are called “markers”.

The localization of the passive markers is process in which the presence of marker is detected by a localization device (locator) and distance between the marker and the antenna of locator is estimated. This localization method is RSSI (Received Signal Strength Indicator) based [2].

In [3] the authors describe localization methods based on damped oscillations and on continuous radiation of electromagnetic waves. The damped oscillation based localization method is modelled by the differential equations and the continuous radiation based localization method is modelled by the algebraic equations and complex impedances. This paper will describe the continuous radiation based method only and it will be analyzed by the differential equations to observe transient phenomena. Next, the serial and parallel resonant LC circuit as locator antenna will be analyzed. The proximity of marker resonant circuit to the locator antenna will be detected by decreasing of the current or voltage in antenna LC circuit (serial or parallel).

## 2. Mutual Inductance

Important quantity in all the models is the mutual inductance $M$ [3], [4]:

$$M = \frac{\sqrt{L_R L_T}\, r_R^2 r_T^2 \cos\theta}{\sqrt{r_R r_T}\left(r_R^2 + x^2\right)^{\frac{3}{2}}}, \tag{1}$$

where $L_R$ and $L_T$ is inductance of locator antenna and marker coils, respectively, $r_R$ is radius of RFID locator antenna, $r_T$ is radius of marker coil, $x$ is distance between the locator antenna and the

marker and $\theta$ is angle between coil of locator antenna and marker coil (note that if $\theta$ = 0 ° then coils are parallel).

## 3. Mathematical Model of Localization Based on GDO Principle

This localization principle assumes that the RFID locator continuously radiates the high frequency waves into the space. In dependence on the distance $x$ between coils the marker resonant circuit influences on the current $i_1(t)$ or voltage $u_{CR}(t)$ in locator antenna circuit.

### 3.1. Serial Antenna Circuit

Schematic diagram of this model is shown in Fig. 1. This model consists of serial resonant circuits in the locator side and on the transponder (marker) side, too. This model can be described by the following system of differential equations:

$$\begin{aligned} L_R \frac{di_1(t)}{dt} + R_R i_1(t) + \frac{1}{C_R}\int_0^t i_1(\tau)d\tau - M\frac{di_2(t)}{dt} &= u_1(t), \\ L_T \frac{di_2(t)}{dt} + R_T i_2(t) + \frac{1}{C_T}\int_0^t i_2(\tau)d\tau - M\frac{di_1(t)}{dt} &= 0. \end{aligned} \tag{2}$$

Next, assume that the signal source in the Fig. 1 is harmonic i. e.:

$$u_1(t) = U_1 \sin(\omega t). \tag{3}$$

The system of integrodifferential equations (2) must be modified into numerically solvable form (4) by substitution $x_1(t)=i_1(t)$, $x_2(t)=di_1(t)/dt$, $x_3(t)=i_2(t)$, $x_4(t)=di_2(t)/dt$. Then we get the 1st order system of differential equations [5]:

$$\begin{aligned} \frac{dx_1(t)}{dt} &= x_2(t) \\ \frac{dx_2(t)}{dt} &= a_1x_1(t) + a_2x_2(t) + a_3x_3(t) + a_4x_4(t) - a_5\omega U_1\cos(\omega t) \\ \frac{dx_3(t)}{dt} &= x_4(t) \\ \frac{dx_4(t)}{dt} &= b_1x_1(t) + b_2x_2(t) + b_3x_3(t) + b_4x_4(t) - b_5\omega U_1\cos(\omega t) \end{aligned} \tag{4}$$

where individual coefficients are given by (5).

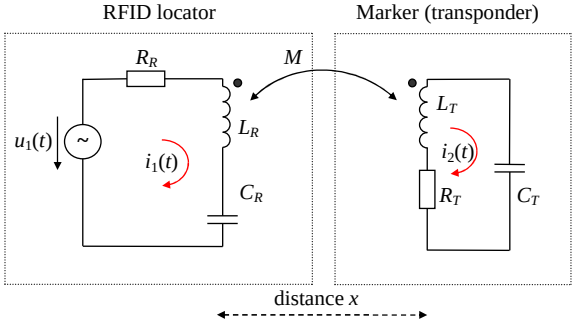


**Fig. 1.** Model of localization based on continuous excitation with serial antenna circuit.

$$a_1 = \frac{L_T}{C_R(M^2 - L_R L_T)} \qquad b_1 = \frac{M}{C_R(M^2 - L_R L_T)}$$
$$a_2 = \frac{L_T R_R}{M^2 - L_R L_T} \qquad b_2 = \frac{R_R M}{M^2 - L_R L_T}$$
$$a_3 = \frac{M}{C_T\left(M^2 - L_R L_T\right)} \qquad b_3 = \frac{L_R}{C_T\left(M^2 - L_R L_T\right)} \tag{5}$$
$$a_4 = \frac{M R_T}{M^2 - L_R L_T} \qquad b_4 = \frac{L_R R_T}{M^2 - L_R L_T}$$
$$a_5 = \frac{L_T}{M^2 - L_R L_T} \qquad b_5 = \frac{M}{M^2 - L_R L_T}$$

If the marker is not in the locator reach i. e. $x \to \infty$ then from (1) it results that the mutual inductance $M$=0. In this case the current $i_1(t)$ has maximum value $I_{1max}$, which is measured in steady state after the time $t$=2.5 ms. The proximity of marker then can be detected if the steady value of current $I_1$ measured after time $t$ = 2.5 ms is decreased by $\Delta I_1$:

$$\Delta I_1 = |I_{1max}| - |I_1| \tag{6}$$

The time course of current $i_1(t)$ in the RFID locator circuit (Fig. 2a) was numerically calculated from the system (4) for these parameters of the whole model:

- Voltage of signal generator $u_1$=10 V, frequency $f$=125 kHz, i. e. $\omega = 2\pi f$=785.4 krad/s
- Distance between coils $x$=0.3 m, angle $\theta$ = 0 °
- Radius of coils $r_R$=0.1 m, $r_T$=0.1 m
- $C_R$=1.621 nF, $L_R$=1 mH, $R_R$=15.7 Ω, i. e. the antenna of locator has resonant frequency $f_R$=125 kHz, the quality factor of $L_R C_R$ tuned circuit is $Q_R$=50
- $C_T$=1.621 nF, $L_T$=1 mH, $R_T$=7.85 Ω, i. e. the resonant frequency of marker is $f_R$=125 kHz, the quality factor of $L_R C_R$ tuned circuit is $Q_R$=100.

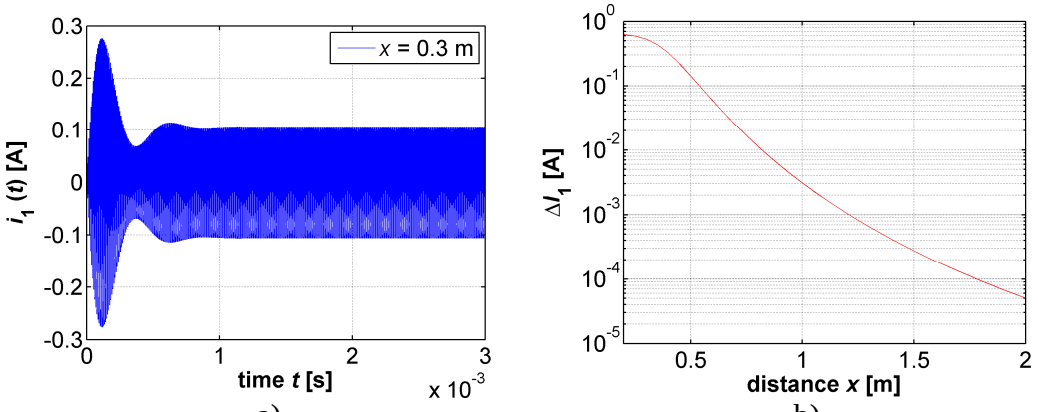


a) b)

**Fig. 2.** a) The time course of current $i_1(t)$, distance $x$=0.3m. b) Detectable current change $\Delta I_1$ versus distance $x$.

### 3.2. Parallel Antenna Circuit

The schematic diagram of this model is shown in Fig. 3. The principle of marker proximity detection is the same as in the previous model but the difference lies in utilization of parallel LC circuit instead of the serial circuit in the locator antenna.

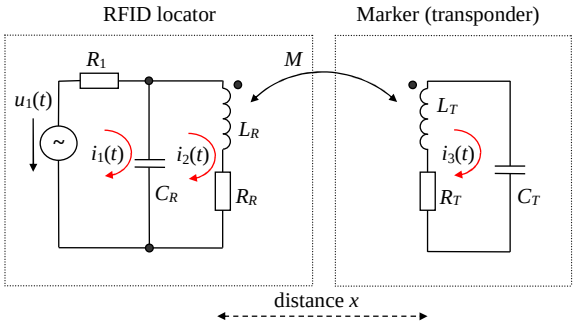


**Fig. 3.** Model of localization based on continuous excitation with parallel antenna circuit

This model can be described by the following system of differential equations:

$$R_1 i_1(t) + \frac{1}{C_R}\int_0^t i_1(\tau)d\tau - \frac{1}{C_R}\int_0^t i_2(\tau)d\tau = u_1(t)$$

$$L_R \frac{di_2(t)}{dt} + R_R i_2(t) + \frac{1}{C_R}\int_0^t i_2(\tau)d\tau - \frac{1}{C_R}\int_0^t i_1(\tau)d\tau - M\frac{di_3(t)}{dt} = 0 \qquad (7)$$

$$L_T \frac{di_3(t)}{dt} + R_T i_3(t) + \frac{1}{C_T}\int_0^t i_3(\tau)d\tau - M\frac{di_2(t)}{dt} = 0$$

The signal source in the Fig. 3 is harmonic in accordance to (3). The system of integrodifferential equations must be modified into numerically solvable form (8) by derivation and by substitution $x_1(t)=i_1(t)$, $x_2(t)=i_2(t)$, $x_3(t)=di_2(t)/dt$, $x_4(t)=i_3(t)$, $x_5(t)=di_3(t)/dt$. Then we get the 1st order system of differential equations:

$$\frac{dx_1(t)}{dt} = \frac{\omega U_1 \cos(\omega t)}{R_1} - \frac{1}{C_R R_1}x_1(t) + \frac{1}{C_R R_1}x_2(t)$$

$$\frac{dx_2(t)}{dt} = x_3(t)$$

$$\frac{dx_3(t)}{dt} = -a_1 x_1(t) + a_2 x_2(t) + a_3 x_3(t) + a_4 x_4(t) + a_5 x_5(t) \qquad (8)$$

$$\frac{dx_4(t)}{dt} = x_5(t)$$

$$\frac{dx_5(t)}{dt} = -b_1 x_1(t) + b_2 x_2(t) + b_3 x_3(t) + b_4 x_4(t) + b_5 x_5(t)$$

where individual coefficients are given by (9).

$$a_1 = a_2 = \frac{L_T}{C_R(M^2 - L_R L_T)} \qquad b_1 = b_2 = \frac{M}{C_R(M^2 - L_R L_T)}$$

$$a_3 = \frac{R_L L_T}{M^2 - L_R L_T} \qquad b_3 = \frac{R_L M}{M^2 - L_R L_T} \qquad (9)$$

$$a_4 = \frac{M}{C_T(M^2 - L_R L_T)} \qquad b_4 = \frac{L_R}{C_T(M^2 - L_R L_T)}$$

$$a_5 = \frac{R_T M}{M^2 - L_R L_T} \qquad b_5 = \frac{R_T L_R}{M^2 - L_R L_T}$$

If the marker is not in the locator reach i. e. $x \to \infty$ then from (1) it results that the mutual inductance $M=0$. In this case the voltage $u_{CR}(t)$ has maximum value $U_{CRmax}$, which is measured in

steady state after the time reaches $t$=2.5 ms. The proximity of marker then can be detected if the steady value of voltage $U_{CR}$ in time $t$ = 2.5 ms is decreased by $\Delta U_{CR}$:

$$\Delta U_{CR} = |U_{\mathrm{CR\,max}}| - |U_{CR}| \tag{10}$$

The time course of voltage $u_{\mathrm{CR}}(t)$ in the RFID locator circuit (Fig. 4a) was numerically calculated from the system (8) for these parameters of the whole model, which are similar as in the previous chapter:

- Voltage of signal generator $u_1$=10 V, frequency $f$=125 kHz, i. e. $\omega = 2\pi f$ = 785.4 krad/s
- Distance between coils $x$=0.3 m, angle $\theta$=0 °
- Radius of coils $r_R$=0.1 m, $r_T$=0.1 m
- Resistor $R_1$=100 kΩ
- $C_R$=1.621 nF, $L_R$=1 mH, $R_R$=5 Ω, i. e. antenna of locator has resonant frequency $f_R$=125 kHz, quality factor of $L_RC_R$ tuned circuit is $Q_R$=70
- $C_T$=1.621 nF, $L_T$=1 mH, $R_T$=7.85 Ω, i. e. resonant frequency of marker is $f_R$=125 kHz, quality factor of $L_RC_R$ tuned circuit is $Q_R$=100.

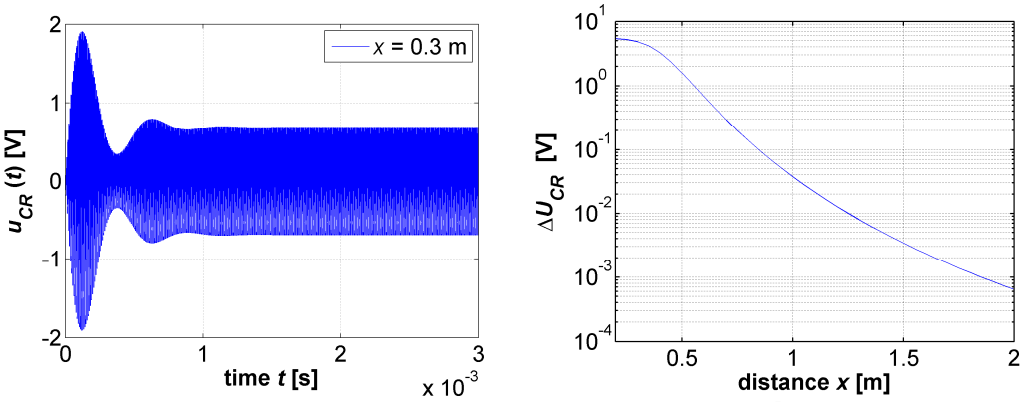


a) b)

**Fig. 4.** a) The time course of voltage $u_{CR}(t)$, distance $x$=0.3 m. b) Detectable voltage change $\Delta u_{\mathrm{CR}}$ versus distance $x$.

## 4. Conclusion

The analyses presented in this paper are a continuation of analyses described in the paper [3] where another method of marker localization (based on periodic marker excitation and response sensing) was described. The signal amplitude returned from marker falls rapidly with increasing distance between locator antenna and marker which is evident from Fig. 2b and Fig. 4b. The signal amplitude depends inversely on the 6$^{\mathrm{th}}$ power of distance $x$, because the mutual inductance $M$ (1) depends inversely on 3$^{\mathrm{rd}}$ power of distance and the analysis based on algebraic equations in [3] showed that the signal amplitude depends inversely on 2$^{\mathrm{nd}}$ power of the mutual inductance. Therefore the real maximum distance of marker proximity detection is no more than 2 – 2.5 m. These mathematical models will be helpful to design new simplified locator antenna consisting of only one coil. At present, the commercial marker locators has two or three coils in antenna.

## Acknowledgement

This paper was supported by KEGA, the Cultural and Educational Grant Agency of Ministry of Education, Science, Research and Sport of the Slovak Republic, grant No. KEGA – 008ŽU – 4/2015: "*Innovation of HW and SW tools and methods of laboratory education focused on safety aspects of IKT solution for safety critical applications within automation*".

# References

[1] FINKENZELLER, K.: *RFID Handbook Fundamentals and Applications in Contactless Smart Cards, Radio Frequency Identification and Near-Field Communication.* Third Edition. John Wiley and Sons, Ltd. Chichester, UK, 2010. ISBN 978-0-470-69506-7

[2] AHMAD, M. Y., MOHAN, A. S.: *RFID Reader Localization Using Passive RFID Tags*. In: Asia Pacific Microwave Conference, APMC 2009, Singapore, December 7th - 10th, 2009, p. 606 – 609, ISBN 978-1-4244-2802-1

[3] VESTENICKÝ, P., MRAVEC, T., VESTENICKÝ, M.: *Mathematical Modelling of Single-bit Passive RFID Marker Localization Methods*. In: ELEKTRO 2014, 10th International Conference, May 19th – 20th, 2014, Rajecké Teplice, Slovakia, p. 504 – 507, ISBN 978-1-4799-3720-2

[4] *RFID made easy*. Application note AN411, EM Microelectronic-Marin SA. Marin, Switzerland, 2002. [online] URL <http://www.emmicroelectronic.com/webfiles/product/rfid/an/an411.pdf>

[5] RŮŽIČKOVÁ, M.: *Discrete and Differential Equations in Applied Mathematics*. In: Communications, Scientific Letters of the University of Žilina, vol. 10, No. 2, 2008, p. 72 – 78. ISSN 1335-4205

**TRANSCOM 2015, 22-24 June 2015**
University of Žilina, Žilina, Slovak Republic

# Power consumption analysis and possibilities of energy saving in WSN applications

[*]Veronika Olešnaníková, *Peter Šarafín, [*]Róbert Žalman, [*]Ondrej Karpiš
[*]University of Žilina, Faculty of Management Science and Informatics, Department of Technical Cybernetics, Univerzitná 8215/1, 010 26 Žilina {veronika.olesnanikova, peter.sarafin, robert.zalman, ondrej.karpis}@fri.uniza.sk

**Abstract.** There is a wide use of WSN technology in many fields. Especially applications placed in terrain need to minimize their energy consumption. In this paper we analyze in which field the consumption may be decreased and using what kind of algorithm we can keep the WSN operating as long as possible. There are discussed three main fields – sensing of signal, preprocessing of the gained signal and communication, especially sending data to the sink node. There is also idea how to use methods of compressed sensing to save energy of nodes.

**Keywords:** WSN, energy consumption, compressed sensing.

## 1. Introduction

Wireless sensor networks are state of the art in the field of intelligent environments. Using WSN, it is possible to monitor required information from surroundings. This system consist of spatial deployed autonomous sensor devices, which are able to interact. Devices are deployed in monitored area and they evaluate status of given object. Basic unit of this networks are modules (nodes) with implemented sensors based on requirements of application. As an example can be mentioned sensing of acoustic emissions from transport, sensing the movement of people in buildings, obtaining of metrological data or wide use of WSN in intelligent buildings. Interaction among individual nodes is ensured via RF communication. According to [1], currently 99% of installed sensors communicates using wires. Expectation for the next 10 years shows that WSN technology should cover 10% of all sensor networks. Currently, there is an expansion of the applications of the “smart” sensors. The difference between standard and intelligent sensor consists in the additional abilities of an intelligent sensor. While standard sensor node sends obtained data only to headquarters, intelligent sensor node is capable of pre-processing this data before transmition and send only partial or complete results and thereby reduce the demand on the transmission channel. Communication in WSN is largely limited. It is often necessary to place the nodes in the places with absence of power source, which results in considerable energy constraints. The power needed for processing and transmission has to be adapted for this requirements. The nodes have defined permeability depending on the application and the available amount of energy. Using WSN technology requires minimum requirements for installation and maintenance. We work with idea how to optimize the consumption of WSN using methods of compressed sensing. The compressed sensing is a method used for capturing signal [2], [3], based on sparse sampling under the conditions that the signal has to be sparse in some domain. This fact results in reduced number of measurements and simplify the process of obtaining data of the surroundings and thus saving energy of network elements.

## 2. Consumption of WSN

One of the reasons for formation of the WSN is the need for placing sensors (static or portable) to remote or inaccessible terrain without established infrastructure. In such an environment there are not any permanent sources of electrical energy accessible, which could be supplying the nodes. In WSN applications, there is still effort to minimize consumption. Electrical power is consumed in the subsystem for capturing signal, the signal processing subsystem and the communication process.

### 2.1. Capturing the signal

To obtain information from environment, it is necessary to capture continuous variables using sensors. This may either be an acoustic, thermal, ultrasonic parameters, data of humidity, pressure or speed and many others. In order to process the data by digital means, they need to be represented in an appropriate digital format. A considerable amount of energy is consumed just in process of analogue to digital conversion of signal samples. Once the signal is digitized, the characteristics of the obtained signal are fixed and there is no possibility to change them. Two basic operations of analog to digital conversion (sampling and quantization) directly affect the characteristics of the digital signal. The conventional approach of signal sampling is to meet the Shannon's theorem, which states that the sampling frequency must be equal to or greater than twice the maximum frequency found in the measured signal. In general, we expect deterministic and periodic (equidistant) sampling. The sampling model, where the signal samples are taken at intervals of constant duration, is the most widely used. It is clear that this approach for obtaining the samples appears to be the most natural and has several advantages. It was introduced some time ago and for some applications is not suitable. For example, when samples should be taken at random intervals or even at random points in time, because of some reasons. Studies show that the randomness of the sampling may not always be negative. Irregularities bring the same benefits, such as suppression of aliasing. Even in case of energy saving randomness can provide good results.

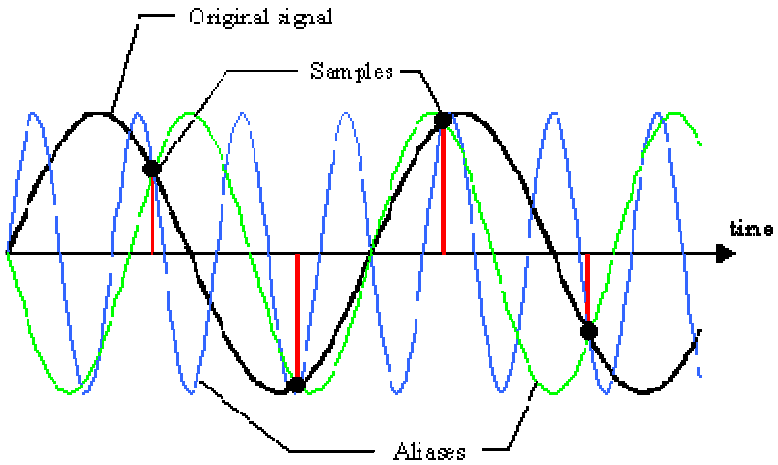


Fig. 1: Periodic sampling – alias effect

Alias effect results to uncertain representation of signal, it can be seen at Fig. 2. These samples of signal can be used in reconstruction for creating original sinusoid. Sine wave plotted in black, corresponds with the data. However, if we follow the possibilities of the reconstruction process, we see that other sinusoids of different frequencies also satisfy the taken samples. There are known methods how to avoid such complications, e.g. using antialiasing filter.

Fig. 3 shows how the alias effect can be avoided by using non-uniform sampling. Sinusoid of the same frequency as in the previous case was sampled. In this case, distances between samples on the time axis are not the same. From the figure it is seen that only one sinusoid fits all samples.

Based on using random sampling, the system for signal processing can be developed. Choosing between periodic and irregular sampling is performed with respect to functionality and quality of output applications. Although the periodic sampling is preferred with high frequencies, the desired sample rate can exceed the capacity of the system, so it is suitable to choose an irregular sampling. However, demands on signal processing increased and it is necessary to use a special and complex algorithms in reconstruction process.

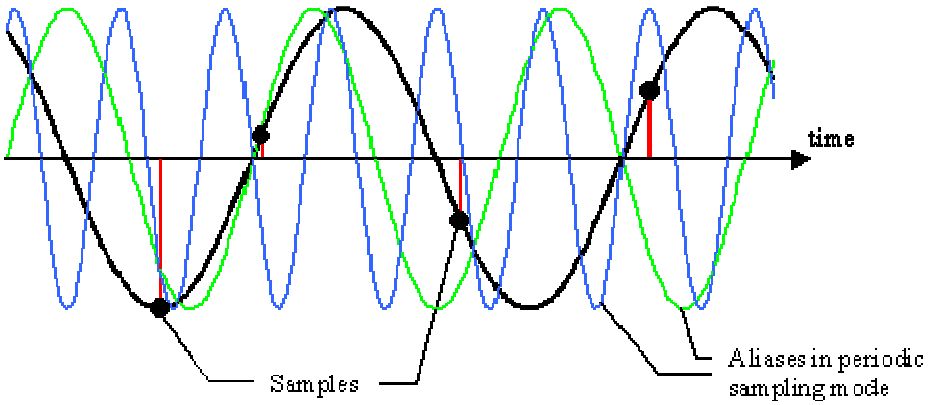


Fig. 2: Aperiodic sampling –alias effect suppression

## 2.2. Preprocessing of the signal

After the sampling process of the signal, the gained samples should be preprocessed in order to extract the required information. In the case of periodic sampling, it is not always necessary to use all collected samples. Therefore exists compression methods of signal preprocessing, which will reduce the number of data. When a compressed sensing is used, signal is directly sampled according to the characteristics of the class of signals, so that samples are taken only in certain random intervals and there is no need for further compression, which reduces the pre-processing and hence saves power of the node.

In digital signal processing, we analyze the signal in different areas, for example in time or frequency domain. Most often a discrete signal is represented in the spectral range in which it is taken using an appropriate transformation. These different transformations are computationally demanding.

## 2.3. Communication – data sending

The most burdensome factor in terms of consumption of WSN is communication, especially sending measured data. Therefore, we try to reduce the volume of data transferred. There are three approaches. The first approach uses signal processing methods to evaluate the data and then only the useful information (final result) is send, which due to the low volume of data minimally spend the energy. In the second approach, characteristics (parameters) of the signal are send. In some cases it is necessary to send the whole captured signal, which is the third case. Using the periodic sampling the volume of transmitted data is very large. Sparse sampling can dramatically reduce the amount and send only useful samples.

In case of selecting sparse sampling, the digital signal processing has to work with algorithm of high computational complexity, which results in an increase of processing power and therefore consumption. In this paper we consider WSN system for collecting data as represented if following figure (Fig. 3). The nodes will be used only for capturing physical quantities using sparse sampling which will save their energy. For sending data to the central node will be used the third type of communication, thus sending all the samples. With the compressed sensing the volume will be

smaller, so it is way to save energy. In the central node there will be applied reconstruction algorithms.

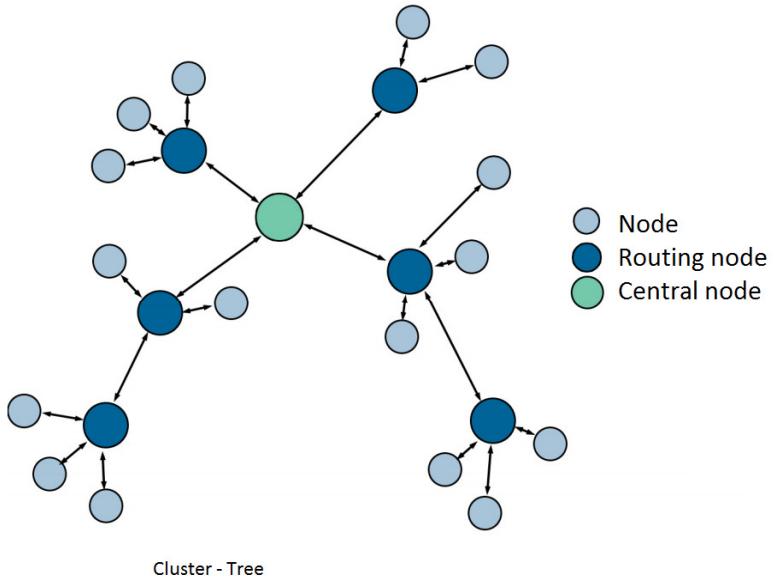


Fig. 3: WSN topology with central computation node

## 3. Compressed sensing in applications

Compressed sensing can potentially be used in all applications, which are designed to reconstruct the signal obtained by linear measurements. In the case of a periodic sampling of a large number of measurements (complete set of measurements), this process is expensive, time-consuming, sometimes dangerous and not always possible. The condition is the sparsity of the signal in a suitable base. In the computational tomography (CT), it is necessary to obtain a picture of the patient's body from different angles using X-rays. Collection of the complete set of measurements would expose the patient long and dangerous dose of radiation, so the number of measurements should be minimized and should guarantee a sufficient quality of image for medical purposes. These images have usually areas whose value is constant, so it is a sparse representation of signals and compression sensing techniques are ideal to use. In fact, this problem led the research and development of methods of compression sensing [4].

Magnetic resonance imaging (MRI) is, like CT essential tool, used for diagnosing patients. Although the patient does not expose hazardous radiation, association with it inherently slow process of data acquisition. The introduction of the compression sensing offers a significant reduction of time required for scanning, benefits for both patients and economics. Other applications where is development in this area are the radar bases. Since they monitored only a small number of targets, the signal sparsity is expected.

There is a big expansion in WSN applications using compression sensing, mainly due to the effectiveness of the node work. The application [5] deals with the collection of scalar physical quantities, e.g. monitoring temperature change in a given geographical area for a certain time. A study [6] deals with deterministic deployment of nodes to detect sparsely occurring events. Event detection is one of the main applications of WSN, this issue using compression sensing is engaged in work[7].

## 4. Conclusion

WSN was analyzed in terms of consumption in each stage of obtaining information. The compressed sensing, field of use and the benefits of a communications subsystem within the WSN

energy-saving individual nodes were described. The main contribution of this work should result in optimal characteristics of WSN. Other benefit would be the classification of various signals with respect to sparse sampling. This work gives and explanation about compressed sensing and formulate the idea how compressed sensing could be used in WSN in order to minimize node energy requirements.

## References

[1] HAROP, P. *Wireless Sensor Networks*, IDTechEx 2008.

[2] EURODASP *Nonuniform sampling*, Application Note, 2001.

[3] HRBÁČEK, R., RAJMIC, P., VESELÝ, V., SPIŘÍK, J. *Řídké reprezentace signálů*, Elektrorevue, 2011.

[4] CAND`ES E. J., TAO T. *Near optimal signal recovery from random projections: universal encoding strategies*, IEEE Trans. Inform. Theory, 52(12):5406–5425, 2006.

[5] CHOU CH. T., RANA R., HU W. *Energy efficient information collection in wireless sensor networks using adaptive compressive sensing*, Local Computer Networks, 2009. LCN 2009. IEEE 34th Conference on , vol., no., pp.443,450, 20-23 Oct. 2009.

[6] JELLALI Z., ATALLAH L. N., CHERIF S. *A study of deterministic sensors placement for sparse events detection in WSN based on Compressed Sensing*, Communications and Networking (ComNet), 2014 International Conference on , vol., no., pp.1,5, 19-22 March 2014.

[7] LIU Y., ZHU X., MA C., ZHANG L. *Multiple event detection in wireless sensor networks using compressed sensing*, Telecommunications (ICT), 2011 18th International Conference on , vol., no., pp.27,32, 8-11 May 2011.

**TRANSCOM 2015, 22-24 June 2015**
University of Žilina, Žilina, Slovak Republic

# A Comparison of Machine Learning Methods for Cancer Classification Using Microarray Expression Data

Jakub Piekoszewski
Kielce University of Technology, Department of Electrical and Computer Engineering,
Al. 1000-lecia P.P. 7, 25-314 Kielce, Poland, e-mail: j.piekoszewski@tu.kielce.pl

**Abstract.** This paper presents a selection of several theoretical tools from the field of artificial intelligence and their application to microarray data classification. Feed forward neural network (multilayer perceptron), neural network with radial basis functions, decision tree, bayesian network, support vector machine, and k-nearest neighbour algorithm have been used for classification. All numerical experiments presented in the paper were performed with the use of four well known in literature datasets: *Leukemia*, *Colon*, *DLBCL*, and *CNS*.

**Keywords:** supervised learning, microarray data analysis, cancer classification, artificial intelligence, decision support system.

## 1. Introduction

During the last two decades, microarray datasets have provided biologists with a powerful tool enabling them to measure the expression levels of thousands of genes in a single experiment. This type of data is used to collect information from tissue and cell samples regarding gene expression differences that could be useful for cancer diagnosis or distinguishing specific types of tumors [2], [8], [12]. The difficulty in microarray analysis is that the number of measurement variables (genes) is very large (tens of thousands), while the number of samples is usually very small (often less than 100 patients). Due to the complexity of the obtained data, any manual analysis is often impossible. Therefore several methods from the field of artificial intelligence have been utilized to build classification models for microarray data. In this study, the four well known cancer classification datasets (*Leukemia, Colon, Diffuse large B-cell lymphomas - DLBCL* and *Central Nervous System - CNS*) have been used to test the proposed classifiers. This paper addresses the supervised classification task where data samples belong to a known class. The following theoretical tools: multilayer perceptron (MLP), neural network with the radial basis functions (RBF), decision tree, bayesian network, support vector machine (SVM), and *k*-nearest neighbor algorithm (*k*-NN) are applied to design six classifiers. A theoretical overview of these tools can be found in [9]. All numerical experiments presented in this paper have been performed with the use of WEKA (Waikato Environment for Knowledge Analysis) software. WEKA is a collection of machine learning algorithms for data mining tasks, available at the WWW server of the University of Waikato in New Zealand (http://www.cs.waikato.ac.nz/ml/weka).

## 2. The classifiers design – an outline

A classification system with $n$ inputs $x_1$, $x_2$, …, $x_n$ and $m$ outputs $y_1$, $y_2$, …, $y_m$ is considered. The number of classes recognized by the system is equal to the number of its outputs. The response of the system on the $j$-th output $y_j \in [0,1]$, $j = 1,2,...,m$ (calculated when the input data are presented to its inputs) represents the degree of membership of input vector for the $j$-th

class. The system is designed from data using the supervised learning scenario and the learning dataset $L_1^{(lrn)}$ in the form of $p$ pairs of the input-output data samples:

$$L_1^{(lrn)} = \{\boldsymbol{x}_s'^{(lrn)}, c_s'^{(lrn)}\}_{s=1}^{p}, \tag{1}$$

where $\boldsymbol{x}_s'^{(lrn)} = [x_{s1}'^{(lrn)}, x_{s2}'^{(lrn)}, ..., x_{sn}'^{(lrn)}]$ ($x_{si}'^{(lrn)} \in \Re$, $i = 1,2,...,n$) is a vector of input data (presented to the classifier inputs), $c_s'^{(lrn)}$ is a class label to which the vector $\mathbf{x}_s'^{(lrn)}$ is assigned. In the frame of the so-called data preprocessing stage, the original learning dataset $L_1^{(lrn)}$ is transformed into a new numerical learning dataset:

$$L_2^{(lrn)} = \{\boldsymbol{x}_s'^{(lrn)}, \boldsymbol{d}_s'^{(lrn)}\}_{s=1}^{p}, \tag{2}$$

where $\boldsymbol{x}_s'^{(lrn)}$ is the same as in (1), whilest $\boldsymbol{d}_s'^{(lrn)} = [d_{s1}'^{(lrn)}, d_{s2}'^{(lrn)}, ..., d_{sm}'^{(lrn)}]$ ($d_{sj}^{(lrn)} \in \{0,1\}$, $j = 1,2,...,m$) is a desirable response of the system, when the input vector $\boldsymbol{x}_s'^{(lrn)}$ is presented to the inputs ($d_{sj}^{(lrn)} = 1$ if the vector $x_s'^{(lrn)}$ is assigned to the $j$-th class and $d_{sj}^{(lrn)} = 0$, otherwise).

During the learning process, the response error $Q_{RMSE}^{(lrn)}$ of the system for the learning dataset $L_2^{(lrn)}$ is minimized:

$$Q_{RMSE}^{(lrn)} = \sqrt{\frac{1}{p}\frac{1}{m}\sum_{s=1}^{p}\sum_{j=1}^{m}(y_{sj}'^{(lrn)} - d_{sj}'^{(lrn)})^2}, \tag{3}$$

where $y_{sj}'^{(lrn)} \in [0,1]$ is a real response of the system on the $j$-th output $y_j$, calculated when the vector $\boldsymbol{x}_s'^{(lrn)}$ is presented to the inputs of the system.. In order to control of the learning process, the response error $Q_{RMSE}^{(tst)}$ of the classifier for the test data $L_2^{(tst)}$ is also calculated in an analogous way as in (3).

## 3. Experiments and results

A typical classification task is to separate healthy patients from cancer patients based on their gene expression profile. There are also dataset in which the goal is to distinguish among different types of tumors. In order to demonstrate the classification methods we use four gene microarray datasets: *Leukemia*, *Colon*, *DLBCL* and *CNS*. Each data set has been divided into two subsets: learning $L_1^{(lrn)}$ and test datasets $L_1^{(tst)}$. The first set contains the 66% of the total number of samples (randomly selected) and the second set contains the remaining 34% of the total number of instances. The appropriate numerical datasets: the learning set $L_2^{(lrn)}$ and test set $L_2^{(tst)}$ have been prepared as it is described in Section 2.

Six classifiers have been designed on the base of: a) two-layer perceptron (2 neurons in the output layer and 50 neurons in the hidden layer) using the backpropagation algorithm (with learning rate equals to 0.3 and momentum rate equals to 0.2; the learning process lasted 1000 epochs), b) neural network with the radial basis function, using *k*-means learning algorithm, c) decision tree, using C4.5 learning algorithm (the minimum number of cases in the leaf equals to 2), d) Support Vector Machine, e) Bayesian network and f) *k*-nearest neighbor algorithm (for the tools d), e), and f) the default parameters provided by WEKA software have been used). The details concerning the learning methods of all considered classifiers used in this paper can be found in [3].

### 3.1. Leukemia dataset

The dataset published in [4] contains 72 samples. Each sample is assigned to one of two possible classes: *acute myeloid leukemia* (AML) or *acute lymphoblastic leukemia* (ALL) and it is described by 7129 gene expression levels. 48 out of 72 samples were used as training data and the remaining 24 as test data. The results of classification for *Leukemia* dataset are presented in Tab. 1.

| Classifier | Learning data set | | | | | | Test data set | | | | | |
|---|---|---|---|---|---|---|---|---|---|---|---|---|
| | Confusion matrix | | | Number of correct decisions | Number of incorrect decisions | $Q_{RMSE}^{(lrn)}$ | Confusion matrix | | | Number of correct decisions | Number of incorrect decisions | $Q_{RMSE}^{(tst)}$ |
| | | ALL | AML | | | | | ALL | AML | | | |
| MLP[1)] | ALL | 32 | 0 | 48 (100.00%) | 0 (0.00%) | 0.0018 | ALL | 15 | 0 | 24 (100.00%) | 0 (0.00%) | 0.1251 |
| | AML | 0 | 16 | | | | AML | 0 | 9 | | | |
| RBF[2)] | ALL | 32 | 0 | 48 (100.00%) | 0 (0.00%) | 0.0000 | ALL | 15 | 0 | 24 (100.00%) | 0 (0.00%) | 0.0000 |
| | AML | 0 | 16 | | | | AML | 0 | 9 | | | |
| Decision tree | ALL | 32 | 0 | 47 (97.92%) | 1 (2.08%) | 0.1421 | ALL | 15 | 0 | 21 (87.50%) | 3 (12.50%) | 0.3437 |
| | AML | 1 | 15 | | | | AML | 3 | 6 | | | |
| SVM[3)] | ALL | 32 | 0 | 48 (100.00%) | 0 (0.00%) | 0.000 | ALL | 15 | 0 | 24 (100.00%) | 0 (0.00%) | 0.0000 |
| | AML | 0 | 16 | | | | AML | 0 | 9 | | | |
| Bayesian network | ALL | 32 | 0 | 47 (97.92%) | 1 (2.08%) | 0.1443 | ALL | 15 | 0 | 23 (95.83%) | 1 (4.17%) | 0.2041 |
| | AML | 1 | 15 | | | | AML | 1 | 8 | | | |
| *k*-NN [4)] | ALL | 32 | 0 | 48 (100.00%) | 0 (0.00%) | 0.0200 | ALL | 15 | 0 | 20 (83.33%) | 4 (16.67%) | 0.4005 |
| | AML | 0 | 16 | | | | AML | 4 | 5 | | | |

[1)] MLP = Multi Layer Perceptron, [2)] neural network with the Radial Basis Functions, [3)] SVM = Support Vector Machine, [4)] *k*-NN = *k*-Nearest Neighbour algorithm.

**Tab. 1.** The results of classification for *Leukemia* dataset

### 3.2. Colon dataset

*Colon* dataset [1] consists of 62 samples and it is described by 2000 gene expression levels. 40 of 62 cases are colon cancer and the remaining are normal healthy tissue. The dataset was divided into training set (41 samples) and test set (21 samples). The results of classification for *Colon* dataset are presented in Tab. 2.

| Classifier | Learning data set | | | | | | Test data set | | | | | |
|---|---|---|---|---|---|---|---|---|---|---|---|---|
| | Confusion matrix | | | Number of correct decisions | Number of incorrect decisions | $Q_{RMSE}^{(lrn)}$ | Confusion matrix | | | Number of correct decisions | Number of incorrect decisions | $Q_{RMSE}^{(tst)}$ |
| | | n[1)] | c[2)] | | | | | n[1)] | c[2)] | | | |
| MLP[3)] | n[1)] | 15 | 0 | 41 (100.00%) | 0 (0.00%) | 0.0028 | n[1)] | 5 | 2 | 16 (76.19%) | 5 (23.81%) | 0.5052 |
| | c[2)] | 0 | 26 | | | | c[2)] | 3 | 11 | | | |
| RBF[4)] | n[1)] | 15 | 0 | 39 (95.12%) | 2 (4.88%) | 0.2056 | n[1)] | 4 | 3 | 16 (76.19%) | 5 (23.81%) | 0.4667 |
| | c[2)] | 2 | 24 | | | | c[2)] | 2 | 12 | | | |
| Decision tree | n[1)] | 15 | 0 | 41 (100.00%) | 0 (0.00%) | 0.0000 | n[1)] | 4 | 3 | 18 (85.71%) | 3 (14.29%) | 0.3780 |
| | c[2)] | 0 | 26 | | | | c[2)] | 0 | 14 | | | |
| SVM[5)] | n[1)] | 15 | 0 | 41 (100.00%) | 0 (0.00%) | 0.0000 | n[1)] | 3 | 4 | 13 (61.90%) | 8 (38.10%) | 0.6172 |
| | c[2)] | 0 | 26 | | | | c[2)] | 4 | 10 | | | |
| Bayesian network | n[1)] | 14 | 1 | 38 (92.68%) | 3 (7.32%) | 0.2601 | n[1)] | 6 | 1 | 16 (76.19%) | 5 (23.81%) | 0.4878 |
| | c[2)] | 2 | 24 | | | | c[2)] | 4 | 10 | | | |
| *k*-NN [6)] | n[1)] | 15 | 0 | 41 (100.00%) | 0 (0.00%) | 0.0233 | n[1)] | 2 | 5 | 12 (57.14%) | 9 (42.86%) | 0.6397 |
| | c[2)] | 0 | 26 | | | | c[2)] | 4 | 10 | | | |

[1)] n = normal healthy tissue [2)] c = cancer, [3)] MLP = Multi Layer Perceptron, [4)] neural network with the Radial Basis Functions, [5)] SVM = Support Vector Machine, [6)] *k*-NN = *k*-Nearest Neighbour algorithm.

**Tab. 2.** The results of classification for *Colon* dataset

### 3.3. CNS dataset

*Central Nervous System* dataset [10] contains 60 patient samples out of which 39 are normal cases and 21 are cancer cases. There are 7129 genes in the dataset. 40 out of 60 samples were used

as training data and the remaining 20 as test data. The results of classification for *Colon* dataset are presented in Tab. 3.

### 3.4. DLBCL dataset

*Diffuse large B-cell lymphomas* dataset contains 77 samples, 58 of which come from diffuse large B-cell lymphoma patients and 19 follicular lymphoma from a related germinal center B-cell lymphoma [11]. Each sample is described by 7070 gene expression levels. The dataset was divided into training set (51 samples) and test set (26 samples).The results of classification for *DLBCL* dataset are presented in Tab. 4.

| Classifier | Learning data set | | | | | | Test data set | | | | | |
|---|---|---|---|---|---|---|---|---|---|---|---|---|
| | Confusion matrix | | | Number of correct decisions | Number of incorrect decisions | $Q_{RMSE}^{(lrn)}$ | Confusion matrix | | | Number of correct decisions | Number of incorrect decisions | $Q_{RMSE}^{(tst)}$ |
| | | c[1] | n[2] | | | | | c[1] | n[2] | | | |
| MLP[3] | c[1] | 14 | 0 | 40 (100.00%) | 0 (0.00%) | 0.0025 | c[1] | 4 | 3 | 14 (70.00%) | 6 (30.00%) | 0.5047 |
| | n[2] | 0 | 26 | | | | n[2] | 3 | 10 | | | |
| RBF[4] | c[1] | 14 | 0 | 39 (97.50%) | 1 (2.50%) | 0.1464 | c[1] | 0 | 7 | 12 (60.00%) | 8 (40.00%) | 0.6325 |
| | n[2] | 1 | 25 | | | | n[2] | 1 | 12 | | | |
| Decision tree | c[1] | 14 | 0 | 40 (100.00%) | 1 (2.08%) | 0.0000 | c[1] | 5 | 2 | 14 (70.00%) | 6 (30.00%) | 0.5477 |
| | n[2] | 0 | 26 | | | | n[2] | 4 | 9 | | | |
| SVM[5] | c[1] | 14 | 0 | 40 (100.00%) | 0 (0.00%) | 0.0000 | c[1] | 4 | 3 | 15 (75.00%) | 5 (25.00%) | 0.5000 |
| | n[2] | 0 | 26 | | | | n[2] | 2 | 11 | | | |
| Bayesian network | c[1] | 14 | 0 | 40 (100.00%) | 0 (0.00%) | 0.0004 | c[1] | 4 | 3 | 14 (70.00%) | 6 (30.00%) | 0.5479 |
| | n[2] | 0 | 26 | | | | n[2] | 3 | 10 | | | |
| *k*-NN[6] | c[1] | 14 | 0 | 40 (100.00%) | 0 (0.00%) | 0.0238 | c[1] | 3 | 4 | 13 (65.00%) | 7 (35.00%) | 0.5778 |
| | n[2] | 0 | 26 | | | | n[2] | 3 | 10 | | | |

[1] c = cancer [2] n = normal, [3] MLP = Multi Layer Perceptron, [4] neural network with the Radial Basis Functions, [5] SVM = Support Vector Machine, [6] *k*-NN = *k*-Nearest Neighbour algorithm.

**Tab. 3.** The results of classification for *CNS* dataset

| Classifier | Learning data set | | | | | | Test data set | | | | | |
|---|---|---|---|---|---|---|---|---|---|---|---|---|
| | Confusion matrix | | | Number of correct decisions | Number of incorrect decisions | $Q_{RMSE}^{(lrn)}$ | Confusion matrix | | | Number of correct decisions | Number of incorrect decisions | $Q_{RMSE}^{(tst)}$ |
| | | d[1] | f[2] | | | | | d[1] | f[2] | | | |
| MLP[3] | d[1] | 38 | 0 | 51 (100.00%) | 0 (0.00%) | 0.0019 | d[1] | 20 | 0 | 25 (96.15%) | 1 (3.85%) | 0.1960 |
| | f[2] | 0 | 13 | | | | f[2] | 1 | 5 | | | |
| RBF[4] | d[1] | 38 | 0 | 51 (100.00%) | 0 (0.00%) | 0.0000 | d[1] | 20 | 0 | 23 (88.46%) | 3 (11.54%) | 0.3397 |
| | f[2] | 0 | 13 | | | | f[2] | 3 | 3 | | | |
| Decision tree | d[1] | 38 | 0 | 50 (98.04%) | 1 (1.96%) | 0.0189 | d[1] | 18 | 2 | 23 (88.46%) | 3 (11.54%) | 0.3375 |
| | f[2] | 1 | 12 | | | | f[2] | 1 | 5 | | | |
| SVM[5] | d[1] | 38 | 0 | 51 (100.00%) | 0 (0.00%) | 0.0000 | d[1] | 20 | 0 | 25 (96.15%) | 1 (3.85%) | 0.1961 |
| | f[2] | 0 | 13 | | | | f[2] | 1 | 5 | | | |
| Bayesian network | d[1] | 38 | 0 | 51 (100.00%) | 0 (0.00%) | 0.0000 | d[1] | 19 | 1 | 24 (92.31%) | 2 (7.69%) | 0.2771 |
| | f[2] | 0 | 13 | | | | f[2] | 1 | 5 | | | |
| *k*-NN[6] | d[1] | 38 | 0 | 51 (100.00%) | 0 (0.00%) | 0.0189 | d[1] | 19 | 1 | 21 (80.77%) | 5 (19.23%) | 0.4306 |
| | f[2] | 0 | 13 | | | | f[2] | 4 | 2 | | | |

[1] d = diffuse large B-cell lymphoma [2] f = follicular lymphoma, [3] MLP = Multi Layer Perceptron, [4] neural network with the Radial Basis Functions, [5] SVM = Support Vector Machine, [6] *k*-NN = *k*-Nearest Neighbour algorithm.

**Tab. 4.** The results of classification for *DLBCL* dataset

## 4. Conclusion

In this paper, six theoretical tools from the area of artificial intelligence have been presented alongside theirs applications to microarray data analysis for cancer classification. Based on the results, it is clear that the methods presented can be useful to support clinical diagnosis for patients. The experimental results might also guide future researches to choose the best classification

approach for their problems in bioinformatics. In the future it is planned to use other alternative methods from the field of computational intelligence, i.e. self-organizing neural networks with growing structures [7] and neuro-fuzzy systems [5], [6].

## Acknowledgement

The numerical experiments reported in this paper have been performed using computational equipment purchased in the framework of the EU Operational Programme Innovative Economy (POIG.02.02.00-26-023/09-00) and the EU Operational Programme Development of Eastern Poland (POPW.01.03.00-26-016/09-00).

## References

[1] ALON, U., BARKAI, N., NOTTERMAN, D. A., GISH, K., YBARRA, S., MACK, D., LEVINE, A. J. *Broad patterns of gene expression revealed by clustering analysis of tumor and normal colon tissues probed by* oligonucleotide arrays. Proceedings of the National Academy of Science, vol. 96(12), 1999, pp. 6745-6750.

[2] BEN-DOR, A., BRUHN, L., FRIEDMAN, N., NACHMAN, I., SCHUMMER, M., YAKHINI, N. *Tissue classification with gene expression profiles.* Journal of Computational Biology, vol. 7, 2000, pp. 559-584.

[3] BISCHOP, C., M. *Pattern Recognition and Machine Learning*. Springer-Verlag, New York, 2006.

[4] GOLUB, T. R., SLONIM, D. K., TAMAYO, P., HUARD, C., GAASENBEEK, M., MESIROV, J. P., COLLER, H., LOH, M. L., DOWNING, J. R., CALIGIURI, M. A., BLOMFIELD, C. D., LANDER, E. S. *Molecular classification of cancer: Class discovery and class prediction by gene-expression monitoring*. Science, vol. 286, 1999, pp. 531-537.

[5] GORZAŁCZANY, M. B. *On some idea of a neuro-fuzzy controller.* Information Sciences, vol. 120, 1999, pp. 69-87.

[6] GORZAŁCZANY, M. B., PIASTA, Z. *Neuro-fuzzy approach versus rough-set inspired methodology for intelligent decision support.* Information Sciences, vol. 120, 1999, pp. 45-68.

[7] GORZAŁCZANY, M. B., PIEKOSZEWSKI, J., RUDZIŃSKI, F. *Generalized tree-like self-organizing neural networks with dynamically defined neighborhood for cluster analysis*. Lecture Notes in Computer Science, vol. 8468, 2014, pp. 713-725.

[8] KHAN, J., WEI, J. S., RINGER, M., SAAL, L. H., LADANYI, M., WESTERMANN, F., BERTHOLD, F., SCHWAB, M., ANTONSCU, C. R., PETERSON, C., MELTZER, P. S. *Classification and diagnostic prediction of cancers using gene expression profiling and artificial neural networks*. Nature Medicine, vol. 7(6), 2001, pp. 673-679.

[9] MITCHELL, T. *Machine Learning*. McGraw Hill, 1997.

[10] POMEROY, S. L., TAMAYO, P., GAASENBEEK, M., STURLA, L. M., ANGELO, M. M., McLAUGHLIN, M. E., KIM, J. Y. H., GOUMNEROVA, L. C., BLACK, P. M., LAU, C., ALLEN, J. C., ZAGZAG, D., OLSON, J. M., CURRAN, T., WETMORE, C., BIEGEL, J. A., POGGIO, T., MUKHERJEE, S., RIFKIN, R., CALIFANO, A., STOLOVITZKY, G., LOUIS, D. N., MESIROV, J. P., LANDER, E. S., GOLUB, T. R. *Prediction of central nervous system embryonal tumour outcome based on gene expression*. Nature, vol. 415(6870), 2002, pp. 436–442.

[11] SHIPP, M. A., ROSS, K. N., TAMAYO, P., WENG, A. P., KUTOK, J. L., AGUIAR, R. C. T., GAASENBEEK, M., ANGELO, M., REICH, M., PINKUS, G. S., RAY, T. S., KOVAL, M. A., LAST, K. W., NORTON, A., LISTER, T. A., MESIROV, J., NEUBERG, D. S., LANDER, E. S., ASTER, J. C., GOLUB, T. R. *Diffuse large B-cell lymphoma outcome prediction by geneexpression profiling and supervised machine learning*. Nature, vol. 8(1), 2002, pp. 68-74.

[12] XU, Y., SELARU, M., Yin, J., ZOU, T. T., SHUSTOVA, V., MORI, Y., SATO, F., LIU, T. C., OLARU, A., WANG, S., KIMOS, M. C., PERRY, K., DESAI, K., GREENWOOD, B. D., KRASNA, M. J., SHIBATA, D., ABRAHAM, J. M., MELTZER, S. J. *Artificial neural networks and gene filtering distinguish between global gene expression profiles of Barrett's esophagus and esophageal cancer*. Cancer Research, vol. 62, 2002, pp. 3493-3497.

**TRANSCOM 2015, 22-24 June 2015**
University of Žilina, Žilina, Slovak Republic

# Comparative Evaluation of GMM and GMM/UBM Speaker Identification Systems

Jozef Polacký, Igor Guoth
Audiolab, Dept. of Telecommunications and Multimedia, Faculty of Electrical Engineering, University of Zilina, Univerzitna 8215/1, 010 26 Zilina, Slovakia, Slovakia, {polacky, guoth}@fel.uniza.sk

**Abstract.** State-of-the-art of speaker recognition is fully advanced nowadays. There are various well-known technologies used to process voice, including Gaussian mixture models (GMM). The paper presents our work on speaker identification from his speech. We build an identity for each person enrolled in our systems using statistical GMM and Universal Background Model (GMM-UBM) developed by using MFCC (Mel Frequency Cepstral Coefficients) speech features. UBM improves GMM statistical computation for decision logic in speaker verification task. As a speech corpus, we used TIMIT database for our experiments. Finally, we compared the recognition accuracy for several different scenarios. The overall accuracy of the system proves advantage of the GMM-UBM approach.

**Keywords:** Speaker identification, GMM-UBM, MFCC features, TIMIT, Matlab

## 1. Introduction

During the past decades, Automatic Speaker Recognition (ASkR) has become a very popular area of research in pattern recognition and machine learning. It is a general term used for any procedure that involves the knowledge of a person's identity on the basis of its speech. ASkR is a general term for speaker identification and speaker verification tasks.

Speaker identification is the process by which the identity of the speaker is not known ahead and system has to decide who it is or put the speaker in a particular group (see Fig. 1). For the identification it must exist the reference speaker model.

Verification process is often used to allow or refuse access to certain resources using the spoken word. In the case of verification the identity of the speaker is known and the role of the system is to verify whether it is really the person for which the speaker is issued.

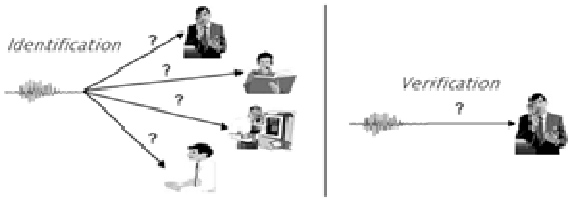


**Fig. 1.** Identification vs. verification process.

ASkR technique is used in many applications such as telephone banking, information security, forensics and so on [1].

One of the biggest problems in ASkR is the mismatch between training and testing conditions caused by several reasons such as channel distortion, different microphones, transmitting channels or utilized encoder. Nowadays, a large number of different solutions to reduce this problem is already known. One of the techniques for noise-robust ASkR is feature enhancement method which attempts to normalize the distorted feature or to estimate undistorted feature from the distorted speech and does not require any explicit knowledge about the noise. Cepstral Mean and Variance Normalization (CMVN) can be mentioned as an example.

In recent years, the Gaussian Mixture Model (GMM) adapted from the so called Universal Background Model (UBM) [2] by Maximum A Posterior (MAP), has become the most popular method in modeling the acoustical space of speech context. These models represent the core technology of majority of the state-of-the-art text-independent speaker recognition systems. This paper presents experiments with the training/testing the ASkR system using either 1) classical GMM, or 2) GMM-UBM approach. The overall accuracy of the system proves advantage of the GMM-UBM approach.

## 2. GMM-UBM verification system

Gaussian Mixture Models used in combination with MAP adaptation [2] represent the main technology of most of the state-of-the-art text-independent speaker recognition systems. In our system the speaker models are derived from a common GMM root model, the so-called UBM, by means of MAP adaptation. Mean, weight vector and covariance matrix adaptation is performed during model training. A speaker is thus represented by the set of the adapted parameters of all the Gaussians of the UBM.

### 2.1. Gaussian Mixture Model

Gaussian Mixture Model [3] is stochastic model, which can be considered as a reference method for speaker recognition. The Gaussian mixture probability density function of model λ consists of a sum of *K* weighted component densities, given by the following equation:

$$p(x \mid \lambda) = \sum_{k=1}^{K} P_k \mathrm{N}(x \mid \mu_k, \Sigma_k) \tag{1}$$

where *K* is the number of Gaussian components, $P_k$ is the prior probability (mixture weight) of the *k*-th Gaussian component, and

$$\mathrm{N}(x \mid \mu_k, \Sigma_k) = (2\pi)^{-\frac{d}{2}} |\Sigma_k|^{-\frac{1}{2}} \exp\left\{-\frac{1}{2}(x-\mu_k)^T \Sigma_k^{-1}(x-\mu_k)\right\} \tag{2}$$

is the *d*-variate Gaussian density function with mean vector $\mu_k$ and covariance matrix $\sum_k$. The prior probabilities $P_k \geq 0$ are constrained as $\sum_{k=1}^{K} P_k = 1$.

For numerical and computational reasons, the covariance matrices of the GMM are usually diagonal. Training a GMM consists of estimating the parameters $\lambda = \{P_k, \mu_k, \Sigma_k\}_{k=1}^{K}$ from a training sample $X = \{\overline{x}_1, .....\overline{x}_T\}$ . The basic approach is to maximize likelihood of *X* with respect to model $\lambda$ is defined as:

$$p(X \mid \lambda) = \prod_{t=1}^{T} p(\overline{x}_t \mid \lambda) \tag{3}$$

The goal is to obtain Maximum-likelihood (ML) parameter estimation. The process is an iterative calculation called the Expectation-Maximization (EM) algorithm [4]. Note that K-means [5] can be used as an initialization method for EM algorithm.

In the identification process, a set of test utterances and its model is compared with each model of the training database. From each comparison between test and training model is obtained a likelihood and the model with the highest score corresponds to the unknown speaker.

Let us assume a group of speakers $S_P=1,2,...S$ represented by GMM´s $\lambda_1$, $\lambda_2$,…$\lambda_S$. Unknown speaker model is identified to each model:

$$\hat{S} = \arg\max_{1 \le k \le S} \sum_{t=1}^{T} \log\left( p\left( \overline{x}_t \mid \lambda_k \right) \right) \tag{4}$$

## 2.2. Universal Background Model

Universal Background Model is an improvement in the field of speaker recognition using GMM. It is typically characterized as a single Gaussian Mixture Model trained with a large set of speakers using the EM algorithm.

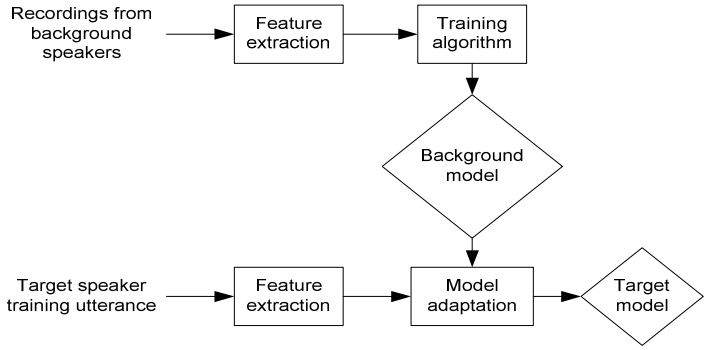


**Fig. 2.** Speaker enrollment

UBM is used for training of the speaker-specific model. The adapted UBM is used as the target speaker model. This process prevents from need for building the speaker model (estimating the parameters) from scratch. There are multiple ways how to adapt the UBM. It is possible to adapt one or more of its parameters as well as all parameters. Adaptation of the parameters is usually done using the MAP. The background model must be built from utterances with common characteristics in the meaning of type and quality of speech. For example, a verification system that uses only telephone channel and female speakers must be trained using only telephone speech spoken by female speakers. For a system where the gender composition is an unknown parameter, the model will be trained using both male and female utterances.

The following average log-likelihood formula gives the final score in recognition process [6]:

$$LLR\left( X, \lambda_{target}, \lambda_{UBM} \right) = \frac{1}{T} \sum_{t=1}^{T} \left\{ \log( p(\overline{x}_t \mid \lambda_{target})) - \log( p(\overline{x}_t \mid \lambda_{UBM})) \right\} \tag{5}$$

where $X = \left\{ \overline{x}_1, ..... \overline{x}_T \right\}$ corresponds to the set of observation or test feature vectors. The higher the score, the more likely the test features belong to the speaker-model with which they are compared.

## 2.3. Feature Extraction

Feature extraction is the process of extracting the speaker and language related feature vectors from the speech signal which can later be used to represent the speaker and the language that the speaker had spoken. It is also known as speech parameterization. VOICEBOX [7] was used on it. The purpose of feature extraction phase is to extract the speaker-specific information in the form of feature vectors which are more compact and more suitable for statistical modeling and the calculation of score. A good feature vector set should have representation of all components of speaker information. The most representative vocal tract acoustic features are Mel Frequency Cepstral Coefficients (MFCC). MFCCs are mostly related to the human peripheral auditory system. The main purpose of the MFCC is to simulate the perception of the human ears [8].

## 2.4. Feature Normalization

The objective of the feature normalization technique is to compensate for the effects of environmental mismatch. The components of the fixed feature vector are scaled or warped so as to

enable more effective modeling of speaker differences. Here, we used short-time mean and variance normalization (STMVN) in one experimental scenario.

In the STMVN technique, *m-th* frame and *k-th* feature space *C* (*m*, *k*) are normalized as:

$$C_{stmvn}(m,k) = \frac{\mathrm{C}(\mathrm{m},\mathrm{k}) - \mu_{st}(m,k)}{\sigma_{st}(\mathrm{m},\mathrm{k})} \tag{6}$$

where *m* and *k* represent the frame index and cepstral coefficients index, *L* is the sliding window length in frames. $\mu_{st}$ *(m, k)* and $\sigma_{st}$ *(m, k)* are the short-time mean and standard deviation, respectively, defined as [9]:

$$\mu_{st}(m,k) = \frac{1}{L}\sum_{j=m-L/2}^{m+L/2} \mathrm{C}(\mathrm{j},\mathrm{k}) \tag{7}$$

$$\sigma_{st}(\mathrm{m},\mathrm{k}) = \frac{1}{L}\sum_{j=m-L/2}^{m+L/2} \left(\mathrm{C}(\mathrm{j},\mathrm{k}) - \mu_{st}(m,k)\right)^2 \tag{8}$$

### 2.5. Evaluation data set

The speaker recognition tests described in this paper were evaluated on the TIMIT Acoustic-Phonetic Continuous Speech Corpus [10]. TIMIT corpus contains recordings of phonetically-balanced English speech. It was recorded using a Sennheiser close-talking microphone at 16 kHz rate with 16 bit sample resolution. TIMIT contains broadband recordings of 630 speakers of eight major dialects regions of the United States, each reading ten phonetically rich sentences resulting in 6300 sentences. The prompts for the 6300 utterances consist of 2 dialect sentences (SA), 450 phonetically compact sentences (SX) and 1890 phonetically-diverse sentences (SI). TIMIT corpus consists of training and test sets. This speech corpus was originally designed as standard database for the speech recognition experiments for several decades and nowadays it is still widely exploited corpus for both speech and speaker recognition experiments [11].

## 3. Experiments and results

The experiment consisted of three different scenarios. One of the tasks was to examine the impact of the speech signal preprocessing and normalization of acoustic features by STMVN on performance of the system for the speaker identification. The second task was to examine the impact of the components number of GMM models of individual speakers. We had two systems. In the first system these models were obtained by basic GMM approach and in the second one were obtained by adaptation of the relevant GMM-UBM model. For each session, the adaptation of all model parameters was applied. Thus, the vectors of weights, mean vectors and the covariance matrix were adapted. Relevance factor was set to 10. For training model was used EM algorithm. The number of iterations of the K-means algorithm was set to 100.

TIMIT database were used for training the UBMs for the proposed system. 630 speakers in total were used for the background model training. For this training, all sentences from all speakers were exploited. For the testing phase, 190 speakers from the first three dialect regions from training set were used. For the speaker specific model training, 5 out of 10 sentences per speaker were utilized and the remaining 5 sentences were used for testing.

This means that two GMM models were obtained for each speaker. The first was trained/adapted by recordings 1-5 from each speaker. The remaining 6-10 recordings were used to test. Reversely, the second one was adapted using recordings 6-10 per speaker, and recordings 1-5 were used to test. Overall, 10x190 tests for each UBM model (different number of components) were conducted. For each session was evaluated recognition performance by calculating success

rate in percentage. These values were statistically averaged and was calculated mean value and variance.

In the first scenario, there were not applied any preprocessing of speech recordings and "raw" recordings were parameterized. For all experiments, 12 MFCC features (excluding log-energy and 0-th coefficient) were used. The analysis frame length was 30 ms with a frame shift of 15 ms with Hamming window.

In the second scenario, the direct component of speech sample was removed, pre-emphasis filter was used and also the normalization of the speech signal was performed. Then silence frames were removed according to the VAD labels. Therein, a basic energy-based VAD was combined with a zero-cross rate based VAD to detect silence frames and MFCCs were calculated.

In the last scenario, feature normalization technique STMVN were additionally applied. Then, a gender-independent basic GMM and UBM models with $2^3$-$2^{10}$ component GMM models were trained for each scenario. Finally, target speakers models were adapted from this UBM models in the second system.

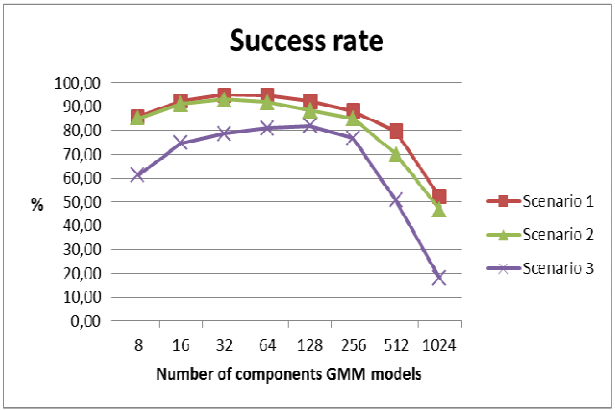


**Fig. 3.** Average success rate for each scenario–basic GMM

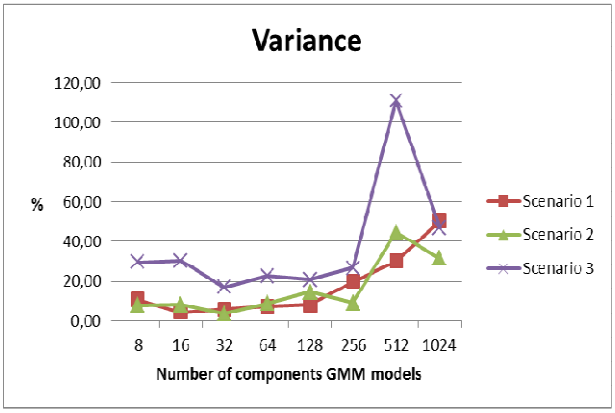


**Fig. 5.** Variance of success rate - basic GMM

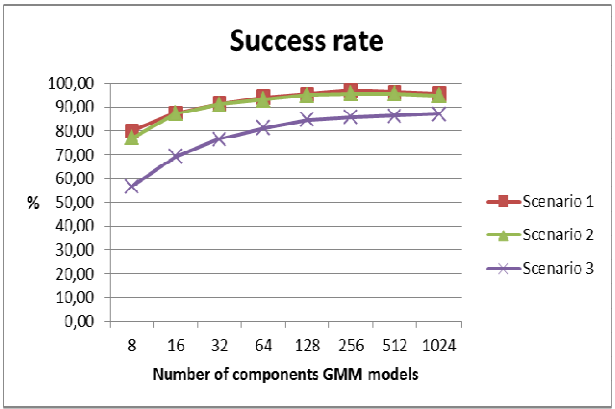


**Fig. 4.** Average success rate for each scenario–GMM-UBM

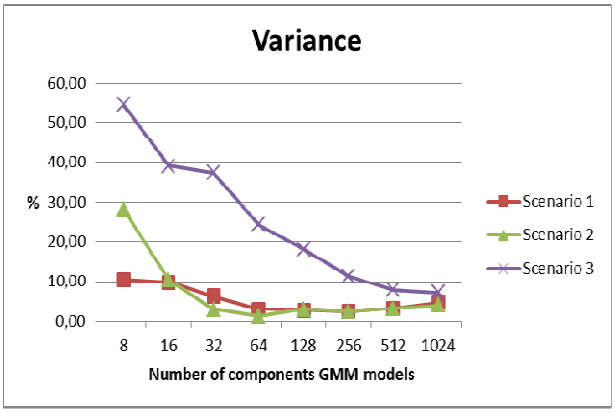


**Fig. 6.** Variance of success rate - GMM-UBM

Figures 3 and 4 show the dependence between success rate of the recognition process and number of components GMM models. At the first one it is seen that success rate grows after 32 component model for the first two scenarios. For scenario 3 it is after 128 component model. For GMM-UBM system it can be seen that success rate grows with the number of components for scenario 3. For the first two scenarios, success rate grows after 256 component model. Then this value slightly decreases for the other two models constellation. From this perspective, together with the time demands associated with the process of training UBM it can be considered as the most appropriate model the one with 256 components in this case. This means that a system with a large number of components of the GMM model may not have always better performance in comparison with the less components model. The similar effect can be seen at the variance of individual sessions when we used GMM-UBM approach. This implies that the results obtained with the

models more components are statistically more balanced and accurate. On the other hand, the opposite effect is in the case of basic GMM approach. From the results it can be seen that the features normalization technique STMVN caused a deterioration of performance in comparison with the other two experiments. The best results were achieved with the use raw speech recordings. From our results it can be seen that the GMM-UBM approach gives better performance in speaker identification tasks. Table 1 shows the complete results for each session.

| GMM components | basic GMM approach | | | | | | GMM-UBM approach | | | | | |
|---|---|---|---|---|---|---|---|---|---|---|---|---|
| | Average success rate [%] | | | Variance [%] | | | Average success rate [%] | | | Variance [%] | | |
| | Sc.1 | Sc.2 | Sc.3 | Sc.1 | Sc.2 | Sc.3 | Sc.1 | Sc.2 | Sc.3 | Sc.1 | Sc.2 | Sc.3 |
| 8 | 85,89 | 85,37 | 61,16 | 10,85 | 8,02 | 29,80 | 79,84 | 77,05 | 56,58 | **10,42** | **28,27** | **54,53** |
| 16 | 92,37 | 91,11 | 74,68 | 4,56 | 8,28 | 30,44 | 87,37 | 87,11 | 69,21 | 9,75 | 10,37 | 39,07 |
| 32 | **94,84** | **93,00** | 78,63 | 5,97 | 3,77 | 17,07 | 91,26 | 91,21 | 76,47 | 6,33 | 3,05 | 37,45 |
| 64 | 94,68 | 91,84 | 81,00 | 7,39 | 8,88 | 22,68 | 93,95 | 93,05 | 81,16 | 3,06 | 1,26 | 24,37 |
| 128 | 92,32 | 88,42 | **81,89** | 8,32 | 14,57 | 21,01 | 95,32 | 94,95 | 84,63 | 2,74 | 3,06 | 18,11 |
| 256 | 88,37 | 85,05 | 76,79 | 19,75 | 9,21 | 26,84 | **97,00** | 95,47 | 85,68 | 2,44 | 2,50 | 11,35 |
| 512 | 79,63 | 70,00 | 50,74 | 30,14 | **44,88** | **111,26** | 95,95 | **95,53** | 86,21 | 3,27 | 3,23 | 7,86 |
| 1024 | 52,26 | 46,74 | 18,05 | **50,47** | 31,51 | 47,15 | 95,47 | 94,79 | **87,00** | 4,66 | 4,07 | 7,15 |

**Tab. 1.** Summary of results for individual conditions.

## 4. Conclusion and future work

In this paper, an analysis of the impact of the number of components of GMM (UBM) model on performance of the system for the speaker identification have been executed. We construct two systems using the GMM and adapted models from UBM for different scenarios described above. We plan to do this analysis with i-vector based strategies as our further step in this research.

## References

[1] YANG, S., ZHAOZHUANG, J., DELIANG, W. An auditory based feature for robust speaker recognition. ICASSP. Taibei, Tanwan. 2009: 4625-4628

[2] REYNOLDS, D.A., QUATIERI, T.F.,DUNN, R.B. Speaker verification using adapted Gaussian mixture models, Digital Signal Processing, vol. 10, no. 1-3, 2000, 19-41

[3] REYNOLDS, D.A., ROSE, R. Robust text-independent speaker identification using Gaussian mixture speakers models, IEEE Trans. On Speech and Audio Processing 3, 1995, 72-83

[4] BISHOP, C. Pattern Recognition and Machine Learning, Springer Science+Business Media, LLC, New York, 2006

[5] LINDE, Y., BUZO, A., GRAY, R. An algorithm for vector quantizer design. IEEE Transactions on Communications 28, 1980, 84-95

[6] KINNUNEM, T., LI, H. An Overwiew of Text-Independent Speaker Recognition: from Features to Supervectors, Speech Communication, 2009

[7] BROOX, M. VOICEBOX: Speech Processing Toolbox for MATLAB. [Online]. Available: http://www.ee.ic.ac.uk/hp/staff/dmb/voicebox/voicebox.html

[8] REYNOLDS, D.A. An overview of Automatic Speaker Recognition Technology, MIT Lincoln laboratory, 244 wood St. Lexinton, MA 02140, USA, IEEE, 2002

[9] ALAM, M. J., OUELLET, P., KENNY, P.,O´SHAUGHNRSSY, D. Comparative Evaluation of Feature Normalization Techniques for Speaker Verification, Canada, 2011

[10] GAROFOLO, J., LAMEL, J. ET AL. DARPA, TIMIT Acoustic-Phonetic Continuous Speech Corpus CD-ROM. National Institute of Standards and Technology, 1990

[11] LOPES, C., PERDIGAO, F. Phoneme Recognition on the TIMIT Database, Speech Technologies, Prof. Ivo Ipsic (Ed.), 2011, ISBN: 978-953-307-996-7, InTech

**TRANSCOM 2015, 22-24 June 2015**
University of Žilina, Žilina, Slovak Republic

# Noise Characteristics of Sensors in Smartphones

[*]Jan Racko
[*]University of Žilina, Faculty of Electrical Engineering, Department of Telecommunications and Multimedia, Univerzitná 1, 01026 Žilina, Slovakia, {jan.racko}@fel.uniza.sk

**Abstract.** Inertial systems generally consist of various sensors, e.g. gyroscope, accelerometer etc. Standard smartphones are equipped with these sensors and data from them can be utilized in position estimation process. Main drawback of the sensors implemented in smartphones is their low quality compared to special external sensors. Therefore, sensors in smartphones are useless separately and data from them had to be fused in order to achieve reasonable accuracy. In order to fuse data from sensors it is necessary to evaluate their characteristics. One of important characteristic is noise characteristic. In this paper we are investigating noise characteristics of sensors implemented in smartphones. There are many negative factors affecting smartphone sensors and some of these factors will be mentioned. Result obtained in paper will be basis for future work.

**Keywords:** gyroscope, accelerometer, inertial system, noise, spectrum.

## 1. Introduction

Location based services (LBSs) have become more and more attractive not only for users, but especially for service providers. Providers recognized huge potential of LBSs and offer plenty of services. LBSs are widespread in outdoor environment using mainly position estimates from GNSS (Global Navigation Satellite Systems). Currently, the idea is to provide LBSs not only in outdoor but also in indoor environment. Therefore, many research teams work on novel positioning systems that will able to provide seamless positioning in outdoor and indoor environment. There are more possibilities how to reach such goal.

Outdoor positioning and navigation do not represent problem these days thanks to GNSS technology. Almost every new mobile device is equipped with at least one GNSS receiver, most commonly represented by GPS. Currently, the issue in development of mobile positing systems is to accurately estimate position in indoor environment. This problem cannot be solved by GNSS, since signals from satellites are highly attenuated by building walls.

Therefore, appropriate solutions usable in indoor represent hot topic for many research teams [1], [2], [3]. One of the possibilities how to implement indoor localization is utilization radio networks. These systems are based on measuring various signal parameters, e.g. ToA (Time of Arrival), AoA (Angle of Arrival), RSS (Radio Signal Strength) [4]. On the other hand, inertial systems represent another possibility for localization in indoor environment and will be discussed in this paper. Inertial system is a self-sufficient navigation system consisting of three orthogonal accelerometers, used for velocity measurements and three orthogonal gyroscopes used for measurements of angular velocity. These sensors form IMU (Inertial Measurement Unit) and can be found in smartphones. Therefore, there is no need to implement additional sensors for position estimation by smartphone.

The question is how sufficient are sensors implemented in a smartphone for position estimation. In this paper the focus will be on noise and its impact on sensor´s accuracy.

Brief principle of particular sensors will be described in Section 2. Adverse effects will be described in Section 3. Section 4 will deal with mathematical models for measured data evaluation and measurement scenario. Evaluation of measurements is analyzed in Section 5.

# 2. Sensors

Nowadays smart phones may contain various sensors, such as pressure sensors, proximity sensor and inertial sensors, e.g. accelerometer, gyroscopes and magnetometer. In this section the main focus will be on description of inertial sensors functionalities.

## 2.1. Gyroscope

There are many types of gyroscopes depending on working principle, e.g. mechanic, optic and Micro Electro Mechanical System (MEMS). MEMS gyroscopes are widely implemented in smartphones due to their small size.

MEMS gyroscopes work on Coriolis force principle. Coriolis force affects an object with mass $m$ [kg], moving by speed $v$ [m/s], in rotating system with angular velocity $\omega$ [rad/s] (Fig. 1.). The resulting Coriolis force $F_C$ is determined by:

$$F_C = 2m\bar{v} \times \bar{\omega} \text{ [N].} \tag{1}$$

The principle is based on a resonating structure attached to inner frame, which moves in a given direction. At the same time Coriolis force equals to angular velocity of rotation, which compresses the outer structure and causes a shift between the measuring surfaces functioning as an air compressor. Output from MEMS gyroscope is given by the change of capacity proportional to angular velocity of device in [°/s].

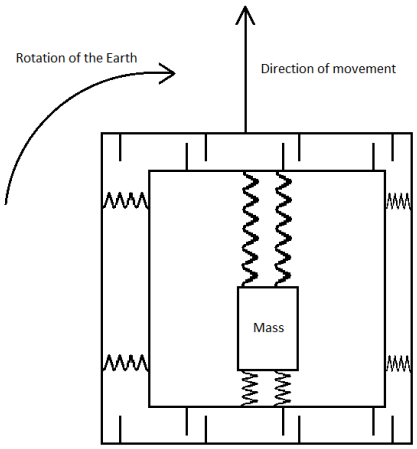


**Fig. 1.** Operation principle of MEMS gyroscope.

To obtain the tilt we have to integrate the output in time:

$$\theta = \int_0^{\infty} \omega(t)dt \,. \tag{2}$$

Here we come to the issue with the integration of noise. Whatever the quality of gyroscope output is, it is always affected by the noise. This causes a deviation from zero value even by simple integration [5], [6], [7].

## 2.2. Accelerometer

Similarly to the gyroscope, accelerometer represents a simple MEMS structure. The main measured unit is acceleration:

$$a = \frac{F}{M} \text{ [m/s}^2\text{].} \tag{3}$$

The output is given by both dynamic acceleration of user and gravity acceleration in [m/s$^2$]. If we leave the device lay still on a solid surface, sensor will exhibit acceleration even though it is not moving. This is caused by accelerometer measuring the gravity acceleration, which needs to be eliminated. In case the device is in free fall, sensors will exhibit zero acceleration, since acceleration towards earth will be equal to gravity acceleration.

Accelerometer sensors work on capacity principle (Fig. 2.). Changes in state of device create a shift of mass against the direction of movement, what changes the distance between conductors. Capacity change is directly proportional to acceleration, therefore, the acceleration in the given axis can be estimated [8], [9].

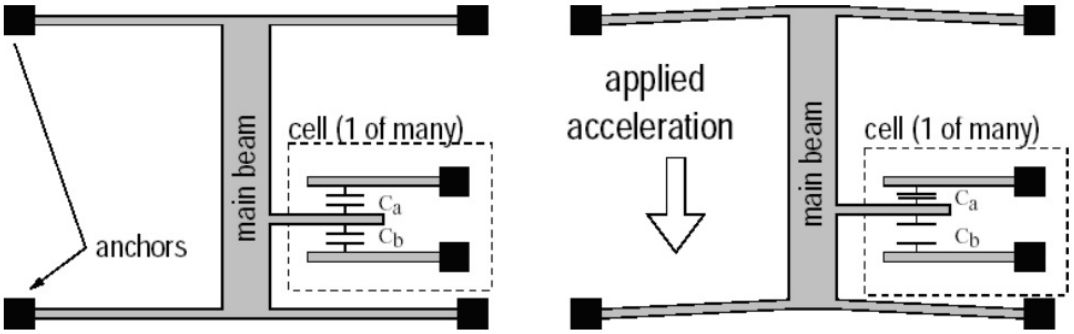


**Fig. 2.** Operation principle of MEMS accelerometer [10].

## 3. Sensors accuracy

Accuracy of sensors is affected by many effects, however, only the most important ones will be described in this section. The most negative effect is Bias. In case of ideal gyroscope it would be possible to get rotation by a simple integration of its output signal. If this was the case, the output would be zero if the device was not rotating. In case of gyroscope we state the bias in °/h or rad/s. The bias of a sensor can be divided to offset and drift. Offset can be estimated by averaging measured values, if no strength affects the device. Drift is a random element and can be determined by probability methods.

Another possible source of errors is deflected axes. This error is given by inaccuracy of manufacturing and it is presented by non-orthogonal axes.

The biggest source of noise in MEMS is thermal noise, which can be found in both accelerometers and gyroscopes. The principle of thermal noise is random movement of charged particles. Theoretically we can say that thermal noise would not represent a problem in systems with temperature equaling absolute zero.

All named effects will combine to localization error. The detailed explanation can be seen in [9], [11], [12].

## 4. Scenario

The objective of the experiment is to find out the frequency characteristic of output signal. Device used during the experiment was Samsung Galaxy S4 smartphone with an LSM 330 chip. Measurements were done on solid wooden surface in calm state without any negative outer interference. Single measurement time was set to 10 minutes, with measurements performed every 5 ms, which result in 200 records per second. Data were recorded from both accelerometer and gyroscope. Noise appears on these sensors and it can cause inaccuracy and errors in positioning. We have transferred the measured values from time domain to frequency domain by using DFT (Discrete Fourier Transform), where frequency compounds affect the output signal:

$$S(k) = \sum_{n=0}^{N-1} s(n) e^{-j\frac{2\pi}{N}kn} . \quad (4)$$

## 5. Results

Negative effects are similar for both. Data measured by accelerometer are shown in time and frequency domain for all axes in Fig. 3. It was assumed that the data should be zero. Impact of bias causes offset from true values, which after double integration will result in error in estimated position. Thermal noise is responsible for effect of random walk. It causes that it looks like smartphone is moving even though it is not.

Bias causes on axis *x* and *y* drift resulting in the shift to higher values. Output data were filtered by a low-pass filter before they were collected. It allowed us to avoid the high frequency compound. Adverse effects have low frequency character with high DC component which causes that data have initial value.

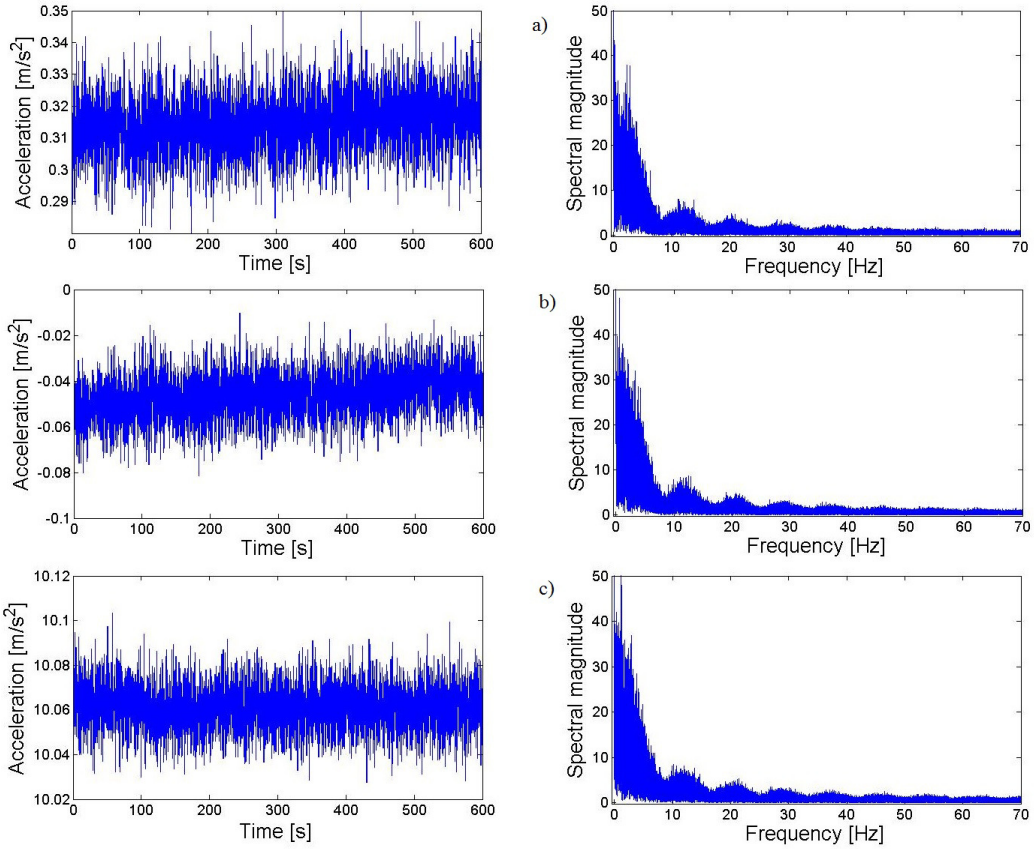


**Fig. 3.** Data measured by accelerometer in time domain and frequency domain a) x-axis b) y-axis c) z-axis.

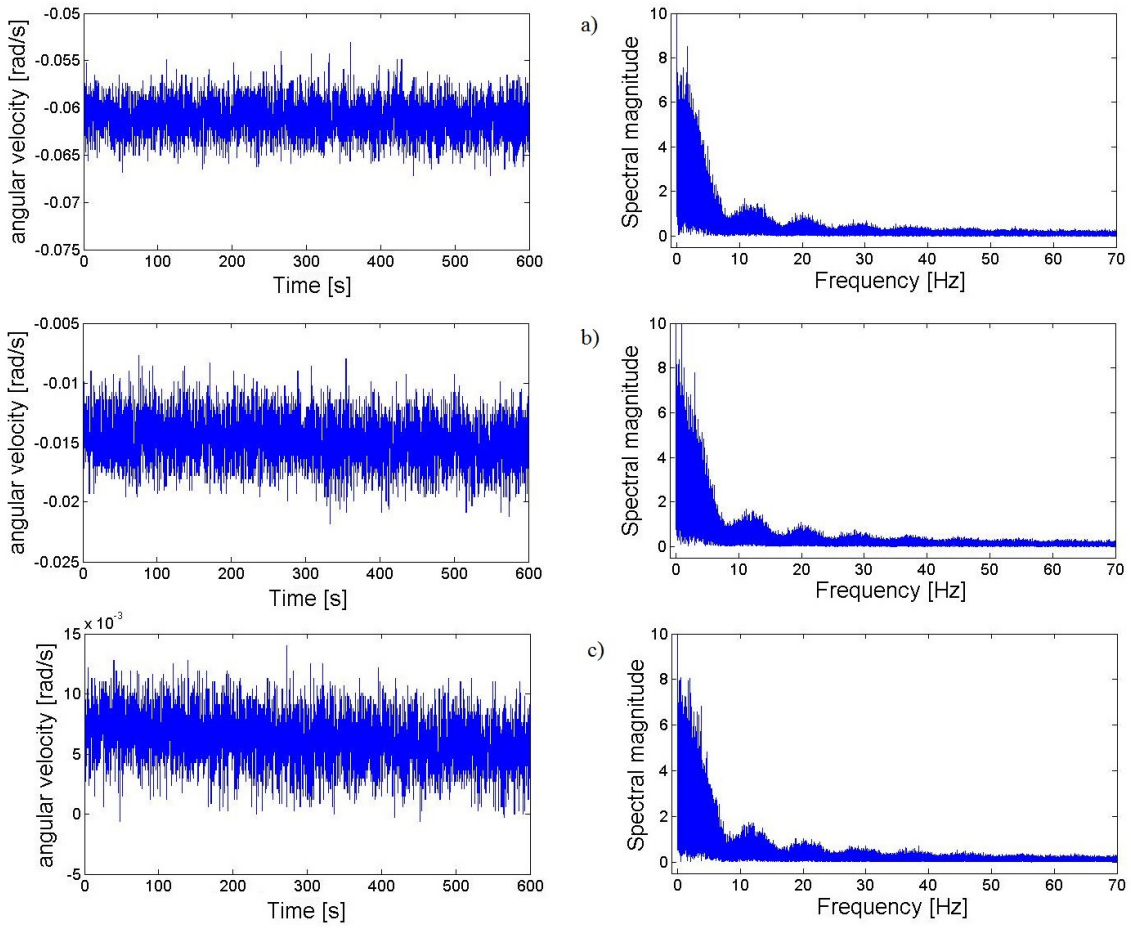


**Fig. 4.** Data measured by gyroscope in time domain and frequency domain a) x-axis b) y-axis c) z-axis.

Data measured by gyroscope are shown in time and frequency for all axes in Fig. 4, where zero values are expected. Real output data shows nonzero values affected by adverse effects. The first negative effect is Bias, which causes rotation error after integration.

Another negative effect is thermal noise. Thermal noise causes smartphone to look like it is changing rotation even though smartphone is still. Bias causes on axis *x* and *y* drift resulting in the shift to lower values. It can be seen that spectral characteristic of gyroscope adverse effect have similar character as accelerometer. Deflected axis and thermal noise cannot be influenced. To gain better results Bias can be reduced by short measuring output data and then averaging them. The result is value which can be subtracted from measured data.

As mentioned above Bias can be reduced by short measuring output data and their averaging. But this gives us only reducing Bias negative effects. Measured data are affected by noise, which causes positioning error after integration and this error rises with time. Output data are more inaccurate if Bias is presented. Output data from accelerometer and gyroscope are separately useless. Therefore Kalman filter has to be used to fuse data from the sensors. Similar results are gained by using Complementary filter, which is easier to use.

## 6. Conclusion

In this paper, basic principles of sensors used in inertial system were described. Spectral characteristics of inertial sensors and determined frequency character of noise, which is affecting measurements was investigated. According to obtained data it is seems, that accelerometer and gyroscope are affected by adverse effects i.e. bias and thermal noise. These results confirmed assumption about low frequency noise character. The future work will be focused on the sensor

fusion and creation of inertial navigation with sensors used in smartphones by utilization of Kalman filter.

## Acknowledgement

This work was partially supported by the Slovak VEGA grant agency, Project No. 1/0394/13 and by Centre of excellence for systems and services of intelligent transport, ITMS 26220120028 supported by the Research & Development Operational Programme funded by the ERDF.

## References

[1] ROMANOVAS, M., GORIDKO, V., KLINGBEIL, L., MANOLI, Y. *A Study on Indoor Pedestrian Localization Algorithms with Foot-Mounted Sensors*. 2012 International Conference on Indoor Positioning and Indoor Navigation IPIN, 2012, pages: 1-10.

[2] HELLMERS, H., NORRDINE A., BLANKENBACH, J., EICHHORN, A. *An IMU/Magnetometer–Based Indoor Positioning System Using Kalman Filtering*. 2013 International Conference on Indoor Positioning and Indoor Navigation IPIN, 2013, pages: 1-9.

[3] ASCHER, CH., WERLING, S., TROMMER, G. F., ZWIRELLO, L., HANSMANN, C., ZWICK, T. *Radio-Assisted Inertial Navigation System by Tightly Coupled Sensors Data Fusion: Experimental Results*. 2012 International Conference on Indoor Positioning and Indoor Navigation IPIN, 2012, pages: 1-7.

[4] FINK, A., BEIKIRCH, H., VOSS, M., SCHRODER, CH. *RSSI-Based Indoor Positioning Using Diversity and Inertial Navigation.* 2010 International Conference on Indoor Positioning and Indoor Navigation IPIN, 2010, pages: 1-7.

[5] PATEL, CH., McMLUSKEY, P. *Modeling and simulation of the MEMS vibratory gyroscope*. 2012 13th IEEE Intersociety Conference on Thermal and Thermomechanical Phenomena in Electronic System, 2012, pages: 928-933.

[6] PATEL, CH., McMLUSKEY, P. *Performance and reliability of MEMS gyroscope at high temperatures.* 2010 13th IEEE Intersociety Conference on Thermal and Thermomechanical Phenomena in Electronic System, 2010, pages: 1-5.

[7] WEN, M., WANG, W., LUO, Z., XU, Y., WU, X., HOU, F., LIU, S. *Modeling and analysis of temperature effect on MEMS gyroscope.* 2014 IEEE 64th Electronic Components and technology Conference, 2014, pages: 2048-2052.

[8] XIONG, X., WU, Y-L., JONE W-B. *Material fatigue and reliability of MEMS accelerometers.* IEEE International Symposium on Defect and Fault Tolerance of VLSI Systems, 2008, pages: 314-322.

[9] SZUCS, Z., NAGY, G., HODOSSY, S., RENCZ, M., POPPE, A. *Vibration combined high temperature cycle tests for capacitive MEMS accelerometers.* THERMIC 2007, 2007, pages: 215-219.

[10] EL-SHEIMY, N. *Inertial Techniques and INS/DGPS Integration.* ENGO 623 Lecture Notes, The University of Calgary, 2013.

[11] TATAR, E., MUKHERJEE, T., FEDDER, G. K. *Simulation of stress effects on mode-matched MEMS gyroscope Bias and scale factor.* Location and Navigation Symposium – PLANS 2014, 2014, pages: 16-20.

[12] DIAO, Z., QUAN, H., LAN, L., HAN, Y. *Analysis and compensation of MEMS gyroscope drift.* 2013 Seventh International Conference on Sensing Technology, 2013, pages: 592-596.

**TRANSCOM 2015, 22-24 June 2015**
University of Žilina, Žilina, Slovak Republic

# Impact of Four-wave Mixing on Optical Transmission Systems

[*]Jana Sajgalikova, [*]Jan Litvik, [*]Milan Dado
[*]University of Zilina, Faculty of Electrical Engineering, Department of Telecommunications and Multimedia, Univerzitna 1, 010 26 Žilina, Slovakia, {jana.sajgalikova, jan.litvik, milan.dado}@fel.uniza.sk

**Abstract.** Most of current core networks utilizes wavelength division multiplex for fulfill of increasing data demands. The most dominant degradation effect in these optical systems is four-wave mixing (FWM) with other nonlinearities. In this paper, impact of four-wave mixing for different channel spacing in multi-channel optical communication system was simulated. This impact is evaluated through Bit Error Rate, eye diagram and output spectrum of transmitted channels. Eliminating of FWM is caused by unequal channel spacing and by varying dispersion and input power. As simulation tool was used VPIphotonic. The simulations show, that impact of FWM is under certain conditions possible suppress and improve then transmission characteristics of optical communication systems.

**Keywords:** FWM, WDM, channel spacing, dispersion, power.

## 1. Introduction

Wavelength division multiplexing (WDM) is commonly used method of multiplexing, which enables high speed transmission information data. Fiber nonlinearities are the one of main degradation effects in high data rate optical communication systems. Optical fiber is nonlinear dispersive medium, which exhibits nonlinear effects, when the high intensity optical signal is launched to the optical fiber, which lead to high levels of power density. The power dependence of refractive index (for amorphous materials) has its origin in the third-order nonlinear susceptibility $\chi^{(3)}$ [1]. The nonlinear phenomenon, knows as four-wave mixing (FWM), also originate from it. In this paper, we have simulated and evaluated the effect of FWM products in WDM by varying channel spacing, dispersion and input power [1-15].

The four-wave mixing is one of the dominating degradation phenomenon in non-linear optics which occurs in multi-channel communication systems. It arises from a third-order optical nonlinearity, as is described in [2] with a $\chi^{(3)}$ coefficient. It occurs when two or more different frequency components propagate together in optical fiber. Interactions between two co-propagating optical signals produce two new group of optical spectral components at different frequencies. The newly produced FWM products can mix with information channels or themselves to produce higher-order FWM products. These cross products cause the interference of information signal with these new products since they often fall near or on top of the desired signals. It can overlap with channels and result in crosstalk. For the future optical multi-channel systems with high-order modulation formats, stochastic nature of FWM will be also the crucial limiting factor and therefore we assume its further investigation will be necessary. Otherwise, FWM can provide beneficial properties and the opportunity for wavelength conversion of WDM channels or signal amplification. FWM can be useful for parametric amplification, optical phase conjugation, wavelength conversion, demultiplexing of OTDM channels or super-continuum generation [1, 2, 5-7, 9, 12, 16, 17].

The paper is organized as follows. The first chapter is focused on origin of FWM. The following chapter deals with the possibility of eliminating of FWM by different channel spacing, different value of dispersion parameter and different value of power. After that are presented results of this simulations.

## 2. Origin of FWM

On a fundamental level, FWM process represents a scattering process in which two photons with energies $\hbar\omega_1$ and $\hbar\omega_2$ are destroyed, and their energy appears in the form of two new photons with energies $\hbar\omega_3$ and $\hbar\omega_4$ (the law of conservation of energy applies) [1].

Mixing of optical energy at the two different frequencies $\omega_1$ and $\omega_2$ causes creates of new frequencies which can be determined as $\omega_{112}$ and $\omega_{221}$ follows [2, 5, 7, 12-14]:

$$\omega_{112} = 2\omega_1 - \omega_2 , \tag{1}$$

$$\omega_{211} = 2\omega_2 - \omega_1 . \tag{2}$$

The Figure 1 shows new created frequencies ($\omega_{112}$, $\omega_{221}$) in multi-channel communication systems caused by FWM.

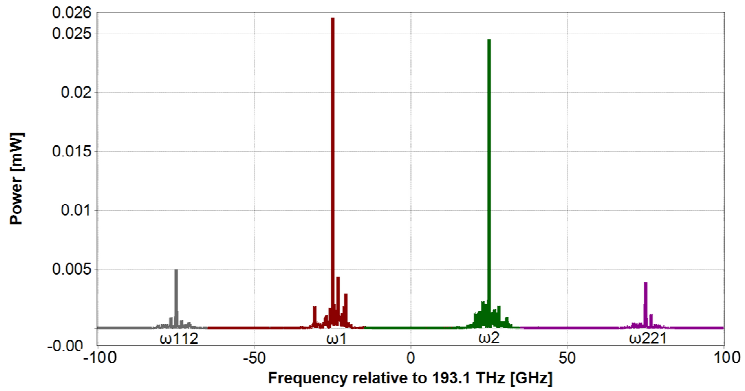


**Fig. 1.** Schematic diagram that shows four-wave mixing in the frequency domain.

For FWM are important two conditions which have to be fulfilled for generating new optical waves; it is a frequency condition and a phase matching condition. The second one is a requirement of momentum conservation. The phase mismatch is the main reason behind FWM. The frequency condition for degenerative and non-degenerative combinations is given by [6-9, 11, 13]:

$$\varpi_{FWM} = \left\{ \begin{array}{l} \varpi_i + \varpi_j - \varpi_k , \text{ if } i \neq j \neq k \\ \quad \rightarrow \text{non-degenerative FWM} \\ \varpi_i + \varpi_j - \varpi_k , \text{ if } i = j \neq k \\ \quad \rightarrow \text{degenerative FWM} \end{array} \right\}. \tag{3}$$

The degenerative FWM is often the dominant process and highly impacts the system performance.

The number of new generated FWM components increases with the increase of information channels in WDM systems. Theoretically, the total number of new generated FWM components $N$ for given number of information channels $M$ can be express as [6, 8, 9]

$$N = \frac{M^2 (M-1)}{2}. \tag{4}$$

The Figure 2 shows the dependence of new generated FWM products on the number of channels. According to (4), it can be easily seen the exponential growth of number of FWM components with increasing number of optical information channel [8].

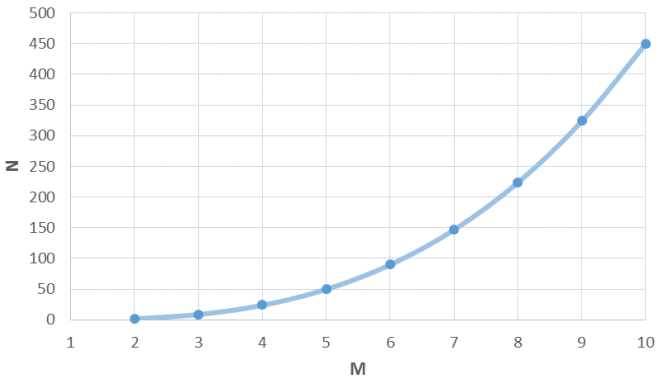


**Fig. 2.** Number of new generated FWM products.

## 3. Eliminating FWM and Simulation Setup

FWM represents serious limits in WDM transmission systems. Impact of FWM can be suppress by increasing the spacing between the channels, increasing the chromatic dispersion of the transmission fiber and decreasing the average input power per channel [1, 3, 5, 6, 12].

In this simulation are used two types of channel spacing in WDM system, equidistant channel spacing (current ITU grid specifies $\Delta f$ = 100, 50, 25 and 12.5 GHz) and non-equidistant channel spacing ($\Delta f \neq$ const.). One way how to suppress FWM impact in transmission system is to increase the spacing between the channels or use unequal channel spacing. In this new scheme of channel arrangement, the new optical waves fall outside of useful optical channels and thus decrease the possibility of intra-channel interference.

In this paper, we use VPIphotonic as simulation tool. It was simulated the effect of FWM in 4 × 10 Gbit/s WDM transmission system configuration (schematic illustration on Fig. 3.). We used DSF fiber (ITU-T G. 653) with nonlinear refraction index $n_2$ = 2.2×10$^{-20}$ m$^2$/W and attenuation $\alpha$ = 0.2 dB/km. Total input power launched into optical fiber was $P_{in}$ = 4 mW and length of optical fiber was $L$= 70 km. Impact of FWM at the propagation information signals are evaluated through BER, eye diagram and optical spectrum by using VPIPhotonicAnalyzer tool.

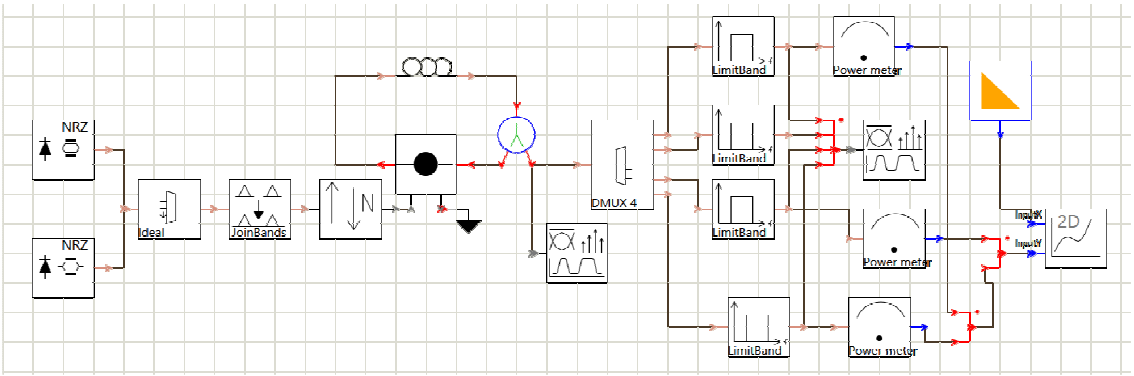


**Fig. 3.** Schematic illustration of a multi-channel transmission system for simulation FWM.

We have investigated the effect of FWM in WDM optical transmission system for two cases. Firstly, the four input signals were launched at 193.1 THz ± 1.5 channel spacing (CHS) and 193.1 THz ± 0.5 CHS, so that they have uniform spacing (100, 50, 25 and 12.5 GHz). In the latter case, we used unequal channel spacing, the four signals at 193.1 THz – 1.5 CHS, 193.1 THz - 0.4 CHS, 193.1 THz + 0.6 CHS and 193.1 THz + 1.5 CHS. The results are presented through BER (Fig. 4.), eye diagram (Fig. 5.) and output optical spectrum (Fig. 6.).

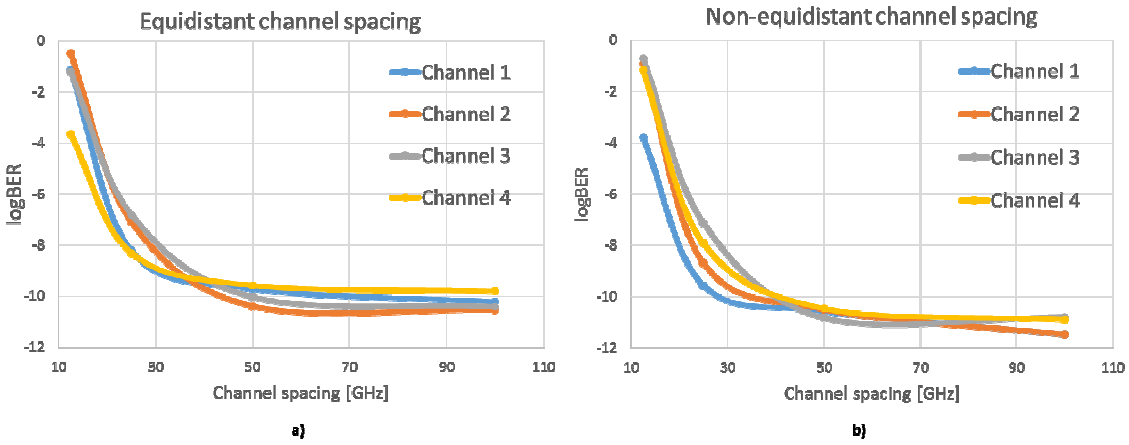


**Fig. 4.** Dependence of BER versus a) equidistant and b) non-equidistant channel spacing, respectively.

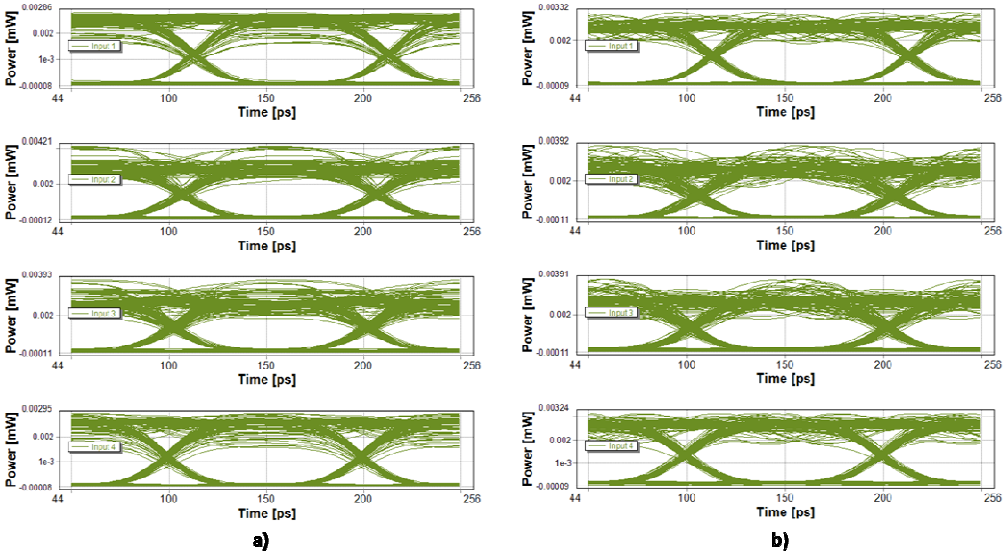


**Fig. 5.** Eye diagram of 4-channel WDM transmission system for a) equidistant and b) non-equidistant channel spacing, respectively.

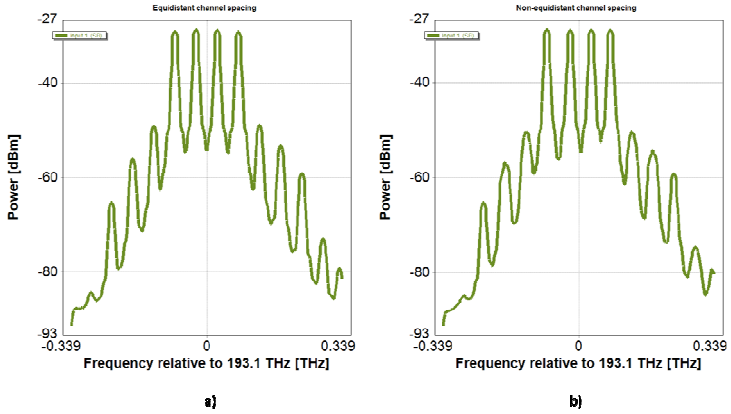


**Fig. 6.** Optical spectrum of 4-channel WDM transmission system for a) equidistant and b) non-equidistant channel spacing, respectively.

Results show that FWM effect depends on channel separation. From Fig. 4., it is seen that the BER improves with increasing channel spacing, because smaller the spacing between input channels, occurs more the interference between information channels. On increasing the spacing between the input information channels, the impact of FWM decreases. Further FWM can be reduced by unequal channel spacing techniques between the channels of the WDM channels.

The result of the unequal channel spacing (right part of figures) is compared with equal channel spacing (left part of figures) for the same system configuration. It is seen, that at channel spacing 50 GHz the BER is about $10^{-10}$ for equal channel spacing and BER about $10^{-11}$ for the same value of channel spacing in the case of unequal channel spacing. This comparison clearly shows the difference in the eye diagrams, which is better for non-equal channel spacing (the wider eye opening).

Also FWM effect was analyzed for different channel separation and by varying the dispersion parameter in the range $D$ = 1 - 7 ps/(nm×km) (Fig. 7.) and input power (Fig. 8.).

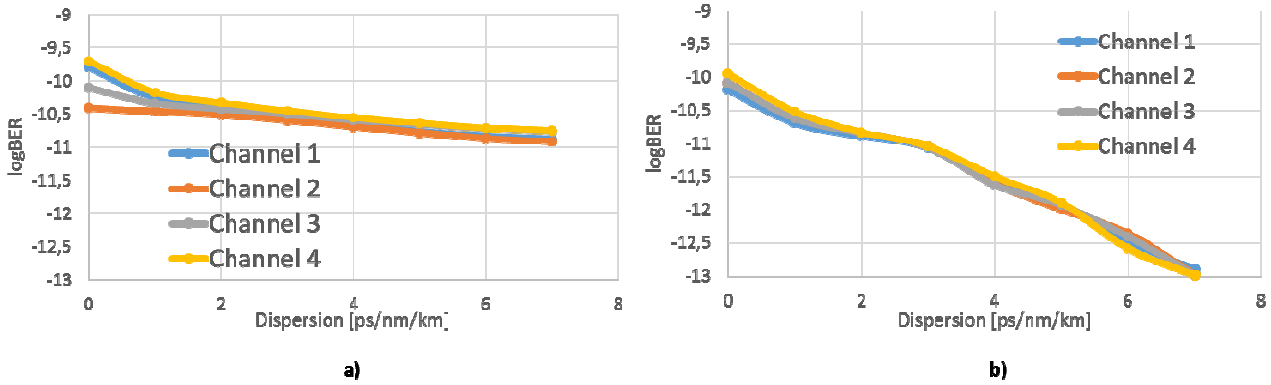


**Fig. 7.** Dependence of BER versus dispersion parameter for a) equidistant and b) non-equidistant channel spacing, respectively.

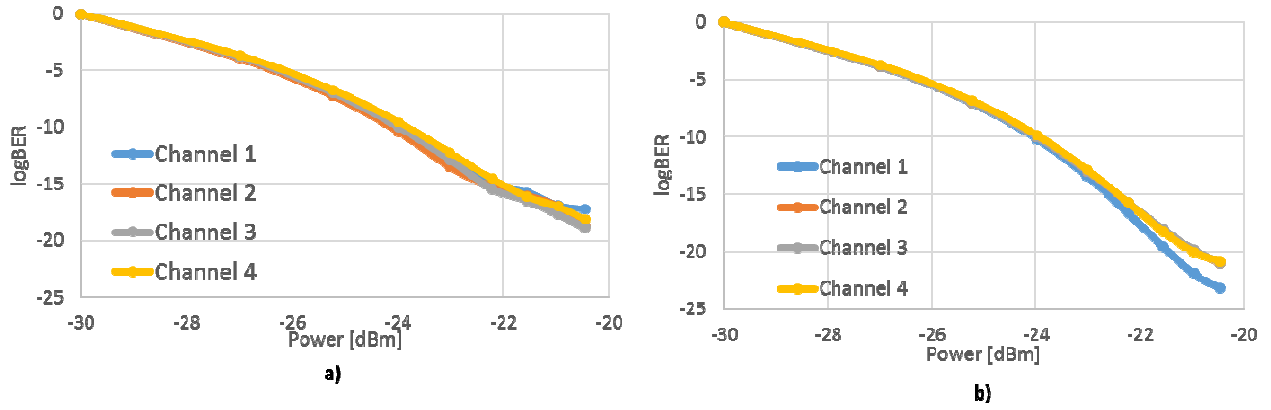


**Fig. 8.** Dependence of BER versus input power for a) equidistant and b) non-equidistant channel spacing, respectively.

From Fig. 7. it is observed as we increase the value of dispersion parameter the BER is getting better, for equal channel spacing it is seen that $D$ = 4.5 ps/(nm×km) the BER is about $10^{-10}$ on the contrary from unequal channel spacing is about $10^{-12}$ for the same of dispersion coefficient. Unequal channel spacing is also useful when input power per channel is required to be increased, then the effect of four wave mixing is tolerable. Unequal channel spacing is found suitable for FWM reduction because no four-wave mixing product term is superimposed on any of the transmitted channels.

## 4. Conclusion

In this paper, analysis of four waves mixing in optical communication systems on the basis of channel spacing, dispersion parameter and input power is presented. The results was obtained by model implemented in VPIphotonics software. It is found that channel spacing of 100 GHz has the best performance according to output BER. Results of simulations show that the effect of four-wave mixing has less impact at the transmitted signal for unequal channel spacing than equal channel spacing. The simulation results show that four wave mixing effect reduces by increasing channel spacing, dispersion and power. The results of our simulation have also important

consequences for understanding multi-channel WDM systems that suffer signal degradation by FWM.

## Acknowledgement

This work is supported by the Slovak Research and Development Agency under the project APVV-0025-12 ("Mitigation of stochastic effects in high-bitrate all-optical networks").

## References

[1] AGRAWAL, G. P. *Fiber - Optic Communication Systems* 4th ed. Rochester, New York: Wiley, 2010.

[2] AGRAWAL, G. P *Nonlinear Fiber Optics* 5th ed. Rochester, New York: Wiley, 2013.

[3] BENEDIKOVIČ, D., LITVÍK, J., KUBA, M., DADO, M., DUBOVAN, J. *Influence of nonlinear effects on WDM system with non-equidistant channel spacing using different types of high-order PSK and QAM modulation formats.* Optical Modelling and Design II, SPIE, vol. 8429, 2012.

[4] BENEDIKOVIČ, D., LITVÍK, J., KUBA, M., DADO, M., DUBOVAN, J. *Modeling of WDM transmission system with high-order phase modulation formats.* 35th International Conference on Telecommunications and Signal Processing (TSP), Prague, p. 325 – 329, 2012.

[5] BENEDIKOVIČ, D., LITVÍK, J., DADO, M., MARKOVIČ, M., DUBOVAN, J. *Numerical investigation of four-wave mixing in DWDM systems with high-order QAM modulation formats.* 18th Czech-Polish-Slovak Optical Conference on Wave and Quantum Aspects of Contemporary Optics, SPIE, vol. 8697, 2012.

[6] ABDUL- MAJID, S. A. *Software simulation FWM in WDM optical communication systems*. Journal of Kirkuk University – Scientific Studies, vol.6, no.1, 2011.

[7] MAHMUD, N. A., BARUA B. *Effects of four wave mixing on an optical WDM system by using dispersion shifted fibre.* International Journal of Engineering and Technology, vol. 2, no. 7, 2012.

[8] AL-MAMUN, S., ISLAM, M. S. *Effect of chromatic dispersion on four-wave mixing in optical WDM transmission system*. Sixth IEEE International Conference on Industrial and Information Systems (ICIIS2011), Kandy, p. 425 – 428, 2011.

[9] RAHMAN, M. Z., ISLAM M. S. *Effect of chromatic dispersion on four-wave mixing in WDM optical transmission system.* Journal of Media and Communication Studies, vol. 3(12), p. 323 – 330, 2011.

[10] BAILLOT, M., CHARTIER, T., JOINDOT M. *Multiple four-wave mixing in optical fibres.* European Conference on Optical Communication, ECOC 2014, Cannes- France, p. 1 – 3, 2014.

[11] KAURA, G., SINGH M.L. *Effect of four-wave mixing in WDM optical fibre systems*. Optik - International Journal for Light and Electron Optics, vol. 120, iss. 6, p. 268 – 273, 2009.

[12] SUGUMARANI, S., ARULMOZHIVARMAN P. *Effect of chromatic dispersion on four-wave mixing in WDM systems and its suppression*. 2013 International Conference on Emerging Trends in VLSI, Embedded System, Nano Electronics and Telecommunication System (ICEVENT), Tiruvannamalai, p. 1 – 3, 2013.

[13] ASO, O., TADAKUMA, M., NAMIKI, S. *Four-wave mixing in optical fibers and its applications.* Furukawa Review, 2000, no. 19.

[14] ARAVIND, P.A., VENKITESH, D. *Measurement of dispersion in a highly nonlinear fiber using four wave mixing.* Communications and Photonics Conference and Exhibition, Asia, p. 1 – 6, 2011.

[15] PACHNICKE, S. *Fiber-Optic Transmission Networks*. Berlin Heidelberg, Springer, 2012.

[16] KAMINOW, I., LI, T. *Optical Fiber Telecommunications IV-B: Systems and Impairments (Optics and Photonics)*, Academic Press, 2002.

[17] TAWADE, L., JAGDALE, S., KADBE, P., DEOSARKAR, S. *Investigation of FWM effect on BER in WDM optical communication system with binary and duobinary modulation format.* International Journal of Distributed and Parallel Systems, vol.1, no.2, 2010.

**TRANSCOM 2015, 22-24 June 2015**
University of Žilina, Žilina, Slovak Republic

# Excel VBA slicer control for OLAP analysis

[*]Ivan Stríček, [*]Martin Hudák
[*]University of Žilina, The Faculty of Operation and Economics of Transport and Communications, Department of communications, Univerzitna 1, 010 26 Žilina, Slovak Republic, {ivan.stricek, martin.hudak}@fpedas.uniza.sk

**Abstract.** The last released versions of Microsoft Excel allow more efficient and faster filtering of pivot tables by slicers. These filters are suitable tool for interactive operation of diagrams and indicators in dashboard. The more complex analysis for exact analyze of multi-dimensional data, is needed to execute in OLAP (Online Analytical Processing) system. For that reason is necessary filtration of pivot tables with more sources of data. The process to create macro to filter more slicers with different data filters is written in the article.

**Keywords:** slicer, Excel, macro, dashboard, OLAP

## 1. Introduction

The information database system (IDS) can be divided into two principal areas. The first one is IDS with OLTP structure and the second area is IDS with more developed OLAP structure. Method of data processing is the main different between them. OLTP systems provide data into data warehouse and OLAP systems help to analyse that data.

OLTP (On-line Transaction Processing) system is characterized with a lot of amount of quick on-line transactions (insert of data, actualization, deleting). The main task of OLTP systems is to allow a fast query processing, maintain the integrity of data in a multi-access environment and efficiency measured by quantity of transactions per second. Actual and detailed data and schemes in OLTP database are used to load transaction database into the entity model.

The access to systems supporting OLAP database structure does not have each company. In case, the acquisition costs are high or ineffective due to the size of company it is better to choose the alternative of data analysis on the basis of OLAP structures.

One of the possible solutions is to create fictitious OLAP filtration in Microsoft Excel in the form of Dashboard application. The dashboard application is managerial analytical application offering the output statistics in form of graphic image with possibility of interactive filtration. At the present, Excel allows easy filtration of data in pivot tables, which are using the same source with, help of slicer. For that reason it is necessary to spar data from pivot table, which uses different data sources.

In this case is needed to create a link between the different kinds of slicers. Microsoft Excel does not support this link in its last released version. It is necessary to create algorithm for mirror settings of filter via macro.

## 2. Setup process functionality

To be able to create a link for filtering the pivot tables according to the hierarchy of data cubes, which are an essential component of the OLAP analysis and create various dimensions of associating elements with values, it must be able to change one element of managing all the pivot tables.

The essence of Microsoft Excel is that with one slicer is possible to manage only pivot tables with one source of data without change of slicer and pivot tables using different data source. This setting is shown on the example of evaluation of data in Slovak Post, specifically for filter of regional centre (OS PPS), error rate and total volume of transactions (figure1).

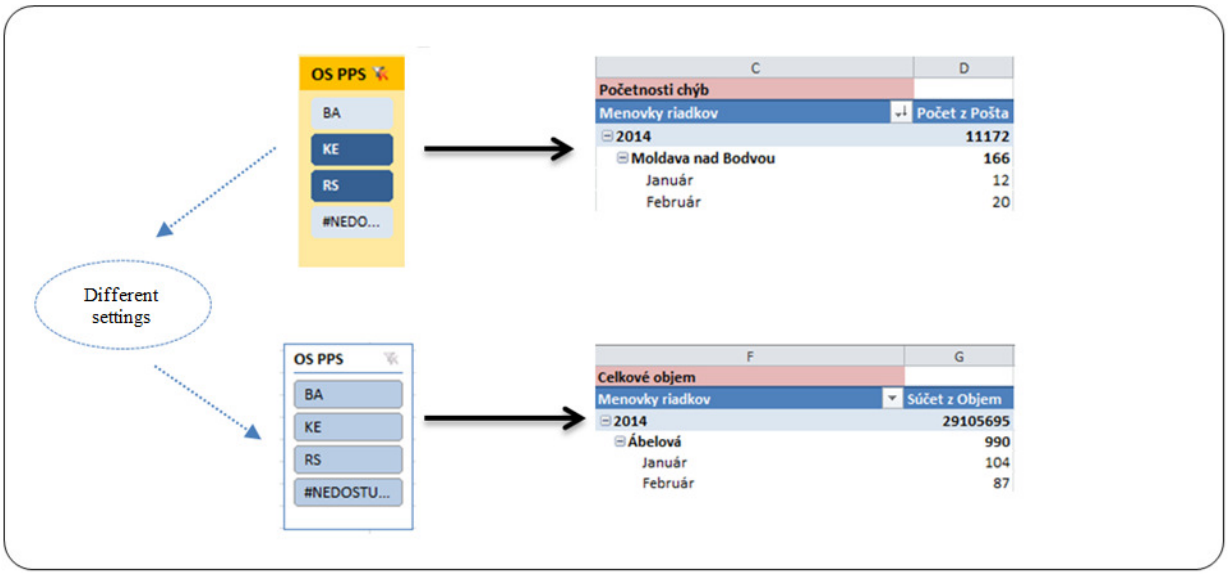


**Fig. 1.** Basic setting of slicers with different data source (Source: Author)

As it is written up, it is not possible to link these two filters only with the default basic setting. Using a macro it is possible to mediate the automatic copy of settings one of the slicers. After that it is possible to set up the second slicer according to settings of the first slicer.

The mirror setting is shown on figure 2.

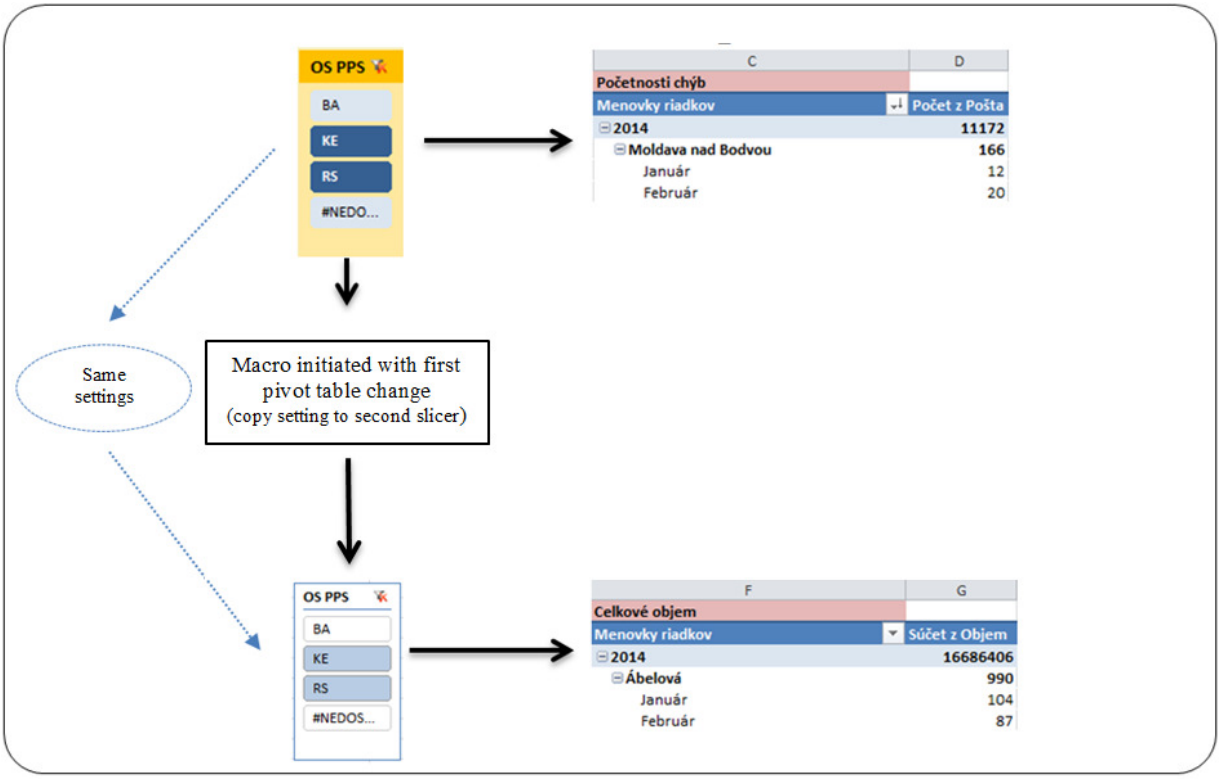


**Fig. 2.** Slicers with same settings set up by macro (Source: Author)

The value #NEDOSTUPNÝ is currently written in all sources tables to prevent the collapse of macros in case of mistake in formulas. This values does not belong to calculation although their status is active or inactive in slicer.

Macro with the algorithm for duplication of setting value of the first slicer to the second slicer with similar names linked with pivot tables of transactions volumes (figure 3).

```
Dim cachSlicer1 As SlicerCache

Dim cachSlicer2 As SlicerCache


Select Case Target

Case "Pivot_OSPPS"


Set cachSlicer1 = ThisWorkbook.SlicerCaches("Rýchly_filter_OS_PPS")

Set cachSlicer2 = ThisWorkbook.SlicerCaches("Rýchly_filter_OS_PPS1")

Dim item As SlicerItem

Dim item1 As SlicerItem

For Each item In cachSlicer1.SlicerItems

        Set item1 = cachSlicer2.SlicerItems(item.Name)

        If item.Selected = True And item.HasData = True Then

            item1.Selected = True

        Else

            item1.Selected = False

        End If


        cachSlicer2.SlicerItems("#NEDOSTUPNÝ").Selected = True

Next item
```

**Fig. 3.** Control macro for second slicer setup (Source: Author)

The value #NEDOSTUPNÝ was chosen permanently visible as helpful value. The aim of this step is to prevent the collapse of macro during the continuous switch-off of all arrays of slicer. This situation cannot occur.

CashSlicer1 presents routing to cash of managing filter and also identification its active items. After that macro cycle „For“ runs truth the all items and sets up their mirror value (true – visible, false - invisible) in the second macro defined by cash memory cashSlicer2.

Using this mirror setting of the secondary slicers that are managing pivot tables of transactions volumes is possible to manage total calculations of final indicators as a single OLAP data cube.

## 3. Conclusion

The introduced way of the filtration in the article is very helpful tool. It helps to create the complex and multidimensional analyses. Every major company should use these analyses especially in managing of quality.

The creation of dashboard applications on the basis of complex interactive filtration and processing information is assumption for cost saving of company not only by reduction of costs for quality. However, the main object is to minimize the needs of expensive programming tools and application that is not possible to manage for company in its own overheads. The tool from

Microsoft Excel is basically accessible for every company. The utilization of Excel full potential requires only training of employees in the beginning of the process and no more capital costs.

## Grant support

This contribution was undertaken, as parts of the research project VEGA 1/0895/13 Research on strategic business management as promoting competitiveness in a dynamic business environment.

## References

[1] BIG DATA IN LOGISTICS A DHL perspective on how to move beyond the hype December 2013, Available at: < http://www.delivering-tomorrow.com/wp-content/uploads/2014/02/CSI_Studie_BIG_DATA_FINAL-ONLINE.pdf>

[2] International Postal Big Data: Discussion Forum Recap May 12, 2014. Available at: < https://www.uspsoig.gov/sites/default/files/document-library-files/2014/rarc-ib-14-002.pdf>

[3] Robert Hillard, Information-Driven Business, How to Manage Data and Information for Maximum Advantage, Library of Congress Cataloging-in-Publication Data, 2010, ISBN 978-0-470-64946-6

[4] Benninga, S. (2014). *Financial Modeling, fourth edition*, Massachusetts Institute of Technology, ISBN 978-0-262-02728-1

[5] Stríček, I. (2013). Costs of quality in company and their measurement, TRANSCOM 2013 Section 2, ISBN 978-80-8070-695-5

[6] *Manažérske systémy*. [online]. [cit. 25.3.2015]. Dostupné na internete:< http://www.dnvba.com/sk/certifikacia/Manazerske-systemy/Kvalita/Pages/ISO-9001.aspx>.

[7] Campbell, J. Y., A. W. Lo, and A. C. McKinley. *The Econometrics of Financial Markets. Princeton University Press*(1996).

[8] Frost, P. A., and J. E. Savarino. *An Empirical Bayes Approach to Portfolio Selection. Journal of Financial and Quantitative Analysis* (1986).

[9] Goldman Sachs. *The Intuition Behind Black-Litterman Model Portfolios. Journal of Finance* (1999).

[10] Jorion, P. *Bayes-Stein Estimation for Portfolio Analysis. Journal of Financial and Quantitative Analysis* (1986).

[11] World Bank, (2007). *Education Quality and Economic Growth, Washington, D.C* : The World Bank, ISBN 0821370588

[12]Time series Forecasting using Holt-Winters Exponential Smoothing Hype .[online]. [cit. 25.3.2015]. Dostupné na internete: <http://labs.omniti.com/people/jesus/papers/holtwinters.pdf>.

**TRANSCOM 2015, 22-24 June 2015**
University of Žilina, Žilina, Slovak Republic

# Analysis of Traffic Identification Methods in Encrypted Voice Transmission

[*]Krzysztof R. Szęszoł
[*]Kielce University of Technology, Faculty of Electrical Engineering, Automatic Control and Computer Science, Department of Telecommunication, Photonics and Nanomaterials, al. Tysiąclecia Państwa Polskiego 7, 25-314 Kielce, Poland {kszeszol}@tu.kielce.pl

**Abstract.** The use of Voice over IP technology is rapidly growing and in the near future it can completely replace traditional PSTN network. The main strong reasons for the use of this technology is a huge reduction of costs, and a significant increase in terms of functionality switched networks. In the past, applications that provide VoIP services were dedicated exclusively to computer users. Today, IP telephony can be used virtually anywhere where one has the access to the Internet and IP networks. The nature of the medium used which is a packet network has some disadvantages, and correcting those is of an interest for telecom operators, telecoms regulators and companies who want to prioritize or block the VoIP traffic for a variety of reasons. Four basic methods of detection are used for this purpose: Port-based filters, keywords, ASCII string patterns, signaling patterns and statistical analysis packages.

**Keywords:** Voice over Internet Protocol (VoIP), encrypted transmission, deep packet inspection (DPI), statistical analysis, tunneling, packet detection techniques

## 1. Introduction

In recent years we have noticed a huge increase in the popularity of *Peer To Peer* applications dedicated for *Voice over IP* communication service, which is due to significantly lower costs in comparison to traditional *Public Switched Telephone Network* services, as well as to a substantial increase of the speed of the transmission links [1],[2]. In case of end-users directly using dedicated applications, voice or video services are usually free of charge. In the majority of popular VoIP protocols are implemented mechanisms that allow circumvent of network security in private or corporate networks. Implementation of non-well known ports, deployment of services into encrypted channels or dynamic and random port assignment are challenges that each network operator must face. Therefore, it's difficult to identify VoIP traffic correctly, afterwards bandwidth management, which ensures the of all services in accordance with the adopted policy of quality assurance. The problem of traffic detection might be even more difficult in case of use of the methods of digital information transmultiplexing for telecommunication services [3]. Despite significant improvements in *Quality of Service* through the use of new routing schemes and packet-grouping [6], accurate identification of encrypted traffic is required due to its nature - a significant temporary load and real time transmission.

Due to the opinion often expressed by various communities and on the need to maintain a high level of privacy between end-users who are recipients of the services offered by the Internet network, the research on the detection of particular types of traffic is rarely ongoing.

Another important reason to perform research on the development of effective methods and mechanisms to detect VoIP traffic is its legality. This is a problem affecting not only business and private telecommunication operators who are exposed mainly to financial losses because of this. It has also a negative influence on the government institutions as the illegal traffic bypasses the settlement points and hence avoiding the payment of taxes.

This paper aims to analyze the main detection techniques of encrypted VoIP traffic and to initiate a discussion on the possibilities of more effective analysis through correlation of the basic

techniques. The further part of this paper will address broader characterization of VoIP traffic in selected countries. Then four basic methods of analysis and detection, their strengths and weaknesses are described. Finally blocking of most popular protocols will be presented.

## 2. VoIP traffic deployment and characterization

Over the last decade, VoIP services have led to a large transformation of the telecommunication market. VoIP has gained a wide acceptance among consumers, service providers and business communities by offering affordable way to communicate. VoIP services and converged networks have changed the definition of telecommunication service providers. The boundaries between network and content have blurred, making it easier for small operators in direct competition without possession of own infrastructure. The elimination of these restrictions allowed to attract new customers based on the properties of the offered services.

In some cases the VoIP may face problems with implementation. It should be noted that the voice, video and high-speed data transmission services have specific requirements, thereby generating variable network load which is the biggest challenge in the provision of the Quality of Service (QoS). In less developed countries the problem may be operation of the network during faults in supply of electricity. The incumbent operators may also receive VoIP as a threat to their PSTN revenues. This is particularly evident in countries where market is monopolistic and not well balanced. The operators who make large investments in broadband networks expect a clear regulatory frameworks to help ensure a rapid return on investments. Currently, the big problem is to offer VoIP services serving emergency calls, due to difficulty in determining a geographical location of the caller.

The biggest market for VoIP services is now East Asia, where Japan plays a dominant role in dissemination of VoIP services. The United States are at the same level of users number. Those two regions together contain almost 2/3 of total number of users in the world. Those statistics should be treated only as an estimate as it is impossible to determine the exact number of computer-to-computer VoIP users in the world at the moment.

Voice traffic transmitted over the Internet does not differ at the first glance from most types of data, so it is difficult to measure its volume. However, the research of estimate ratio of transmitted voice traffic over the IP networks in the world is still ongoing. It shows a strong trend to grow. A key issue of the estimates are revenues from IP telephony services. Despite the fact that each year number of users are doubled, overall revenues from voice services are consistently falling. In the face of such a large increase in the VoIP market, reactions in the form of regulations can be divided in view of countries. In some countries, VoIP was banned in order to protect the revenues of national operator (usually these are lower developed countries). In some countries consciously VoIP is not regulated by law, which gives free rein for telecom operators. Very often it is a subject to the same regulations as the PSTN. Depending on the technology used, it can be a subject of a part of the laws or all of the regulations. Significant difficulties in controlling VoIP traffic are noticeable on the international transit points of contact. There were created for this purpose *International Clearing Houses*. However, they are not always an effective tool for the proper calculations to charge taxes on VoIP services [12].

Potential, considerable threat for the computer may be an application such as Skype or Google Hangouts, due to their primary aims which are to ensure the best possible quality of transmission between subscribers. Let Skype *End User License Agreement* to be evidence, which contains a rather controversial clause, saying that the application can have control over owners computer resources such as *Central Processing Unit* or *Network Interface Controller*. Furthermore, due to the nature of connection, Skype application is also vulnerable to the risks of P2P networks. This can be associated with various attack types from buffer overflows to *Denial Of Service* attacks or simply network bandwidth limitations. Therefore, many companies and government institutions want to block such applications in their local networks.

## 3. Methods of VoIP detection

The simplest method of network applications detection in view of implementation is the analysis of TCP/IP ports. Depending on the protocol or a specific application, VoIP services can use dedicated ports defined by the *Internet Assigned Number Authority*. Having a list of defined ports, it is easy to control the flow of data by placing appropriate rules in firewall. However, the effectiveness of this approach is low, since the applications use enumeration of the dynamic port range [17]. Many application developers gave up to use predefined ports in favor of dynamic ports, which is intended to provide higher availability and better Quality of Service. Applications adjust their configuration to the network in order to bypass firewalls or proxy servers. Ports of popular protocols, such as HTTP, HTTPS or SSH (respectively 80, 443 and 22 ports) are used to create simple Virtual Private Network tunnels (in application layer of OSI model) in order to circumvent of blocking traffic [18].

| **Protocol** | SIP | H.323 | Skype | XMPP | MGCP | Megaco |
|---|---|---|---|---|---|---|
| **Default ports** | 5060, 5061 | 1300, 1718-1720 | 23399, 33033, (when blocked – 80, 443) | 5222, 5269 | 2427, 2727 | 2944 |

**Tab. 1.** Standard ports of popular VoIP protocols.

The signature based method can overcome some disadvantages of analysis based on ports of services. Software for monitoring and analyzing the content of packets which is often referred as Deep Packet Inspection, is used for this purpose. Intrusion Detection Systems designed for deep analysis of network traffic fulfill their tasks largely based on database of signatures used for detection and identification. The disadvantage of such systems is that software which analyze content of packets in terms of certain keywords and ASCII string also analyzes the data flow patterns that are characteristic for different types of services and applications [4, 9, 16].

The disadvantage of this detection approach is a need to determine the patterns of keywords or traffic flow models for each newly created application which packets have to be detected. This means there is a need to know each application in terms of behavior in network before introduce it into a general use. Taking into account their number and rate of issuing new applications, it is very difficult or even impossible to keep pace with constant changes. In addition, the use of encryption techniques leads to increase complexity of this method. Here are two ASCII strings that identify the Skype application, when log on to the login server [9, 16, 17].

*16 03 01 00 ** 42 cd ef e7 40 d7 2f 1d*

*16 03 01 00 cd 41 03 00 09 8040 04 08 c0 01*

The identification is additionally difficult due to the lack of a fixed position during occurrence of information string, but it usually occurs between third and twentieth packet after three-way handshake TCP connection is established.

| | **Google Talk** | **Skype** | **Yahoo** | **Online Game** | **Streaming Video** | **MSN Text Chat** |
|---|---|---|---|---|---|---|
| Average packet size | 178B | 166B | 125B | 423B | 737B | 414B |
| Average packets/sec. | 21 | 24,9 | 27,5 | 2,1 | 8,5 | 4 |
| Average Bytes/sec. | 3709 | 4146 | 3450 | 890 | 6305 | 1668 |

**Tab. 2.** Comparison of selected traffic features in different types of applications.

As can be seen from the Table 2, traffic of VoIP packets shapes differently in relative to packets unrelated with voice traffic. It allows to determine the packet flow models taking into account appropriate set of coefficients [5]. Most characteristic index is the number of transmitted packets per second and it is clearly higher for VoIP applications.

The most common way for VoIP traffic tunneling is HTTP protocol. Studies on the use of HTTP to hide VoIP calls proposes detection model based on following five parameters [4, 10, 14]:

- Size of HTTP request
- Size of HTTP response

- Inter-arrival time between requests
- Number of requests per page
- Page retrieval time.

The two first parameters are relatively simple to evaluate. Time intervals between generated requests are defined as time between two consecutive request of the same subscriber to the same server, about the same website. Therefore there is a fixed time interval in which a requests can be interpreted as a requests for single website. The last two parameters are calculated based on previously measured values of 1 to 3 parameters. In order to assess anomalies occurring in WWW traffic there are carried out two types of tests based on statistical analysis: chi-square test and Kolmogorov-Smirnov test [10, 14].

Traffic analysis based on signaling mechanisms patterns is the development of communication model between two clients. The detection process consists of analyzing in details the procedure of log on to server including the way in which client sends a request to the VoIP server. Such methods have already been a subject of an extensive research on proprietary protocols. Skype is a frequent topic of that research because of the very large number of users as well as distinct way of communication. Pattern based techniques can be a good solution in some cases for detecting of encrypted traffic in VoIP applications. This depends largely on the signaling mechanisms, so characteristic for each VoIP application. The use of tunneling at the network layer (IP protocol) makes that pattern based technique becomes useless.

## 4. Realization of Skype protocol flow blocking

Construction of the Skype network as opposed to the SIP where there is a client-server model is more complex. Three basic elements can be distinguished [4, 7, 8, 15]. *Skype Client* (SC) is a software application installed on the end user workstation that initiates connection, logging, and processing of income calls. *Super Nodes* (SN) are selected SC who have additional functionality in form of routing requests and answers to the SC. In some cases they act as intermediary in the login process, when the login server is not available directly. In order to be selected as a SN user must meet some requirements including high speed Internet access, no firewalls or other restrictions of access to the public network, and own public IP address. There are some bootstrap SN that are hard coded in SC and which are owned by Skype. The third element is the logon server. It is one of few central points in the Skype network where each user is subject to authentication.

Skype has a mechanism to recognize network configuration and existing limitations [11]. Mechanism involves sending by SC UDP requests to SN. Depending on that test a suitable model of network functionality is chosen. Hence, in order to create good pattern of Skype signalization ensuring application blocking, there is a need to analyze of multiple client scenarios. Correct analysis should take into account possible configurations of the firewall, SCs with private or public addresses, possible connectivity scenarios, various Skype user statuses, creating account and login to network.

After successful verification of the network configuration, the SC starts the login procedure. When communication takes place with bootstrap SN, destination port is 33033. Otherwise, port number is randomized in range of above 1024. In order to authenticate on login server, at least one previously established TCP session is required. When this connection cannot be established on a random port, SC tries to establish a connection on port 443 and 80 [13, 18]. It should be noted that despite the use of HTTPS and HTTP ports, Skype does not utilize corresponding network protocols. Established TCP connection allows SC to authenticate to login server. Reference 7 gives two addresses such servers that are verified and described in other articles [4, 8]: 192.215.8.141 and 212.72.49.141.

After first correct login since time of registration, the user's credentials for further logins are stored encrypted on local drive. Default location is in file:
C:\Documents and Settings\user_name\Application Data\Skype\user\config.xml

This behavior makes login process automatic and no connections to any login server at startup is required. Analysis of described procedures and statistical analysis of TCP/UDP packets, including discussed parameters of traffic enables to provide an algorithm to identify and block calls described in Fig 1 [4, 11].

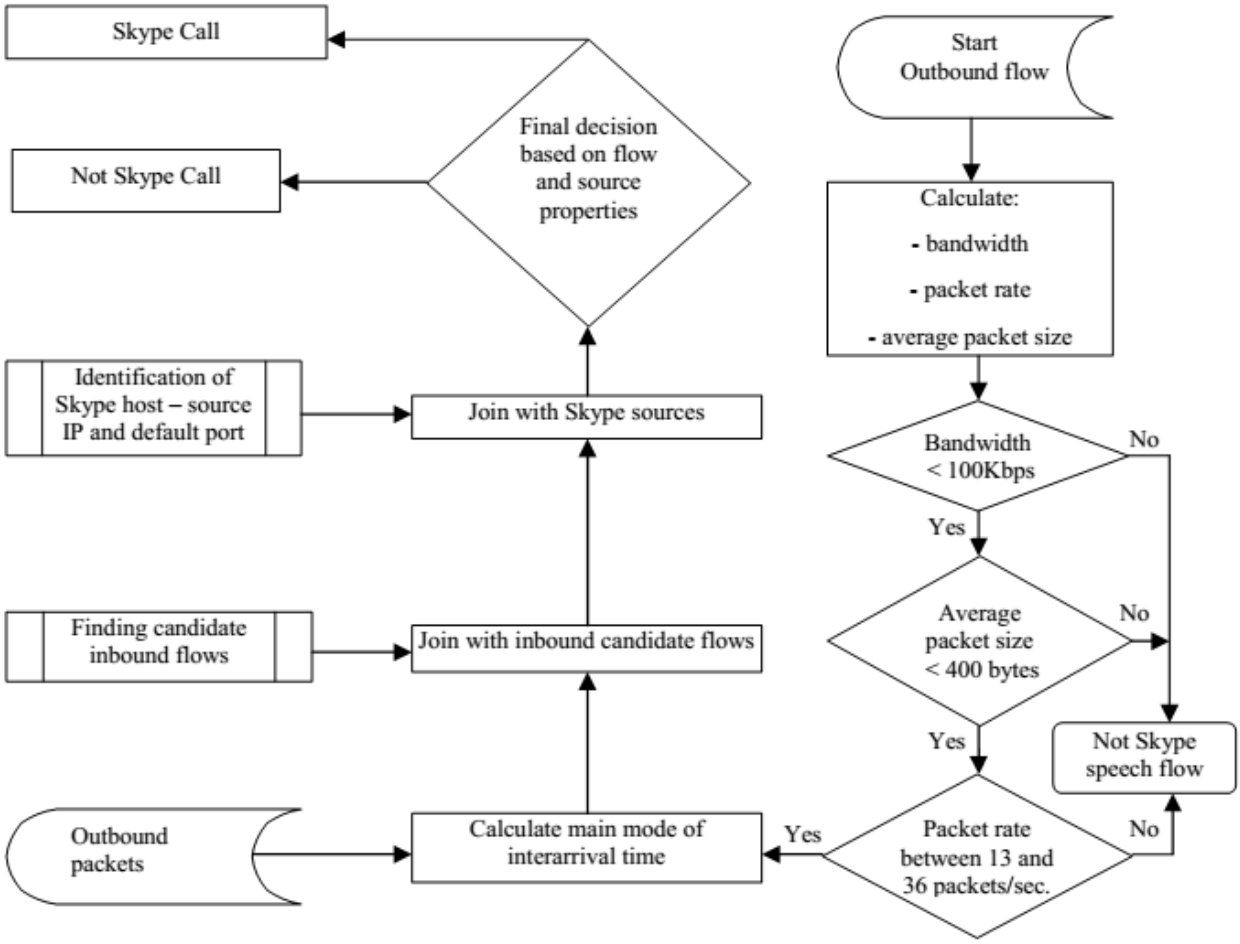


**Figure 1.** Process of Skype calls identification.

## 5. Summary and conclusions

Detection and classification of network traffic is a key issue for telecom operators because of security, Quality of Service and economic policy. All these techniques, e.g. analysis based on ports, signatures, traffic patterns or statistical analysis have their limitations. The complexity of VoIP protocols and data encryption makes the total information flow control is not possible.

This paper reviews proposed VoIP detection methods. Analysis of ports and packet signatures can be applied to both voice, data, and signaling detection. These techniques may be effective for some protocols, but in cases, where traffic is encrypted, only patterns of signaling and statistical analysis can be applied. Port based analysis can be used to detect the encrypted transmission only if data tunneling takes place higher than in network layer. Due to its performance limitations, the statistical analysis is not the best solution, but correctness of encrypted and not encrypted traffic detection puts it in first place in term of effectiveness. Except statistical analysis, all these methods have good scalability.

Current research on VoIP detection can be divided into two categories. The first one is characterized by detection based on VoIP traffic distinctive parameters. There are several algorithms in this group, which detect various protocols without detailed identification of application. The second category of algorithms is based on communication models which are

defined in order to detect anomalies that occur in the network. Existing communication models are successfully used for detecting traffic tunneling based on HTTP protocol.

Possible solutions of using the techniques listed above should be determined considering VoIP traffic detection regardless of protocol, encryption mechanisms and network security policies. Analyzing research in this field raises to an observation that there is still a lack of generic tool with high scalability and performance, which would allow detection of VoIP traffic in real time.

## References

[1] MARCINIAK M. – *100/1000 Gbit/s Ethernet and beyond.* Journal of Telecommunications and Information Technology, nr 1/2009.

[2] CHODOREK A., CHODOREK R. – *A simple and effective TCP-friendly layered multicast content distribution*. Polish Journal of Environmental Studies, vol: 18/4B, 2009.

[3] CIOSMAK J. – *Algorytm wyznaczania nieseparowalnych dwuwymiarowych zespołów filtrów dla potrzeb systemów transmultipleksacji*. Przegląd Elektrotechniczny, vol: 87/11, 217-220, 2011.

[4] FONSECA H., CRUZ T., SIMOES P., SILVA J., GOMES P., CENTEIO N. – *A comparison of classification techniques for detection of VoIP traffic.* Eighth International Conference on Next Generation Mobile Apps, Services and Technologies, Oxford 2014.

[5] IDREES F., KHAN U. A. – *A generic technique for Voice over Internet Protocol (VoIP) traffic detection.* International Journal of Computer Science and Network Security, vol. 8, nr 2, luty 2008

[6] KLINKOWSKI M., CAREGLIO D., SOLE-PARETA J., MARCINIAK M. – *A performance overview of quality of service mechanisms in optical burst switching networks.* Current research progress of optical networks, Springer 2009.

[7] BASET S. A., SCHULZRINNE H. G. – *An analysis of the Skype peer-to-peer Internet telephony protocol.* INFOCOM 2006. 25th IEEE International Conference on Computer Communications.

[8] EHLERT S., PETGANG S. – *Analysis and signature of Skype VoIP session traffic*. Fraunhofer Focus technical report NGNI-SKYPE-06b, 2006.

[9] RENALS P., JACOBY G. A. – *Blocking Skype through Deep Packet Inspection.* 42nd Hawaii International Conference on System Sciences. 2009. HICSS '09.

[10]FREIRE, E.P. ; Mil. Inst. of Eng. (IME), Rio de Janeiro ; Ziviani, A. ; Salles, R.M. - *Detecting VoIP calls hidden in web traffic.* IEEE Transactions on Network and Service Management, (Volume:5, Issue: 4 ).

[11]PERENYI M., MOLNAR S. – *Enhanced Skype traffic identification.* Proceedings of the 2nd international conference on Performance evaluation methodologies and tools. Brussels 2007.

[12] RASHEED A., KHALIQ A., SAJID A., AJMAL S. – *Identification of hidden VoIP (Grey traffic).* Journal of Computer Networks, 2013, Vol. 1, No. 2, 15-27.

[13] LEUNG CH., CHAN Y. – *Network forensic on encrypted Peer-to-Peer VoIP traffic and the detection, blocking and prioritization of Skype traffics.* 16th IEEE International Workshops on Enabling Technologies: Infrastructure for Collaborative Enterprises, 2007. WETICE 2007.

[14] FREIRE W. P., ZIVIANI A., SALLES R. M. – *On metrics to distinguish Skype flows from HTTP traffic*. Network Operations and Management Symposium, 2007. LANOMS 2007. Latin American

[15] MOLNAR S., PERENYI M. – *On the identification and analysis of Skype traffic*. International Journal of Communication Systems. 2011; No. 24, 94-117.

[16] LU F., LIU X., MA Z. – *Research on the characteristics and blocking realization of Skype protocol.* International Conference on Electrical and Control Engineering (ICECE), 2010.

[17] RATHORE M.M.U., MEHMOOD T. – *Research on VoIP traffic detection.* International Symposium on Performance Evaluation of Computer and Telecommunication Systems (SPECTS), 2012.

[18] OKABE T., KITAMURA T., SHIZUNO T. – *Statistical traffic identification method based on flow-level behavior for fair VoIP service.* 1st IEEE Workshop on VoIP Management and Security, 2006.

**TRANSCOM 2015, 22-24 June 2015**
University of Žilina, Žilina, Slovak Republic

# Methods of Input Shapers Realization

[*]Peter Šarafín, [*]Veronika Olešnaníková, [*]Róbert Žalman, [*]Peter Ševčík
[*]University of Žilina, Faculty of Management Science and Informatics, Department of Technical Cybernetics, Univerzitná 8215/1, 01026 Žilina, Slovakia, {Peter.Sarafin, Veronika.Olesnanikova, Robert.Zalman, Peter.Sevcik}@fri.uniza.sk

**Abstract.** Input shaping is a technique that operates by filtering reference command so that the modified command does not invoke natural frequencies of the system. Residual vibrations occurring in positioning systems can be reduced by forming the reference control signal by the notch filters, low pass filters and input shapers. In this paper, an adaptive input shaping technique and advantages of using extra sensors are discussed too.

**Keywords:** Input shaper, damping, adaptive input shaper.

## 1. Introduction

When controlling weakly damped dynamic system, method of input shaping is often used. The method should ensure control of the movement of the system with flexible elements so the system does not start to oscillate. In practice, there are often limitations that need to be considered in the theoretical proposal of the shaper. These limitations include especially limitation of input variable magnitude and relatively low resolution of the output elements performance [1].

Among the interesting applications we can include, for example, motion control of speed elevators, cranes, production lines, especially in the food industry.

## 2. Input Shapers

In general we can say that the problem of the input shaping occurs always when controlling positioning systems with flexible elements. With the development of mechatronic systems, the issue of input shaper becomes actual again. The role of the shaper is to modify frequency spectrum of control signals so that the resonant frequency of controlled system is avoided. On this basis, we can conclude that in a principle we are talking about proposal for a serial correction element (Fig. 1) with the task to adjust the frequency characteristics of the controlled system.

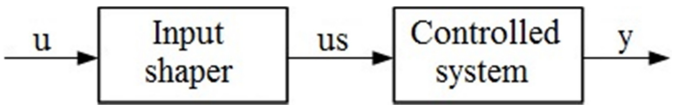


**Fig. 1.** Representation of the input shaper application.

Input shaping is the process of modifying the control commands in a way to disable the resonant system output. In other words, the input shaper filters frequencies of these commands that cause resonance in the system. Parameters of input shaper are formed so that the response of the system to input signals corresponds to the desired resonance characteristics.

### 2.1. ZV input shaper

For various applications, a wide range of input shapers has been developed. Often used input shaper is Zero Vibration (ZV) shaper. This shaper takes the shortest time needed to implement arithmetic operations of the system using only positive pulses. This time is important because the convolution with the input shaper increases the reaction time of the shaper throughput. If the ZV

shaper is designed with a perfect model, all vibrations are canceled. If the model is incorrect, some vibrations occur [3]. The ZV shaper can be defined as (1), where $\omega$ and $\varsigma$ are inherent frequencies and damping of the flexible system respectively.

$$ZV: \begin{bmatrix} A_j \\ t_j \end{bmatrix} = \begin{bmatrix} \frac{1}{1+K} & \frac{K}{1+K} \\ 0 & T \end{bmatrix}, \qquad where\ T = \frac{\pi}{\omega\sqrt{1-\varsigma^2}}, K = e^{\frac{-\varsigma\pi}{\sqrt{1-\varsigma^2}}}. \qquad (1)$$

## 2.2. ZVD input shaper

If it is desired to ensure the fault tolerance against modeling errors, Zero Vibration Derivative (ZVD) input shaper can be used. This shaper forces the function derivation with respect to the modeling error to be equal to zero (2). The tax for adding this extra robustness is increased execution time of shapers arithmetic operations, and thus the time of the system transition.

$$ZVD: \begin{bmatrix} A_j \\ t_j \end{bmatrix} = \begin{bmatrix} \frac{1}{1+2K+K^2} & \frac{2K}{1+2K+K^2} & \frac{K^2}{1+2K+K^2} \\ 0 & T & 2T \end{bmatrix}, \qquad (2)$$

where *T* and *K* are defined exactly as those near ZV shaper.

## 2.3. EI input shaper

Another type of shaper is Extra-Insensitive (EI) shaper. Time needed for the shapers arithmetic operations is the same as in the case of using ZVD shaper, but its insensitivity is considerably higher [2]. The insensitivity of EI shaper depends on the size of allowed vibrations in exact model. In general, the size of allowed vibrations is determined to be equal to the upper limit of acceptable residual vibration. The reason for this procedure is that increasing the allowable size of the vibration increases insensitivity to modeling errors. The relation representing the EI shaper can be defined as (3), where *V* stands for rate of insensitivity to system vibrations.

$$EI: \begin{bmatrix} A_j \\ t_j \end{bmatrix} = \begin{bmatrix} \frac{1+V}{4} & \frac{1-V}{2} & \frac{1+V}{4} \\ 0 & \frac{T}{2} & T \end{bmatrix}, \quad where\ T = \frac{\pi}{\omega\sqrt{1-\varsigma^2}} \qquad (3)$$

Figure 2 represents the relation of residual vibrations and normalized frequency for ZV, ZVD and EI shapers [3].

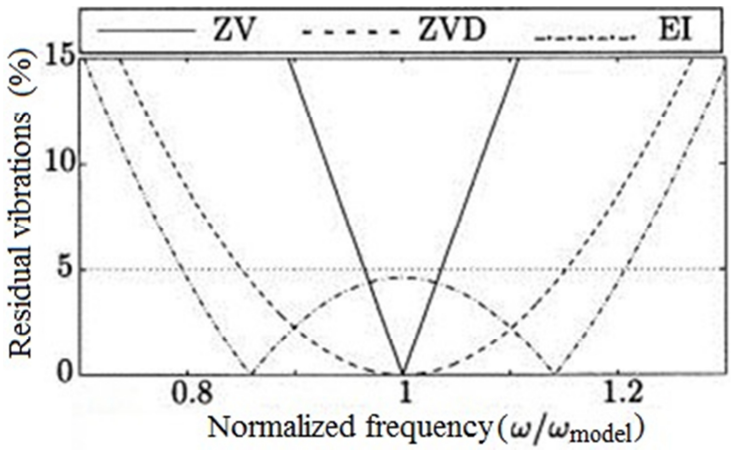


**Fig. 2.** Comparison of ZV, ZVD and EI input shapers.

## 2.4. Using conventional filters as input shaper

For input shaping, various conventional filters can be used [4], [5]. The impulse response of real systems is too long for modelling by FIR filter, because this response is infinite. To reduce the impulse response, a certain part is only maintained, which damages the frequency response.

Therefore, it is necessary to determine the relatively large window with respect to the period of oscillation.

The main advantage of the IIR filters over FIR filters is that they generally meets the specifications of much lower filter order, as the corresponding FIR filters [6]. By using IIR filter relatively good vibration reduction is achieved, but the arising time delay in their use is too large.

Ideal notch filters, as well as an ideal low pass filters are not feasible. As the size of the response during the notch suddenly drops to zero and the next pass band becomes again unitary, it can be claimed that the filter has an infinite length. In an ideal band-pass filter Hamming window can be applied. Windowing produces feasible filters with the frequency responses close to the responses of an ideal filter. The response obtained by using this filter contains a significant residual vibration.

## 3. Adaptive input shapers

To adjust the input commands online, direct design method of adaptive shaping control signal can be used. The task of this method is to ensure that residual vibrations are suppressed in the final time, as soon as possible. The more general filtering using discrete FIR filter can achieve the same objectives. Different approaches leading to improved error robustness in the model were examined. However, increasing robustness requires an increase in the period of input shaper implementation and the corresponding increase in stabilization time or the introduction of usage of negative pulses.

Obviously, the vibration reduction in the system should be adapted to the characteristics of the input shaper as measured by current oscillations. The disadvantage of this approach is the need to add further sensors and increase the complexity of controller. Despite these complications, it is necessary to consider the potential benefits in applications in systems with unknown or time-varying dynamics.

One approach to adaptive input shaping is based on the use of methods of system identification. In this case, the shaper is defined to meet the requirements of the proposal, which is already known as a function of identifiable parameters in the system transfer function. The identification system in the frequency domain was first proposed to adjust the time interval of shapers pulses [7]. Such identification systems are also considered computationally less demanding [8]. How can these systems be successfully applied to multimodal systems is still an open issue, especially when significant noise occurs. These systems prevent the unambiguous identification of the model parameters.

Method of direct adaptive input shaping (Direct Adaptive Input-Shaping - DAIS) is based on the measurement of residual oscillations and may be directly applicable for multimodal systems. This method includes a sufficient number of pulses in the shaper sequence and it can be used to set only the amplitudes of the pulses. Zero vibrations can then be obtained with any times of the pulse occurrence.

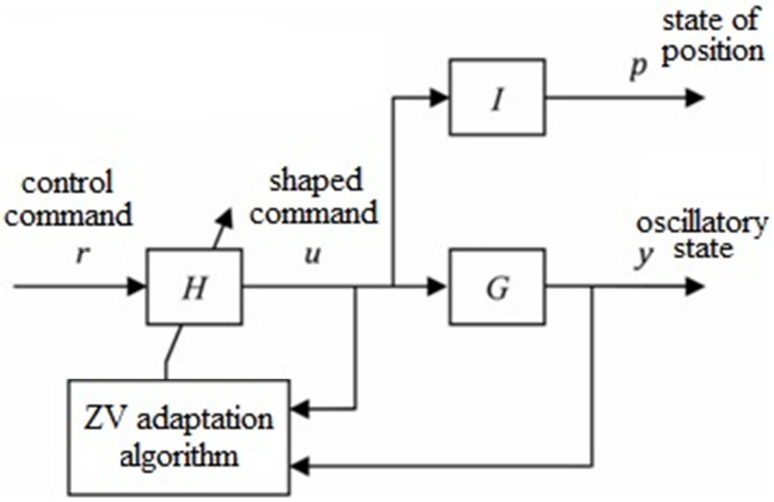


**Fig. 3.** The structure of adaptive input shaper.

### 3.1. Direct design method using input and output data

Input shaping requires the determination of the filter *H*, which ensures that when the input command *r* reaches and remains at zero or other stable value, the output *y* reaches and remains at zero in finite time. This condition is known as zero vibrations. It is expected that the achievement of the zero state at *y* causes the elimination of undesirable oscillation components at the state of position *p*. The output *y* occurring in response to the command *r* is the convolution of $y = f * r$, where $f = g * h$ is the impulse response of the system [9].

Consider input shaper *H* defined by the number of coefficients *K*, which is connected in series with a stable linear system *G* with infinite impulse response $= \{g_0, g_1, g_2, \ldots\}$. Shaper has an impulse response $h = \{h_0, h_1, h_2, \ldots, h_K\}$, that is the aim of optimization / adjustment, and *G* and *I* represent controlled system, as shown in Fig. 3.

In the case that we do not know the mathematical model of the system *G*, we can use the direct method proposal using input and output signals. The following matrix (4) derived from the convolution equation describes the relationship between inputs and outputs:

$$\begin{bmatrix} y_N & y_{N-1} & \cdots & y_{N-K} \\ y_{N-1} & y_{N-2} & \cdots & y_{N-K-1} \\ \vdots & \vdots & & \vdots \\ y_{K+1} & y_K & \cdots & y_1 \\ y_K & y_{K-1} & \cdots & y_0 \end{bmatrix} =$$

$$= \begin{bmatrix} u_N & u_{N-1} & \cdots & u_{N-K} \\ u_{N-1} & u_{N-2} & \cdots & u_{N-K-1} \\ \vdots & \vdots & & \vdots \\ u_{K+1} & u_K & \cdots & u_1 \\ u_K & u_{K-1} & \cdots & u_0 \end{bmatrix} \begin{bmatrix} g_0 & 0 & \cdots & 0 \\ g_1 & g_0 & \cdots & 0 \\ \vdots & \vdots & \ddots & \vdots \\ g_K & g_{K-1} & \cdots & g_0 \end{bmatrix} + \tag{4}$$

$$+ \begin{bmatrix} u_{N-K-1} & u_{N-K-2} & \cdots & u_0 \\ u_{N-K-2} & u_{N-K-3} & \cdots & 0 \\ \vdots & \vdots & & \vdots \\ u_0 & 0 & \cdots & 0 \\ 0 & 0 & \cdots & 0 \end{bmatrix} \begin{bmatrix} g_{K+1} & g_K & \cdots & g_1 \\ g_{K+2} & g_{K+1} & \cdots & g_2 \\ \vdots & \vdots & & \vdots \\ g_N & g_{N-1} & \cdots & g_{N-K} \end{bmatrix}$$

This relation can be simplified as (5):

$$Y_N = U_N \Phi + V_N \Gamma_N \,. \tag{5}$$

If *h* satisfies the condition of zero oscillations, eg. $\Gamma_N h = 0$ and we know that $\Phi h = f$ , then:

$$Y_N h - U_N f = 0 \,. \tag{6}$$

Even though knowledge of the system dynamics contained in $g$ is not necessary for the synthesis, the approximate values of the natural frequencies may be helpful for choosing the appropriate duration of the shaper.

## 4. Conclusion

In this paper, conventional input shapers, filters and adaptive input shaper were considered. Each of these input shaping schemes succeeded in reducing residual vibrations. It was stated that with the cost of additional time delay a greater reduction in endpoint vibrations is obtained. Creating adaptive input shaper represents different approach than adding extra robustness. It is obvious that the adaptation algorithm is more computationally demanding, because shaper's coefficients are modified based on the information obtained by the sensors. The method of direct adaptive input shaping using input and output data does not require the knowledge of system transfer function. This fact means, that coefficients of the shaper will be adjusted correctly even if parameters of the system change.

When designing input shaper, one of the factors is the execution time of shapers arithmetic operations. This time may be significantly reduced by designing proper adaptive input shaper. It can be stated that more accurate information is received from sensors applied to the system, input shaper with less coefficients has to be proposed to suppress residual vibrations.

## References

[1] MIČEK J., JURÍČEK J. *Design of multimode shaper of control signals and proper choice of sampling frequency. Canadian Journal on Automation*, Control and Intelligent Systems, Vol.2, No.3, April 2011, ISSN 1923-1709.

[2] SINGER N., SINGHOSE W., SEERING W.: *Comparison of filtering methods for reducing residual vibration. European Journal of Control*, 1999.

[3] SINGER N., SEERING W. *Design and comparison of command shaping methods for controlling residual vibration*, *Proc. IEEE Int. Conf. Robot. Autom.*, Scottsdale, AZ, Vol. 2, pp. 888–893, 1989.

[4] MIČEK J. *Alternatívny prístup k návrhu tvarovača riadiacich signálov*, *AT&P journal 3*, 2010, ISSN: 1335-2237.

[5] FORTGANG J., MARQUEZ J., SINGHOSE W. *Reducing vibration by digital filtering and input shaping*, *IEEE Trans. Control Syst. Technol.*, Vol. 19, No. 6,pp. 1410-1420, Nov. 2011.

[6] MURPHY B., WATANABE I. *Digital shaping filters for reducing machine vibration*, *IEEE Trans. Robot. Autom.*, Vol. 8, No. 2, pp. 285–289, Apr. 1992.

[7] PEREIRA E., TRAPERO J., DIAZ I., FELIU V. *Adaptive input shaping for manoeuvring flexible structures using an algebraic identification technique*, Automatica, Vol. 45, No. 4, pp. 685–693, 2009.

[8] RHIM S., BOOK W. *Noise effect on adaptive command shaping methods for flexible manipulator control*, *IEEE Trans. Control Syst. Technol.*, Vol. 9, No. 1, pp. 84–92, Jan. 2001.

[9] ŠEVČÍK P., KAPITULÍK J. *Moderné prostriedky implementácie metód číslicového spracovania signálov II*. Žilina: Žilinská univerzita, 2013, ISBN 978-80-554-0676-3.

**TRANSCOM 2015, 22-24 June 2015**
University of Žilina, Žilina, Slovak Republic

# Extension of Automatic System For Animal Recognition to animal classification in the infrared domain

[*]Tibor Trnovszký, [*]Róbert Hudec
[*]University of Žilina, Faculty of Electrical Engineering, Department of Telecommunications and Multimedia, Univerzitna 2, 01026 Žilina, Slovakia, {tibor.trnovszky, robert.hudec}@fel.uniza.sk

**Abstract.** In this paper, the description a reasons why the ASFAR system have to be extended into infrared domain for animal classification in night is presented. Moreover, some behavioral and migration characteristic of wild animals and reasons for their movements were described. Thus, the physiological background of Animal Visual System in opposite to Human Visual System we described in detail. Following the analysis of visual behavior, the concept of sensing the wild animal in the natural environment and appropriate time migration was developed. Regarding to the dominant migration time, the original ASFAR system was extended to infrared domain. There are some infrared subparts different in wavelength. Thus, the decision that kind of infrared domain is more suitable for animal capturing and classification in the night was discussed, too.

**Keywords:** animal, classification, infrared, night, ASFAR

## 1. Introduction

ASFAR (Automatic System For Animal Recognition) is system developed at the Laboratory of Digital Video Processing, FEE, University of Zilina. It provides very good results for automatic recognition of wild animals from captured video streams. This system was developed for classification of animals occurring the area of Slovak republic like deer, bear, wild boar, fox and wolf. It is detailed described here [1].

It was developed for animal detection on scene with good illumination in the daytime. In evening or in night when the light is too low it is impossible to capture good images in visible spectrum. It is impossible to classify the animal on captured images, which are almost black corrupted by a lot of Gaussian noise. If we use additional visible light source we will improve the illumination on scene but this light can disturb or scare animals. They can see it and they usually do not come to this areas in the middle of night, they instinctively run away from this areas. Therefore we have to improve this system for the video stream capturing in the night with enough image quality and make this system invisible for animals at the same time.

The paper organization is as follows. Section 2 is devoted to the general migration information of wild animals and section 3 to the visual characteristics of animal eye. In the section 4, the state of the art in the capturing and classification domain are introduced. In the final, the enhancement of previously developed system ASFAR are presented in section 5. The last section contains the conclusion and future work.

## 2. Behavioral and migration characteristics of wild animals

There are a lot of kinds of wild animals in Slovakia. We are focusing especially on animals defined in chapter 1. Foxes (*lat. Vulpes vulpes*) are very territorial animals and their territory can cover almost 20 km$^2$, but younger ones can migrate up to 15 km far away. Deer (*lat. Capreolus capreolus*) in the summer usually stay in one place, but they usually migrate in winter to find food.

Different behavior have wild boars (*lat. Sus scrofa*). Because they are still in move, they can migrate up to 40 km per day. On the other hand, deers (*lat. Cervus elaphus*) periodically migrate to find food and also during the rut. Bears (*lat. Ursus arctos*) and wolves (*lat. Canis lupus*) migrate to long distances, they walk hundreds of kilometers.

Main reasons for migration are finding water and food, seasons, changes of temperature or mating seasons [2]. The most of this migration routes may cross the roads, railways and highways. It is very dangerous for animals and people in cars. Especially in the night, there is bigger chance of collision between car and animal because they are active mainly during sunrise or sunset and also during the nighttime, when the light condition is very poor for our eyesight.

## 3. Impact of infrared domain on animal eyesight

### 3.1. Animal eyesight

There are some key differences between human eye and other mammalian eye. Especially between the eye with *Tapetum lucidum* see Figure 1. All previously mentioned animals have this special reflective layer. We can compare this layer with a mirror. When the light enters into eye, a part of this light is being absorbed by photoreceptors and the rest is reflected back by this layer. It means that photoreceptors can absorb reflected light again. Human eye is missing this layer so we can absorb light only once, but for example deer can absorb light twice. This is the main reason why some kinds of animals can see better in the dark and it is also the reason why their eyes shine at night.

The second difference is the count of rods (low light photoreceptors) and cones (color receptors). Deer has a lower concentration of cones and have only two types of color receptors, see Figure 1. Human eyes have three types of cones. That is why they can see less colors as human. On the other side, they have a higher concentration of rods cells. Thus, they are more sensitive to light intensity and they can see a much more better in the dark.

Finally, third difference is pupil. Deer`s pupil is much more bigger and can open wider. They can gather more light than human eye. Mentioned animals from chapter 2 can see far more better in the dark as human. All mentioned facts are reasons, why they are so active in the evening, morning and during the night [3], [4].

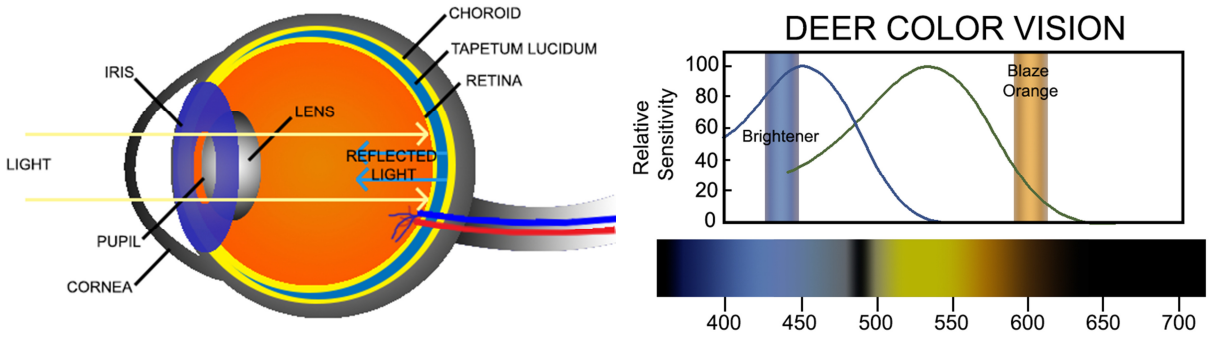


a) b)

**Fig. 1.** Animal eye with Tapetum lucidum, a) cross section, b) spectrum.

### 3.2. Infrared domain

The most of wild animals are primary active in night. Therefore we need to monitor them in the night too. We can realize this task by using cameras in infrared spectrum, see Figure 2. Infrared spectrum is a part of the light which cannot be seen by humans, because longer wavelength light has lower energy and it is too low for our eyes to see it. We can see the light between 380-700nm wavelength only and we call it the visible light. Infrared domain is between 780nm to 1mm wavelength.

With special sensors and cameras we can detect and convert this part of light into an electrical impulses and construct image. Infrared light is divided into three dominant parts based on ISO 20473 specification. The first one is NIR (Near-InfraRed) light within the range from 780nm to 3000nm. Next one is MID (Medium-InfraRed) light in range from 3 000 to 50 000nm and last one is FIR (Far-InfraRed) light up to 1mm wavelength [5].

The key difference between NIR, MIR and FIR is that the NIR is usually used as infrared light as illumination in the dark environments. Then we can capture reflected light from objects. Lighter areas are closer to light source or have bigger reflection. Darker areas are farther from light source or have smaller reflection. The MIR, FIR capture directly emitted light from objects as thermal radiation, where lighter areas are hotter and darker areas are colder. It is also called thermo-vision [6].

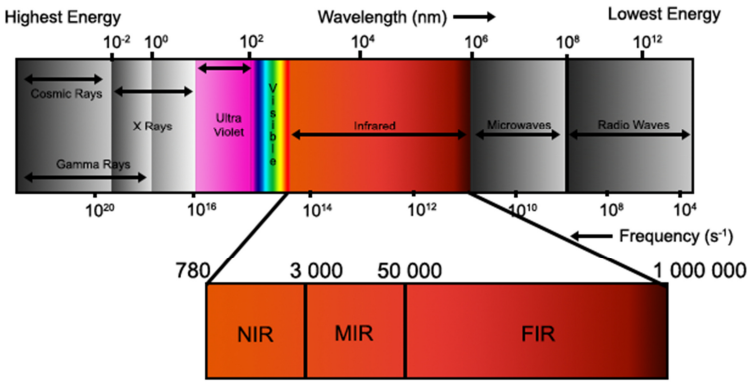


**Fig. 2.** Infrared spectrum based on ISO 20473.

### 3.3. IR light visibility by mammals

We do not want to disturb or scare animals with our system. At first we needed to make sure that animal cannot see or notice IR light. Based on study [7], animals should not be able to notice or see infrared light. Due to low energy of IR light animals cannot visualize stimulation in infrared light domain. On the other side, deer are able to see UV light, because they have not UV filter and that is reason why they cannot see as much details as human.

## 4. Other IR classification systems in night

There are many ways how we can realize human or animal classifications in night. First difficult task is hardware realization of the system. In [8] they used FIR camera for capturing thermal images. Then they converted this images to grayscale, where hotter areas are brighter and colder ones are darker. Animals on images are brighter than a background. Next they use thresholding to create a mask containing the animal pictogram which is used for classification.

Most of this systems like this [9], [10] are based on using thermal cameras. The advantages of this systems are that they do not need any source of light. Capturing by thermal camera is independent on visible light condition and can produce good images with good contrast even in absolute dark areas. Animals or humans do not perceive that they are monitored. The disadvantages are low resolution of output stream and low frames per second ratio. Moreover, they are also quite expensive.

The thermal IR camera cannot be used as ordinary camera for capturing visible light. ASFAR system was developed by using ordinary cameras, therefore we need to expand system with one extra thermo-vision camera for nighttime. For our purposes, this configuration is unacceptable. The reasons are expensive hardware and financial realization, power consumption, etc.

The other way how to capture the video in the night was used in [11], [12]. They used NIR camera with additional infrared illumination for pedestrian recognition. This systems capture grayscale images only. The advantages of NIR cameras are high resolution with good frames per

second ratio and they are also cheaper than MIR or FIR cameras. The big disadvantages are worse contrast of images and requirement of additional IR illumination. Overall quality of illumination depends on numbers of IR LEDs and total power. Common NIR cameras with integrated IR LEDs can illuminate scene up to 30 - 100 meters.

In our solution, the additional IR light reflectors to illuminate monitored area will be used. The most of NIR cameras are equipped with standard CCD or CMOS sensors which can capture light in visible spectrum and also in infrared spectrum up to 1000nm. For the video capturing in night, additional IR filter and IR LED diodes are used. Based on this facts, NIR camera is the best solution how to extend our ASFAR system for monitoring in night. In Figure 3, a samples acquired by NIR camera AXIS Q1765-LE and Thermal camera FLIR TAU 2 640 are introduced [13].

a) b)

**Fig. 3.** Acquired images, a) NIR camera, b) Thermal camera.

## 5. Our solution for ASFAR extension

In figure 4, the block diagram of extended ASFAR system with infrared domain is shown. For our purpose will be used security outdoor camera with night vision Axis Q1765-LE. This camera have four infrared LED diodes for scene illumination. Each diode emit light around 850nm wavelength peak. It allow to see the objects up to 40m distance during the night for capturing enough good quality video stream. Switching between daytime and nighttime mode can be automatically controlled by the camera. Based on used mode, the system will be switched between block for detection and feature extraction during the daytime and during the nighttime. Animal classification during the daytime has already been developed in laboratory. Now, the extension in IR object-based classification will be designed.

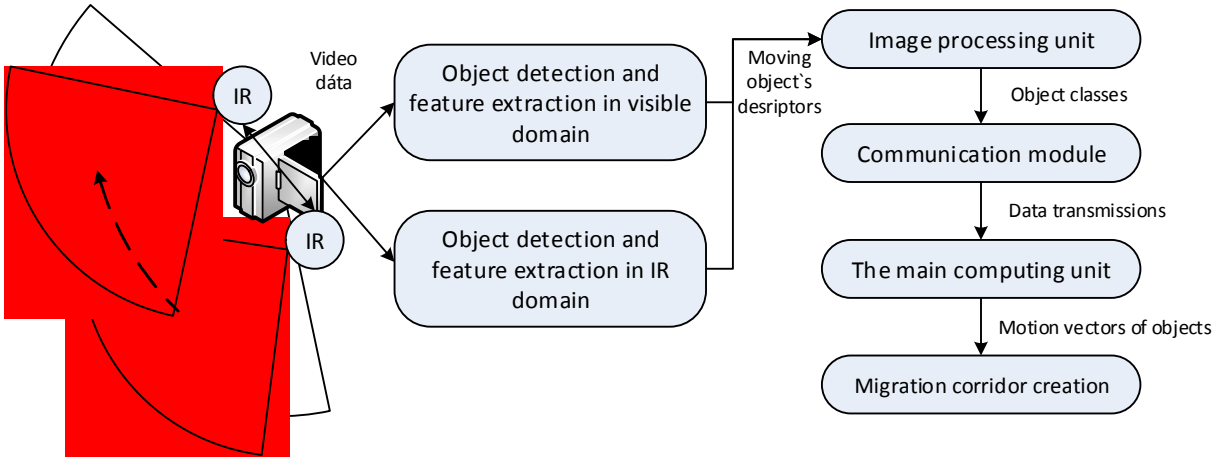


**Fig. 4.** Extended ASFAR system.

## 6. Conclusion

In this paper, the extension of existing ASFAR system was presented. In detail, we described the importance to extend this system for animal classification during the nighttime working. Based on animal eyesight and their behavioral characteristic, we tried to find out the best solution for proposed expansion. We deduced that best area of infrared light for ASFAR system will IR domain, namely, near-infrared light sub-domain. As source of light, the IR LED diodes emitting light around 850nm wavelength will be used. This light is for animals invisible, thus it will not scare or disturb animals in their natural environment. In the future, final version of ASFAR system will provide 24-hour monitoring with automatic animal classification for better migration corridor creation. Moreover, it can be used for planning roads, highways, railways and precede car-animal collision and etc.

## Acknowledgement

The work presented in the paper has been supported by EUREKA project no. E!6752 – DETECTGAME: R&D for Integrated Artificial Intelligent System for Detecting the Wildlife Migration.

## References

[1] MATUSKA, S.; HUDEC, R.; BENCO, M.; KAMENCAY, P.; ZACHARIASOVA, M., *A novel system for automatic detection and classification of animal*, ELEKTRO, 2014 , vol., no., pp.76,80, 19-20 May 2014

[2] MINISTERSTVO DOPRAVY, VÝSTAVBY A REGIONÁLNEHO ROZVOJA SR, *Migračné objekty pre voľne žijúce živočíchy*, Available at: http://www.telecom.gov.sk/index/open_file.php?file=doprava/dopinfra/cesinfra/tech_predpisy/2012/tp_2_2012.pdf, [online], march 2015 (in Slovak)

[3] BRIAN MURPHY, *What do deer see?*, Available at: http://www.qdma.com/corporate/what-do-deer-see, [online], March 2015

[4] BRIAN P. MURPHY, KARL MILLER, AND R. LARRY MARCHINTON, JESS DEEGAN II, JAY NEITZ, GERALD H. JACOBS, *How Whitetail Deer view their world!*, Available at: http://home.comcast.net/~gefferts/deervis.htm, [online], March 2015

[5] ISO, *ISO 20473:2007*, Available at: https://www.iso.org/obp/ui/#iso:std:iso:20473:ed-1:v1:en, [online], March 2015

[6] FLIR, *What`s the difference between thermal imaging and night vision?*, Available at: http://www.flir.com/cvs/americas/en/view/?id=30052, [online], March 2015

[7] DONG-GEN LUO, WENDY W. S. YUE, PETRI ALA-LAURILA, KING-WAI YAU, *Activation of Visual Pigments by Light and Heat. Science*, 10 June 2011: Vol. 332 no. 6035 pp. 1307-1312 DOI: 10.1126/science.1200172

[8] DEBAO ZHOU; DILLON, M.; EIL KWON, *Tracking-based deer vehicle collision detection using thermal imaging*, Robotics and Biomimetics (ROBIO), 2009 IEEE International Conference on , vol., no., pp.688,693, 19-23 Dec. 2009

[9] FORSLUND, D.; BJARKEFUR, J., *Night vision animal detection*, Intelligent Vehicles Symposium Proceedings, 2014 IEEE , vol., no., pp.737,742, 8-11 June 2014, doi: 10.1109/IVS.2014.6856446

[10] Apatean, A.; Rogozan, A.; Bensrhair, A., "Objects recognition in visible and infrared images from the road scene," Automation, Quality and Testing, Robotics, 2008. AQTR 2008. IEEE International Conference on , vol.3, no., pp.327,332, 22-25 May 2008, doi: 10.1109/AQTR.2008.4588938

[11] Andreone, L.; Bellotti, F.; De Gloria, A.; Lauletta, R., "SVM-based pedestrian recognition on near-infrared images," Image and Signal Processing and Analysis, 2005. ISPA 2005. Proceedings of the 4th International Symposium on , vol., no., pp.274,278, 15-17 Sept. 2005, doi: 10.1109/ISPA.2005.195422

[12] Cheng Chang Lien; Wen Kai Yu; Chang Hsing Lee; Chin Chuan Han, "Night Video Surveillance Based on the Second-Order Statistics Features," Intelligent Information Hiding and Multimedia Signal Processing (IIH-MSP), 2014 Tenth International Conference on , vol., no., pp.353,356, 27-29 Aug. 2014, doi: 10.1109/IIH-MSP.2014.94

[13] HD Thermal Core FLIR TAU 2 640 9hz, Available at: http://www.rtfdrones.co.uk/product/thermal-core-flir-tau-2-640-9hz/, [online], March 2015

**TRANSCOM 2015, 22-24 June 2015**
University of Žilina, Žilina, Slovak Republic

# Relationship between the quality coefficients signal and rainfall intensity

[*]Jacek Wilk, [*]Marian Marciniak
[*] Politechnika Świętokrzyska, Wydział Elektrotechniki, Automatyki i Informatyki, Al. 1000-Lecia Państwa Polskiego 7, 25-314 Kielce, jwilk@tu.kielce.pl, marian.marciniak@ieee.org

**Abstract.** This article presents the impact of rain attenuation contributing to the overall loss of signal propagation along Earth-space paths in Poland in the area of Kielce city. This area is the representative region in Poland, especially due to the central location, environment and morphology of terrain. Close to this city from 1974 at Psary-Kąty, was a large satellite ground station, operated by TP SA once, with up to seven large parabolic antennas. In the general theory the presence of rainfall has an influence on the quality of microwaves links. In this paper we present the example result measurements to show the impact of rainfall intensity on the horizontally and vertically polarized radio waves in both (upper and lower) frequency band. In practice the quality coefficients allow to determine the reception range of digital satellite systems. We can estimate the influence of rain intensity on the quality coefficients signal such as: *Channel power*, *CNR* (Carrier-to-Noise Ratio), *MER* (Modulation Error Ratio), *CBER* (BER before FEC – Forward Error Correction, Channel BER), *VBER* (BER after Viterbi, Viterbi BER) and *LBER* (BER after LDPC – Low Density Parity Check). In future all collected data can be used to determine the impact of rainfall intensity, polarization and frequency of microwaves on the received satellite signal quality to provide information about signal attenuation due to rain.

**Keywords:** signal attenuation due to precipitation, *Channel power*, *Link margin*, *CNR*, *CBER*, *VBER*, *LBER*.

## 1. Introduction

The Kielce University of Technology was the member of the international research project COST Action IC0802 – *Propagation Tools and Data for Integrated Telecommunication, Navigation and Earth Observation Systems* [10]. Some part of this study connected with the impact of rainfall intensity on the quality coefficients is presented in this article [10]. All of measurement data were used to estimate the impact of the rainfall intensity, polarization and radio wave frequency on the quality of received microwave satellite signals in Poland. We analyze the microwave satellite signals transmitted via the active satellites Hot Bird on geostationary earth orbit: (1) Hot Bird 13A; (2) Hot Bird 13B and (3) Hot Bird 13C. From this orbital position (13 degrees East) we can receive 2216 Ku-band transmissions: (1) 1649 television programs – include 1197 free-to-air transmissions; (2) 384 radio stations and (3) 183 transfers data. For satellite Hot Bird 13A minimum declination is 0,01º and the maximum – 0,04º, for satellite Hot Bird 13B minimum declination is 0,07º and the maximum – 0,09º and for satellite Hot Bird 13C minimum declination is 0,02º and the maximum 0,03º. In this article we present only the sample data which can illustrate the general regularities (see Tab. 1., Tab. 2, Tab. 3, Tab. 4). The owned meter can be used to change the reference level of the satellite bandwidth in the range of 70 dBuV to 130 dBuV. In the case of digital systems we use the noise level detector to determine the carrier level with an average value (filter bandwidth of 4 MHz) on the same adjustments bandwidth.

## 2. Tables

Rainfall intensity *R* is defined as the ratio of the total amount of rain (rainfall depth) falling during a given period to the duration of the period. We present below the examples of measurements (standard signal: *DVB-S*, modulation: *QPSK*) obtained in the area of Kielce city (*R = 0 mm/h*, *R= 0,3 mm/h*, *R = 0,9 mm/h*). Full study include also many results of measurements for signals with the same and different transmission parameters (*Symbol Rate*, *FEC*, *Bitrate*) also in standard *DVBS-2* and modulation *8PSK* in a wide range of changes in rainfall intensity which are not presented here due to the finite volume of the article. On this basis we can overall illustrate the impact of rainfall intensity on the frequency of the microwave satellite signals for each polarization (horizontal and vertical). See some examples.

| The frequency of the signal before transformation [MHz] and the number of the corresponding transponder | Quality coefficient | Unit | Rainfall intensity | | |
|---|---|---|---|---|---|
| | | | *R* = 0 mm/h | *R* = 0,3 mm/h | *R* = 0,9 mm/h |
| 11977 (63) | *Channel power* | dBμV | 77,8 | 77,2 | 76,9 |
| | *MER* | dB | 14,4 | 13,8 | 13,6 |
| | *Link margin* | dB | 7,2 | 6,6 | 6,4 |
| | *CBER* | | $< 1 \cdot 10^{-6}$ | $< 1{,}8 \cdot 10^{-6}$ | $< 2{,}9 \cdot 10^{-6}$ |
| | *VBER* | | $< 1 \cdot 10^{-8}$ | $< 1 \cdot 10^{-8}$ | $< 1 \cdot 10^{-8}$ |
| 12054 (67) | *Channel power* | dBμV | 77,4 | 76,6 | 76,4 |
| | *MER* | dB | 13,8 | 13 | 12,9 |
| | *Link margin* | dB | 6,6 | 5,8 | 5,7 |
| | *CBER* | | $< 2{,}1 \cdot 10^{-6}$ | $< 1{,}3 \cdot 10^{-5}$ | $< 1{,}5 \cdot 10^{-5}$ |
| | *VBER* | | $< 1 \cdot 10^{-8}$ | $< 1 \cdot 10^{-8}$ | $< 1 \cdot 10^{-8}$ |

* Standard signal: *DVB-S*, modulation: *QPSK* (*FEC* =5/6).

**Tab. 1.** The result of measurements for horizontally polarized radio waves .

| The frequency of the signal before transformation [MHz] and the number of the corresponding transponder | Quality coefficient | Unit | Rainfall intensity | | |
|---|---|---|---|---|---|
| | | | *R* = 0 mm/h | *R* = 0,3 mm/h | *R* = 0,9 mm/h |
| 11565 (153) | *Channel power* | dBμV | 76,8 | 76,1 | 75,9 |
| | *MER* | dB | 15 | 14,2 | 14,1 |
| | *Link margin* | dB | 8,9 | 8,1 | 8 |
| | *CBER* | | $< 1 \cdot 10^{-6}$ | $< 1 \cdot 10^{-6}$ | $< 1 \cdot 10^{-6}$ |
| | *VBER* | | $< 1 \cdot 10^{-7}$ | $< 1 \cdot 10^{-7}$ | $< 1 \cdot 10^{-7}$ |
| 12169 (73) | *Channel power* | dBμV | 74,2 | 73,3 | 72,5 |
| | *MER* | dB | 14,3 | 13,5 | 13,1 |
| | *Link margin* | dB | 8,2 | 7,4 | 7 |
| | *CBER* | | $< 1 \cdot 10^{-6}$ | $3{,}2 \cdot 10^{-6}$ | $6 \cdot 10^{-6}$ |
| | *VBER* | | $< 1 \cdot 10^{-7}$ | $< 1 \cdot 10^{-7}$ | $3{,}5 \cdot 10^{-7}$ |

* Standard signal: *DVB-S*, modulation: *QPSK* (*FEC* =3/4).

**Tab. 2.** The result of measurements for horizontally polarized radio waves.

| The frequency of the signal before transformation [MHz] and the number of the corresponding transponder | Quality coefficient | Unit | Rainfall intensity | | |
|---|---|---|---|---|---|
| | | | $R$ = 0 mm/h | $R$ = 0,3 mm/h | $R$ = 0,9 mm/h |
| 11316,5 (6) | *Channel power* | dBμV | 77,4 | 76,1 | 75,9 |
| | *MER* | dB | 15,8 | 14,9 | 14,8 |
| | *Link margin* | dB | 9,7 | 8,8 | 8,7 |
| | *CBER* | | $< 1 \cdot 10^{-6}$ | $< 1 \cdot 10^{-6}$ | $< 1 \cdot 10^{-6}$ |
| | *VBER* | | $< 1 \cdot 10^{-7}$ | $< 1 \cdot 10^{-7}$ | $< 1 \cdot 10^{-7}$ |
| 12111 (70) | *Channel power* | dBμV | 75,3 | 74,4 | 73,6 |
| | *MER* | dB | 14 | 13,3 | 13,1 |
| | *Link margin* | dB | 7,9 | 7,2 | 7 |
| | *CBER* | | $1{,}1 \cdot 10^{-6}$ | $5{,}7 \cdot 10^{-6}$ | $5{,}8 \cdot 10^{-6}$ |
| | *VBER* | | $< 1 \cdot 10^{-7}$ | $< 1 \cdot 10^{-7}$ | $< 1 \cdot 10^{-7}$ |

* Standard signal: *DVB-S*, modulation: *QPSK* (*FEC* =3/4).

**Tab. 3.** The result of measurements for vertically polarized radio waves.

| The frequency of the signal before transformation [MHz] and the number of the corresponding transponder | Quality coefficient | Unit | Rainfall intensity | | |
|---|---|---|---|---|---|
| | | | $R$ = 0 mm/h | $R$ = 0,3 mm/h | $R$ = 0,9 mm/h |
| 11881 (58) | *Channel power* | dBμV | 77 | 76,3 | 75,5 |
| | *MER* | dB | 14,7 | 13,9 | 13,1 |
| | *Link margin* | dB | 8,6 | 7,8 | 7 |
| | *CBER* | | $< 1 \cdot 10^{-6}$ | $< 1 \cdot 10^{-6}$ | $3{,}5 \cdot 10^{-6}$ |
| | *VBER* | | $4{,}7 \cdot 10^{-7}$ | $< 1 \cdot 10^{-7}$ | $< 1 \cdot 10^{-7}$ |
| 12225 (76) | *Channel power* | dBμV | 76,8 | 75,3 | 74,3 |
| | *MER* | dB | 13,6 | 13,5 | 12,3 |
| | *Link margin* | dB | 7,5 | 7,4 | 6,2 |
| | *CBER* | | $2{,}1 \cdot 10^{-6}$ | $8{,}3 \cdot 10^{-6}$ | $4{,}5 \cdot 10^{-5}$ |
| | *VBER* | | $< 1 \cdot 10^{-7}$ | $< 1 \cdot 10^{-7}$ | $< 1 \cdot 10^{-7}$ |

* Standard signal: *DVB-S*, modulation: *QPSK* (*FEC* =3/4).

**Tab. 4.** The result of measurements for vertically polarized radio waves.

Increase in the rainfall intensity causes the decrease in *Channel power*. Generally, with the increase in the rainfall intensity we can observe that *MER*, *Link margin* and *CBER*, *VBER* coefficient decreases slowly. With the increase in the frequency these rules are more noticeable. In practice the Hot Bird satellites are equipped with *AGC* systems (Automatic Gain Control). It may give rises to lack of correlation between change of power of signals transmitted by satellite operators and power of signals received by the end user in decrease or increase in power. The study show that the greater rainfall intensity causes the increase in signal attenuation and thus degradation of signal quality coefficients such as: *Channel power*, *MER*, *Link margin*. Increase in the rainfall intensity causes a gradual reduction of error rates: BER before Forward Error Correction (Channel BER) and BER after Viterbi (Viterbi BER) for *DVB-S* standard signals and BER after Low Density Parity Check (signals in the *DVB-S2*), wherein – depending on the signal coefficients and polarization – increase in the rainfall intensity does not always result in the visible changes of coefficients: *CBER*, *LBER* or *VBER*.

## 3. Conclusion

The overall result measurements may be important when high reliability of microwave link is needed to calculate the link budget analysis in the design of telecommunication systems. In practice systems engineers can improve the design and performance of satellite links in adverse weather conditions and consequently they may reduce the risk of interruption or lack of communication between the terminal and active satellites *EUTELSAT* Hot Bird on geostationary earth orbit. The overall collected results of the international research project COST Action IC0802 – *Propagation Tools and Data for Integrated Telecommunication, Navigation and Earth Observation Systems* indicate (on the basis of the comparative results of the analysis of measurements for vertical and horizontal polarization) that the signal attenuation (with the same frequency and rainfall intensity) of horizontally polarized radio waves is greater than the signal attenuation of vertically polarized radio waves that empirically confirm the theory from literature for propagation radio waves (the elaboration model is developed in accordance with series of the ITU-R Recommendations in up-to-date) [1, 3, 4, 5, 6].

Ongoing research may be used in the further to analyze the propagation of microwave satellite signal (on the direction of the satellite-Earth and Earth-satellite) in the area of Kielce with the best possible quality including the atmospheric attenuation, combine the signal by transmultiplexer, analysis of absorption, ionosphere phenomena and other factors in the troposphere [2, 7, 8, 9, 10].

## References

[1] BEM J.: *Antennae and radiowave propagation*, Wydawnictwa Naukowo-Techniczne, Warszawa 1973.

[2] CIOSMAK J.: *An algorithm of determining non-separable two-dimensional filer arrays for transmultiplexion systems*. Przegląd Elektrotechniczny 2011, nr 11.

[3] IPPOLITO L. J.: *Satellite communications. Systems engineering. Atmospheric effects, satellite link design and system performance*. JohnWiley & Sons, Chichester 2008.

[4] ITU, *Radio regulations*. *Edition of 2008*, http://www.itu.int/opb/itemdetails.aspx? lang=e&item=R-REG-RR-2008-A5-ZPF-E&folder=R-REG-RR-2008.

[5] KATULSKI R. J.: *Radiowave propagation in wireless Communications*. Wydawnictwa Komunikacji i Łączności, Warszawa 2009.

[6] KOLAWOLE M. O.: *Satellite communication engineering*. Marcel Dekker, Inc., New York 2002.

[7] LLORET J., DIAZ J. R., BORONAT F., ESTEVE M.: *A satellite connections approach based on spatial footprints*, http://ieeexplore.ieee.org/stamp/stamp.jsp? tp=&arnumber =4362395.

[8] MARAL G.: *VSAT Networks*. JohnWiley & Sons, Chichester 2003.

[9] MARCINIAK M., ZINENKO T. L,. NOSICH A. I: *Accurate Analysis of Light Scattering and Absorption by an Infinite Flat Grating of Thin Silver Nanostrips in Free Space Using the Method of Analytical Regularization*. IEEE JOURNAL OF SELECTED TOPICS IN QUANTUM ELECTRONICS 2013, no 3.

[10] WILK J. Ł.: *Total signal degradation due to rain precipitation in the troposphere in the area of Kielce city*. Zeszyty Naukowe. Scientific Journal 262. Telekomunikacja i Elektronika. Telecommunications and Electronics 2013, no 17, red. J. Flizikowski, Wydawnictwo Uniwersytetu Technologiczno-Przyrodniczego im. Jana i Jędrzeja Śniadeckich w Bydgoszczy.

**TRANSCOM 2015, 22-24 June 2015**
University of Žilina, Žilina, Slovak Republic

# Aspects of a wireless telemetry station

Vasilios Zarikas[1], Theofilos Chrysikos[2], K. E. Anagnostou[1], Stavros Kotsopoulos[2], P. Avlakiotis[1], C. Liolios[1], T. Latsos[1], G. Perantzakis[1], A. Lygdis[1], D. Antoniou[1], A. Lykourgiotis[2]
[1]ATEI of Central Greece, Department of Electrical Engineering, Lamia, Greece,
E-mail: vzarikas@teilam.gr
[2]University of Patras, Department of Electrical & Computer Engineering, Patras, Greece,
kotsop@ece.upatras.gr

**Abstract.** A telemetric station measuring continuously various physicochemical parameters of hot spring waters is presented. The work describes the final full operation stage of the integrated system. Challenges of the wireless connection are presented as well as statistical inferences regarding the measured data. The measuring station is able to dynamically measure, process and transmit the following key factors of hydrogeological significance: Radon, Geomagnetic field strength, redox potential OPR, acidity PH, Conductivity and water Temperature. The presented statistical analysis concerns data for the time period 28-4-2014 till 21-6-2014. Some interesting results refer to statistically significant correlations that emerged between the involved physico-chemical factors

**Keywords:** Wireless Telemetry, Hydrogeology Engineering Geology, Modeling/Statistics

## 1. Introduction

This work concerns a measuring station built in order to investigate the physical and chemical characteristics of the Thermopylae natural hot water springs. The scope of this study is first to describe aspects of the developed wireless measurement system and second to present some thorough statistical inferences coming out of the statistical analysis of the data taken by the full operation phase of the integrated system. The whole measuring system provides a realisation to a challenge stated in [1], where the need for a system of continuous monitoring of physicochemical hydrogeological parameters is stated.

An early development and preliminary results of the integrated measuring station are presented in [2], [3]. A Similar sensor system for environmental monitoring (Slovenian hot springs) as well as seismic detection is described [4]. The developed measuring station belongs in the broad category of Wireless Sensor Networks (WSN). A WSN includes various spatially distributed autonomous sensors that monitor physical or environmental conditions. WSNs cover a great variety of different domains, such as weather parameters monitoring, seismic or acoustic detection, health monitoring, inventory tracking, army surveillance or process monitoring.

The measured factors are of hydrogeological importance. During geological deformations which most probably take place in different depths various variations are produced such as: changes in the temperature and/or chemical composition, variations both in the gas discharge flow-rates and in the chemical and isotopic composition of the gases (especially 222Rn), hydrostatic pressure, electrical conductivity etc.

In the full operating system under study six parameters were introduced and measured which are important to geological deformations too. Radon to study the influence of deformations to gases flow/composition, Geomagnetic field strength and temperature to study the flow rate and depth variations, PH to study acidity variations, Redox potential to study the biologic load variations, and electrical conductivity to study the salanity variations.

Since geological phenomena are time dependent it is expected that measured physicochemical parameters to follow the same variation in time. In addition occasionally certain abrupt geological realignments occur in a few minutes. In these circumstances in a time scale of a few minutes it is possible to extract critical information for the geological phenomenon. In the present research measuring station, physicochemical parameters have been measured underwater. This means that their values are considered to vary on a time scale of hours. However, a sampling period (or data collection time) of 15 minutes has been implemented in order to capture both common and spontaneous geological phenomena.

In what follows, the implemented telemetry system and the statistical methods are presented in the second section. Some selected statistical inferences of the data analysis are presented in the third section.

## 2. Materials and Methods.

### 2.1 Wireless link setup.

The investigation of a reliable wireless link between the data collection measuring station of Thermopylae, Greece and the campus of Technological Educational Institute (ATEI) of Central Greece, located at Lamia, Greece was thoroughly investigated in [2],[3].

Line of Sight (LOS) was assumed for this link. Antenna heights were considered so as to provide LOS and avoid obstruction or severe fading by local foliage. In order to estimate the average level of local mean strength at the receiver, two different path loss models were employed: the Free Space and the Log-Distance path loss model [5-7]. The Free Space Model takes into consideration only the distance-dependent losses due to free space propagation [8]. On the other hand, the Log-Distance model incorporates the excess path loss, defined by Jakes as “the difference (in decibels) between the computed value of the received signal strength in free space and the actual measured value of the local mean received signal” [9]. In this scenario, since LOS is considered, the excess path loss stands for the losses due to terrain and other geographical irregularities.

The average path loss (in dB) is provided by the following formula [8] for the Free Space Model:

$$P_L = 32.45 + 20\log_{10} f(MHz) + 20\log_{10} d(km) \qquad (1)$$

The mathematical expression of the Log-Distance path loss model is given by [9]:

$$L_{total} = PL(d_0) + N\log_{10}\left(\frac{d}{d_0}\right) + X_\sigma \qquad (2)$$

Where $PL(d_0)$ is the path loss at the reference distance, usually taken as (theoretical) free-space loss at 100 m or 1 km, for outdoor propagation scenarios, $N$ is the path loss distance exponent (set to 2 in this work) and $X$s is a Gaussian random variable with zero mean and standard deviation of $\sigma$ dB (set to 6 dB in this paper). $N$ and $\sigma$ are derived from experimental data. During our work a coverage probability of 95% was assumed and thus:

$$\mathrm{X}_\sigma = z \times \sigma(dB) = 1.645 \times \sigma(dB) \qquad (3)$$

Both models are suitable [9] for open areas unlike others which are more appropriate for urban or suburban areas, such as the Hata and Okumura model [10]-[11].

The distance required for signal propagation (T-R separation is approximately 38 km) calls for the employment of specific wireless technologies such as WiMax or LTE. In [2,3], the 1800 MHz frequency band was investigated since major telecommunications providers in Greece have

introduced LTE in band 3 (1800 MHz). A bandwidth of 20 MHz was assumed and a medium-range LTE Base Station (BS) is assumed, with a maximum transmit power of 38 dBm.
Results provided a signal reception level critically close to the threshold set by the receiver sensitivity level. Clearance of first Fresnel zone for ensuring LOS communications was deemed essential for the avoidance of outage. Moreover, if any unexpected excess path loss occurred, then the link was compromised. Since distance-dependent free space losses were considered, it was imperative to provide a more efficient solution. Understanding that free space losses are also frequency dependent [5] and in compliance with the inverse-square law, in this work we have introduced a LOS link based on band-28 LTE. Therefore, a 700 MHz carrier frequency is investigated in this work. According to LTE specifications [12], or the 700 MHz carrier frequency, an additional margin of 6 dB for interference mitigation needs to be considered, leading to a threshold of -85 dBm.

Three propagation scenarios were examined for the band-28 solution or our wireless link of 38 km: a free space/LOS propagation scenario where only distance-dependent free space path loss is considered, a LOS-dominant propagation scenario with an excess path loss (attributed to various mechanisms such as scattering or partial impairing of the 1$^{st}$ Fresnel zone) with a shadow depth of 3 dB (a total excess path loss of 4.94 dB), and a more severe case of excess path loss with a shadow depth of 6 dB and a total excess path loss of 9.88 dB. A medium-range BS of 38 dBm has been employed and results are presented in the following graph.

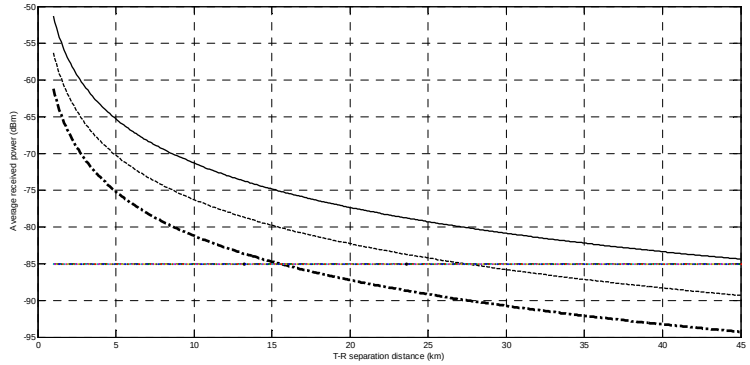


**Fig. 1.** Local mean value of received power as a function of distance

As it can be seen from the graph, for the free space-LOS scenario, the link is never compromised as the receiver threshold is approached for distances up to 45 km. Concerning the T-R separation distance of 38 km, there is a fade margin of a few dB. For the excess path loss scenarios however, the link is compromised: in the case of a mild excess path loss (standard deviation of 3 dB), the receiver threshold is reached at ~ 27.5 km (this refers to the threshold that incorporates the 6 dB margin for interference mitigation, as the actual sensitivity level is never reached for distances up to 45 km). For the more severe excess path loss scenario (standard deviation of 6 dB), the link is compromised at ~ 15 km, whereas the receiver sensitivity level is crossed at around 30 km of T-R separation distance.

## 2.2 Statistical methods

The under consideration data from the full operation measuring station in Thermopylae refer to the time duration 28-4-14 till 21-6-14. The various parameters of hot waters that are measured are: Geomagnetic Field strength, Radon in pCi/L, temperature in Celsius degrees, potential of redox (ORP) in milli-Volts, PH and conductivity in milli-Siemens. Data analysis was performed with the help of commands in SPSS v21 software.

First descriptive statistics was performed on data. It includes measures of skewness and kyrtosis in order to study deviation from normality. Furthermore Kolomorov-Smirnov test was evaluated. The tests of normality overlay a normal curve on actual data, to assess the fit. A

significant test means the fit is poor. Finally in order to explore the type of distribution P-P plots and Q-Q plots were drawn for each factor [13]. A P-P Plot is made by plotting a variable's cumulative proportions against the cumulative proportions of any of a number of test distributions. Probability plots are generally used to determine whether the distribution of a variable matches a given distribution. If the selected variable matches the test distribution the points cluster around a straight line. Similarly in Q-Q Plots we draw the quantiles of a variable's distribution against the quantiles of any of a number of test distributions. These probability plots are also used to determine whether the distribution of a variable matches a given distribution. If the selected variable matches the test distribution, the points cluster around a straight line.

Correlations are measures of linear association. Correlations were investigated using various methods. The Pearson correlation coefficient measures the linear association between two scale variables. However, the Pearson correlation coefficient works best when the variables are approximately normally distributed and have no outliers. The Spearman's rho and Kendall's tau-b statistics measure the rank-order association between two scale or ordinal variables. They work regardless of the distributions of the variables.

Partial Correlations method usually denotes an algorithm that computes partial correlation coefficients. These coefficients describe the linear relationship between two variables while controlling for the effects of one or more additional variables. Even if two variables are perfectly related, if the relationship is not linear, a correlation coefficient is not an appropriate statistic for measuring their association. The Partial Correlations table shows both the zero-order correlations (correlations without any control variables) of all three variables and the partial correlation of the first two variables controlling for the effects of the third variable.

## 3. Results and discussion

We have evaluated the time series of all measured factors. The analysis of them indicates that statistically significant peak occurred for temperature and OPR variables. Indeed one significant temperature modification had occurred during the studied time period affecting OPR too. Results from the descriptive statistical analysis have also been investigated. A very brief summary of them follows: *T* (Celcius) = 39.987 ± 0.6278, *OPR* (mV) = 279.008 ± 40.6826, *PH* = 6.428 ± 0.068, *Conductivity* (mS) = 19.704 ± 0.896, *GMagnetic Stength* = 44887.34 ± 282.968 and *Radon* (pCi/L) =4.089 ±0.7220. Examining the values of skewness and kyrtosis it can be concluded that data concerning the Temperature *T* and *PH* are close to normality while the rest are not. However, some factors can be handled as a skewed normal distributions with the help of parametric statistical methods that are not very sensitive to normality.

In addition the magnitude of the departure from normality can be shown with the help of P-P and Q-Q plots. As an example Figure 2 shows clearly the large departures from normality of the Radon.

The statistical study Table 1, reveals some statistically significant correlations estimated between the factors as follows: Temperature and ORP, Temperature and PH, Temperature and Conductivity, PH and OPR, PH and Conductivity, Conductivity and OPR and Radon and Geomagnetic Strength. However, most of them are only mild associations. Both parametric “Pearson correlation” and non parametric methods “Kendall tau” and “Spearman's rho” for the investigation of possible associations have been evaluated and found to agree.

Furthermore, in order to test correlations we have investigated if there is a control variable that will cancel some of the correlations appeared in our analysis. For this reason, a partial correlation analysis was accomplished taking into account all the possible combinations of the six factors under investigation. The whole partial correlation analysis suggests that all mentioned correlations remain.

| | | | T (Celcius) | OPR (mV) | PH | Conductivity (mS) | GMagnetic Stength | Radon (pCi/L) |
|---|---|---|---|---|---|---|---|---|
| **Kendall's tau_b** | **T (Celcius)** | Correlation Coefficient | 1.000 | .047** | .131** | -.601** | .011 | -.006 |
| | | Sig. (2-tailed) | . | .000 | .000 | .000 | .265 | .505 |
| | | N | 5201 | 5201 | 5201 | 5201 | 5201 | 5201 |
| | **OPR (mV)** | Correlation Coefficient | .047** | 1.000 | .143** | -.184** | -.004 | -.007 |
| | | Sig. (2-tailed) | .000 | . | .000 | .000 | .661 | .484 |
| | | N | 5201 | 5201 | 5201 | 5201 | 5201 | 5201 |
| | **PH** | Correlation Coefficient | .131** | .143** | 1.000 | -.066** | -.006 | -.008 |
| | | Sig. (2-tailed) | .000 | .000 | . | .000 | .545 | .408 |
| | | N | 5201 | 5201 | 5201 | 5201 | 5201 | 5201 |
| | **Conductivity (mS)** | Correlation Coefficient | -.601** | -.184** | -.066** | 1.000 | -.009 | .007 |
| | | Sig. (2-tailed) | .000 | .000 | .000 | . | .326 | .492 |
| | | N | 5201 | 5201 | 5201 | 5201 | 5201 | 5201 |
| | **GMagnetic Stength** | Correlation Coefficient | .011 | -.004 | -.006 | -.009 | 1.000 | -.143** |
| | | Sig. (2-tailed) | .265 | .661 | .545 | .326 | . | .000 |
| | | N | 5201 | 5201 | 5201 | 5201 | 5201 | 5201 |
| | **Radon (pCi/L)** | Correlation Coefficient | -.006 | -.007 | -.008 | .007 | -.143** | 1.000 |
| | | Sig. (2-tailed) | .505 | .484 | .408 | .492 | .000 | . |
| | | N | 5201 | 5201 | 5201 | 5201 | 5201 | 5201 |
| **. Correlation is significant at the 0.01 level (2-tailed). | | | | | | | | |

**Table1.** Non parametric correlations.

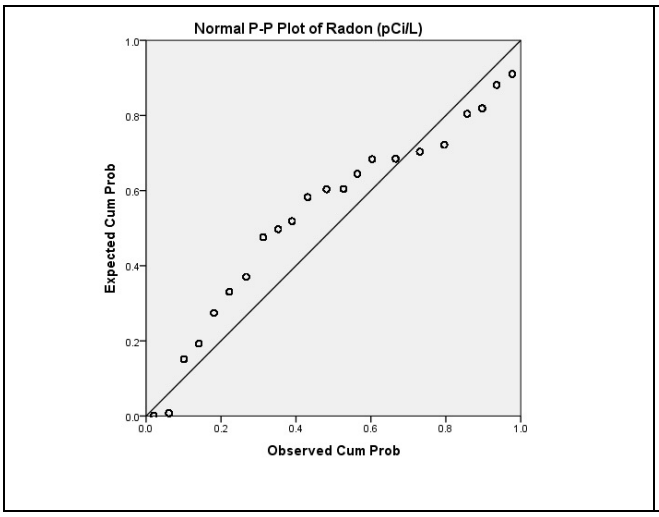


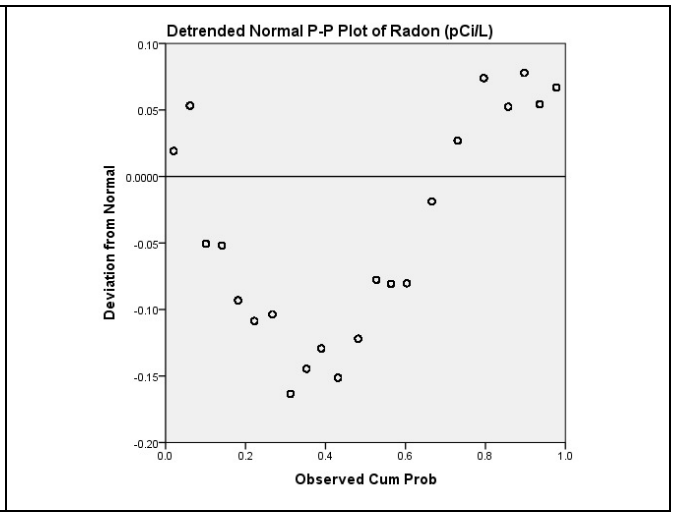

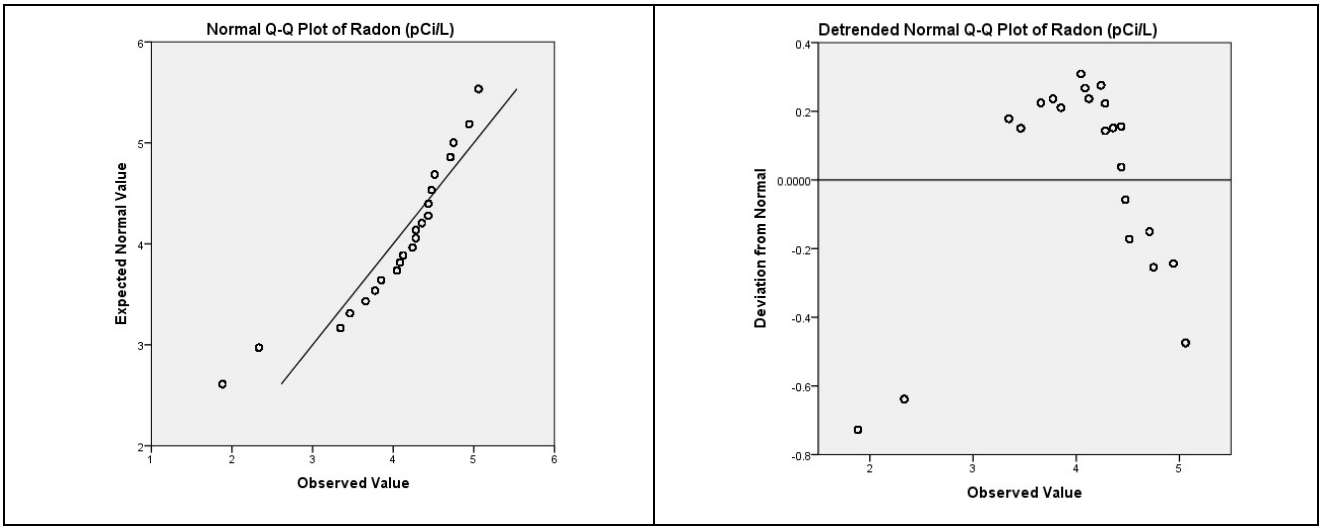


**Fig. 2**. P-P and Q-Q plots showing deviation from normality for radon

## Acknowledgements

This work is part of "ARCHIMEDES III" project, entitled: "Measurement of Environment Physical-Chemical Parameters by Development Autonomous Data Collection Processing Transmission Systems with use of green Power and most optimal management", funded by the European Union.

## References

[1] POPIT A., VAUPOTIC J., DOLENEC T. 2005, Geochemical and geophysical monitoring of thermal waters in Slovenia in relation to seismic activity, Annals of Geophysics, Vol. 48, N. 1.

[2] VASILIOS ZARIKAS, THEOFILOS CHRYSIKOS, K. ANAGNOSTOU, S. KOTSOPOULOS, P. AVLAKIOTIS, C. LIOLIOS, G.T. LATSOS, C. PERATZAKIS, A. LYGDIS , D., ANTONIOU A. LYKOYRGIOTIS, "WirelessTelemetry: Channel characterization and statistical imputation of missing values", Communications Journal: Scientific Letters of the University of Zilina, 2015 (in print) ;

[3] VASILIOS ZARIKAS, K.E. ANAGNOSTOU, P. AVLAKIOTIS, STAVROS KOTSOPOULOS, C. LIOLIOS, T. LATSOS, G. PERANTZAKIS, A. LYGDIS, ASIMAKIS LYKOURGIOTIS, D. ANTONIOU «Measurement and Analysis of Physicochemical Parameters Concerning Thermopylae Natural Hot Spring Waters» Journal of Applied Sciences 01/2014; 14(19):2331-2340.

[4] ZMAZEK, B.; ITALIANO, F.; ZIVCIC, M.; VAUPOTIC, J.; KOBAL, I.; AND MARTINELLI, G., 2002, *Geochemical monitoring of thermal waters in Slovenia: relationships to seismic activity*, Elsevier Applied Radiation and Isotopes Journal, Vol. 57, pp. 919-930.

[5] GOLDSMITH, A.: *Wireless Communications*. Cambridge: Cambridge University Press, 2005.

[6] PARSONS, J. D.: *The Mobile Radio Propagation Channel*. Hoboken : NJ: Wiley Interscience, 2000.

[7] RAPPAPORT, T.: *Wireless Communications: Principles & Practice. Upper Saddle River*, NJ: Prentice Hall, 1999.

[8] SEYBOLD, J.: Introduction to RF Propagation. Hoboken, NJ: Wiley Interscience, 2005.

[9] JAKES, W. C. (Ed.): Microwave Mobile Communications. New York : Wiley Interscience, 1974.

[10] HATA, M. : Empirical Formula for Propagation Loss in Land Mobile Radio Services, IEEE Transactions on Vehicular Technology, vol. 29, No. 3, pp. 317-325, August 1980.

[11] OKUMURA, Y., OHMORI, E., KAWANO, T., FUKUDA, K. : Field Strength and its Variability in VHF and UHF Land-Mobile Radio Service, *Review of the Electrical Communication Laboratory*,vol. 16, No. 9-10, pp. 825-873, September-October 1968.

[12] 3GPP TS36.104 version 11.8.2. R11

[13] KOTZ, S., AND N. L. JOHNSON, eds. 1988. Encyclopedia of statistical sciences. New York: John Wiley & Sons, Inc.

**TRANSCOM 2015, 22-24 June 2015**
University of Žilina, Žilina, Slovak Republic

# Analysis of acoustic signals in transport systems using WSN

[*]Róbert Žalman, [*]Veronika Olešnaníková, [*]Peter Šarafín, [*]Ján Kapitulík
[*]University of Žilina, Faculty of Management Science and Informatics, Department of Technical Cybernetics, Univerzitná 8215/1, 010 26 Žilina, Slovakia, {robert.zalman, veronika.olesnanikova, peter.sarafin, jan.kapitulik}@fri.uniza.sk

**Abstract.** The paper deals with the recognition of acoustic signals in transport systems. It uses a Fast Fourier Transform to create frequency spectra. This spectrum is used to create clusters due to which we are able to identify the vehicle passing near the nodes in a wireless network.

**Keywords:** Distributed Sensor Network, Acoustic Signal, Fast Fourier Transform, Cluster analysis.

## 1. Introduction

We are dealing with the analysis of acoustic signals in transport system. Acoustic signal transmits acoustic energy and it also represents information. This information represents a change of physical quantity in time. The simplest change can be represented as periodic sinusoidal signal [1]. The composite signal can be analysed using transformation to simpler harmonic signals, thus spectrum of original signal can be obtained this way. In spectrum, the key parameters of the signals may be found.

Using the WSN, acoustic emissions can be detected in transport system, sensing the movement of people in the building can be provided, also as obtaining meteorological data or wide use of WSN in intelligent buildings.

### 1.1. Monitoring of the transport systems

Monitoring of the transport systems serves primarily to:

- Vehicle Detection – to set up the traffic lanes crossings.
- Counting the vehicles – to determine the number of vehicles at crossroads, important information to control traffic lights.
- Vehicle classification – identification of the type of the vehicle for various applications.
- The measurement of the intensity of the traffic flow – the information necessary for the effective maintenance of road surface or traffic control.
- The measurement of vehicle speed – supports the safety and efficiency of travel.

Monitoring of emergency vehicles allows safe passage through crossroad. Since those emergency vehicles are using sirens, monitoring of these vehicles is reliably secured by acoustic sensors.

Monitoring of weather allows the driver to adjust driving style to avoid accidents [2]. Monitoring of environmental conditions is used to gather information of air pollution: emissions of $CO_2$, dust concentration, acoustic noise associated with the operation in this area. Such information is valuable for development of applications for the protection of public health.

This paper is focused on vehicle classification using cluster analysis. Processed acoustic signals by using Fast Fourier Transform form the input data for cluster analysis.

## 2. Fast Fourier Transform

The calculation of the Discrete Fourier Transform (DFT) is relatively simple, which results in quadratic time complexity $N^2$. For this reason Fourier Transform was in practical applications used not so often. Finally, in 1942, Danielson and Lanczos develop a version of the algorithm known under the name of Fast Fourier Transform (FFT). The time complexity of this algorithm is already logarithmic *Nlog2N*. Danielson and Lanczos showed that the DFT of length *N* can be calculated as the sum of the two Fourier Transform length *N/2* [3, 4]. One of it can be counted with the even points (points located at even spot) and other can be counted with the odd points (points located at odd spot) spot of the original Fourier Transform, which is expressed by the formulae:

$$X(k) = \sum_{n=0}^{\frac{N}{2}-1} x(2n) W_{\frac{N}{2}}^{k} + W_N^k \sum_{n=0}^{\frac{N}{2}-1} x(2n+1) W_{\frac{N}{2}}^{nk}, \qquad W_N = e^{\frac{-2j\pi}{N}}, \tag{1}$$

where $k = 0,1,2,\ldots,N-1$. From the relation it can be seen that the calculation of the Fast Fourier Transform (with period *N*) is reduced. The essence of the algorithm is to reduce the number of needed complex multiplication of the number from $N^2$ to *Nln2*. Taking the Fourier Transform of length 1 (with a period length 1), it is the same value. The advantage of this algorithm is therefore in its recursive. However, the limitation of the number of points entering into transform that have to be $N = 2^r$, $r > 0$.

The formulae for the inverse Fourier Transform is:

$$X(k) = \frac{1}{N} \sum_{n=0}^{N-1} x(n) e^{\frac{-j2\pi nk}{N}}. \tag{2}$$

### 2.1. Utilization of the Fast Fourier Transform for analysis of the acoustic signals in transport systems

Acoustic signal in transport system can be analysed via frequency analysis. FFT can be effectively applied here, which results into the spectral graph as can be seen in Fig.1. In this picture passing vehicle is captured nearby monitoring node of wireless network. The picture shows the dominant frequency is approximately 1 kHz. These data serve as input for cluster analysis.

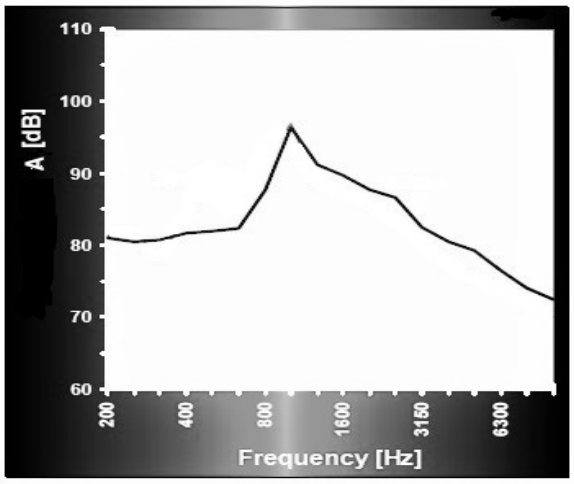


**Fig. 1.** The frequency spectrum of passing vehicle obtained by using FFT.

### 2.2. Clustering

The aim of clustering is to determine the inner grouping of the unmarked data. Therefore, we have to decide what is appropriate grouping. It can be demonstrated that there does not exist the

best criterion which would be independent of the final aim of clustering [5]. Consequently, this criterion is supplied by the user in such a way that the result of clustering is subject of his needs.

### 2.3. Clustering based on the linking of clusters

Clustering based on the data fusion can be divided into several categories. We are going to mention the hierarchical tree, based on the measurements of distances of clusters or based on the linking clusters rules. Clustering by measuring the distance of clusters differs in how we calculate the distance between clusters. For this purpose we can use the Euclidean distance.

Euclidean norm is probably the most frequently chosen type of distance measurement. It is the geometric trace of multi-dimensional space. It is calculated as the distance between *x* and *y*:

$$(x, y) = \sqrt{\sum_i (x_i - y_i)^2}, \tag{3}$$

Testing the clustering was tested for division of passing cars into two clusters on the basis of the amplitude and frequency of Fig. 2. The input data for clustering were the result of frequency analysis. Maximum amplitude at a given frequency of these data was send.

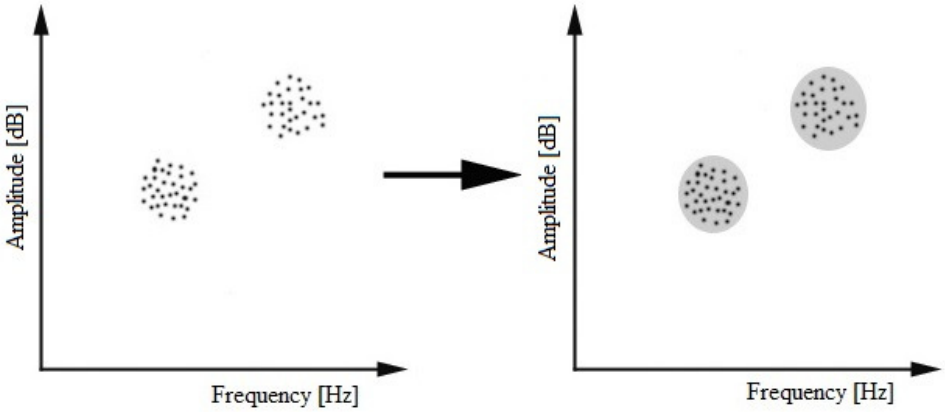


**Fig. 2.** Simple clustering based on the distance - division into two clusters.

## 3. Requirements for the sensor node

Each sensor network is composed of many simple sensors located in the area. Every node should be able to perform the following basic functions:

- Data collection.
- Data Processing.
- Communication.
- Automatic detection of a position in the case where the WSN is not structured, GPS allows us to solve the localization problem. Another solution is based on the principle of evaluation of the intensity of RF signal [6, 7].
- Time synchronization of network elements is required in most applications. This problem can be solved by GPS [8, 9] or by using synchronization algorithms [10].

It is important to note that it is not possible to create a universal wireless network which meets all these requirements. Also, each node in WSN has to ensure the implementation of these three basic functions: data collection, data processing and data transfer.

### 3.1. Sensor node

The basis of the node is ATSAM4S microcontroller. This model includes a core Cortex-M4 and is equipped with RISC. It works at the frequency of 120 MHz and it includes 12-bit AD Converter with Programmable Gain Amplifier and consumption is 180u/1MHz – max. Furthermore, sensor node is equipped with a microphone to capture the acoustic signal and preamplifier. Input signal has to pass through band-pass filter with a range of 200 Hz – 2kHz. On the circuit board, it is also located RF module. Communication between the MCU and nRF24L01 module is realized by SPI communication interface. For testing purposes the sensor is also equipped with SD card slot with which the MCU communicates via HSMC interface.

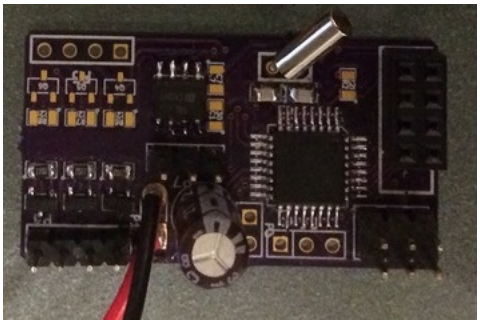

**Fig. 3.** Testing sensor node the ATSAMS4S view from above without RF module.

## 4. Conclusion

Collected results are used to create a database which is compare with the recorded acoustic signals in real environments. This database is acting as a learning system and it is adjusted according to the function, depending on the its suitability for signal processing in a particular environment.

For better identification, the passing vehicles are captured by a magnetometer and ultrasonic sensors. Information from these sensors are used for better identification of the vehicle and subsequent correction of the system. The biggest problem of the system is the acoustic noise which disrupts frequency spectrum.

In the future, the system will be modified for the use of estimates using hidden Markov models (HMM) or neural networks. Thanks to this model, the system should identify the vehicle more precisely. However, the problem with unwanted noise still persists. It is therefore necessary to increase the robustness of these algorithms or to find suitable alternatives.

## References

[1] EVEREST A.F., POHLMANN C. K. *Master Handbook of Acoustics Fifth Edition*, - ISBN 978-0-07-160333-1.

[2] MIČEK J., KAPITULÍK J. *WSN sensor node for protected area monitoring*, FedCSIS, 2012: IEEE. - ISBN 978-83-60810-51-4.

[3] MIČEK J., JURE ČKA M. *Moderné prostriedky implementácie metód číslicového spracovania signálov I.*, Žilina : Žilinská univerzita, 2013. - ISBN 978-80-554-0714-2.

[4] ŠEVČÍK P., KAPITULÍK J. *Moderné prostriedky implementácie metód číslicového spracovania signálov II.*, Žilina: Žilinská univerzita, 2013. - ISBN 978-80-554-0676-3.

[5] MURPHY, KEVIN P. *Machine learning: a probabilistic perspective*, Adaptive computation and machine learning series, ISBN 978-0-262-01802-9.

[6] SAVARESE Ch., RABAEY J. M., BEUTEL J. *Locationing in distributed ad-hoc wireless sensor networks*, 2001.

[7] MAO G., FIDAN B., ANDERSON B. D. O. *Wireless sensor network localization techniques*, p.p. 2529-2553, Computer Networks 51, 2007.

[8] ELSON J., ESTRIN D. *Time synchronization for wireless sensor networks*, Proceedings of 15th International Parallel and Distributed Proccesign Symposium, IEEE 2001.

[9] SOMMER P., WATTENHOFER R.: *Gradient clock synchronization in wireless sensor networks*, Proc. IPSN09, USA 2009.

[10]CHOVANEC M., PÚCHYOVÁ J., HÚDIK M., KOCHLÁŇ M. *Universal synchronization algorithm for wireless sensor networks - FUSA algorithm*, FedCSIS, 2014, Warsaw, Poland: IEEE. - ISSN 2300-5963.

**TRANSCOM 2015**

Proceedings, Section 3

Published by University of Žilina
First Editions
Printed by EDIS - Žilina University publisher
Printed in 500 copies

ISBN 978-80-554-1045-6
ISSN of Transcom Proceedings CD-Rom version: 1339-9799
ISSN of Transcom Proceedings online version: 1339-9829
(http://www.transcom-conference.com/transcom-archive)


9 788055 410456